Metamorphism of eclogites and associated metamorphic rocks in the Chandman district, Lake Zone, SW Mongolia

A dissertation submitted to the Department of Geoscience in partial fulfillment of the requirement for the Degree of Doctor of Science (D.Sc) at the Interdisciplinary Graduate School of Science and Engineering, Shimane University, Japan

Javkhlan Otgonkhuu

July, 2014

Supervisor: Prof. Dr. Akira Takasu

Abstract

Chandman district is located in the southeast part of Lake Zone, SW Mongolia, which is situated in the Central Asian Orogenic Belt. Chandman district consists of four major geologic units, i.e. Neoproterozoic ophiolites of Khantaishir Formation, eclogite-bearing orthogneisses of the Alag Khadny metamorphic complex, marbles of the Maykhan Tsakhir Formation, which lie in contact with eclogite bodies, and the basement block of the Zamtyn Nuruu Formation.

Eclogites in the Chandman district have two modes of occurrences, i.e. lenses and boudins of eclogites surrounded by orthogneisses of the Alag Khadny metamorphic complex (eclogite-1) and eclogites in marbles of the Maykhan Tsakhir Formation (eclogite-2). The marbles contain small lenses of garnet-chloritoid schists, which occur close to a body of eclogite-2. Eclogite-1 is intruded by veins of orthogneisses.

Eclogite-1 consists mainly of porphyroblastic garnet (<2 mm), clinopyroxene (omphacite, aegirine-augite), sodic, sodic-calcic, and calcic amphiboles (glaucophane, taramite, barroisite, winchite, pargasite, tschermakite, Fe/Mg-hornblende, and actinolite) with minor amounts of epidote, phengite, paragonite, plagioclase, biotite, K-feldspar, rutile, titanite, quartz, calcite, hematite, ilmentite and zircon. Eclogite-2 consists mainly of garnet (<0.3 mm), omphacite, and minor amounts of sodic-calcic calcic amphiboles (barroisite, Mg-taramite, tschermakite, pargasite, Mg-hornblende and actinolite), epidote, paragonite, plagioclase, chlorite, calcite, biotite, quartz, titanite and rutile.

Both eclogites (eclogite-1 and -2) experienced four metamorphic events i.e. precursor metamorphism (M1) of high-temperature amphibolite facies; high-pressure metamorphism (M2)

of the eclogite facies; and medium-pressure metamorphism (M3) of the epidote-amphibolite facies. Some of eclogite-1 does not preserve the evidence of M3 metamorphism.

M1 event indicate an early and relatively high-temperature metamorphism before the eclogitic metamorphism. Porphyroblastic garnets of eclogite-1 show a prograde zoning. The core of the garnets contains polyphase and discrete grain inclusions of high TiO_2 (up to 1.32%) taramite, Fe-pargasite, tschermakite, aegirine-augite (Jd=13) + taramite + quartz, plagioclase (An<19) + biotite + epidote. Those inclusions indicate relatively high-temperature metamorphism of amphibolites facies conditions (M1).

M2 event with prograde and peak stages of metamorphism represents relatively high pressure and low temperature metamorphism of the blueschist to eclogite facies, causing continuous subduction resulted in cooling of the hangingwal after the initial early M1 event. The prograde and peak stages of the high-pressure metamorphic event (M2) is characterized by cores of glaucophane in barroisites and coexisting assemblage of rim of garnets, omphacite (Jd<46%), phengite (6.51-7.11), barroisite, rutile and quartz, respectively. THERMOCALC (v.3.33) calculations for the peak stage of eclogite yielded P-T conditions of 565 ± 69ºC and 22.5 ± 2.6 kbar. The retrograde stage of M2 is characterized by symplectite of sodic plagioclase (An=1-18) + amphibole ± Na-poor clinopyroxene (Jd=2-25). These mineral assemblages give 450-560°C and 4-11 kbar.

M3 event is represents medium pressure metamorphism. The M3 metamorphism is characterized by prograde zoned amphiboles with winchite, actinolite, tremolite core and barroisite rim. Large prograde zoned poikiloblastic barroisitic amphibole also developed in the eclogite-2. They contain inclusions of garnet, omphacite and symplectite of amphibole + clinopyroxene+sodic plagioclase suggesting that the amphiboles crystallized after the M2

metamorphism. The cores of the amphiboles indicate 300-400°C and 3-8 kbar, whereas the rims indicate >400-600ºC and 3-12 kbar.

Garnet-chloritoid schists consist mainly of garnet, chloritoid, phengite, chlorite and quartz, with minor amounts of kyanite, rutile, and zircon. Prograde zoned garnet and associated minerals suggest that garnet-chloritoid schists experienced pre-peak (500-510°C and 7-8 kbar) and peak stages (560-590°C and 10-11 kbar) of medium-pressure metamorphism, corresponding with M3 metamorphism of eclogites (-1 and -2).

The fourth metamorphic event (M4) defined in the amphibolized eclogites-1 can be corresponding with metamorphism of the vein-type orthogneisses which suffered two metamorphic events, i.e., first (M1) greenschist facies metamorphism (~380°C and 3 kbar), second (M2) amphibolite facies metamorphism (~500°C and 4 kbar). The P-T conditions of peak stages of M1 and M2 for vein-type orthogneiss correspond to geothermal gradients of ~35 °C/km and ~30 °C/km, respectively. The peak temperature conditions of M2 event (~ 500 °C) for the vein-type orthogneiss are lower than peak temperature of M4 metamorphic event of intruded amphibolized eclogites-1 (550-640 °C) whereas the pressure conditions of vein-type orthogneiss (4 kbar) correspond with peak pressure of M4 for amphibolized eclogites-1 (2-5 kbar). This feature suggests that geothermal gradient of M4 metamorphic event of amphibolized eclogites-1 same as vein-type orthogneiss.

Trace elements of Ba, Ce, Nb, Sc, Sr, Y and Zr contents of eclogites are comparable with MORB compositions. Major and trace element compositions of eclogites are comparable with ophiolitic metabasalts of Khantaishir Formation. Khantaishir metabasalts are plotted in the field of calc-alkaline series by AFM diagram.

We obtained K-Ar ages of c. 500-480 Ma from the vein-type orthogneiss intruded into eclogite-1 as well as c. 500-460 Ma from the orthogneisses surrounding eclogite bodies. These ages indicate that an exhumation ages of eclogite-1 and vein-type orthogneisses.

Based on the textural and geochronoligical evidence, after the exhumation of eclogite blocks which were decoupled from subducted oceanic slab, eclogites were suffered by the medium-pressure prograde collisional metamorphism (M3) together with garnet-chloritoid schists. Metamorphosed orthogneisses intruding into and surrounding eclogite-1 suggest the M4 event of low-pressure metamorphism took place during the collision, and subsequent exhumation at c. 500-460 Ma.

The P-T-t evolution of the Chandman metamorphic rocks reconstructs the entire tectonic sequence from initiation of subduction (M1 and M2) to collision events (M3 and M4).

CONTENTS

CHAPTER 1 INTRODUCTION

1.1 Geological framework of Mongolia

Mongolia is composed of a number of tectonic zones situated within the Central Asian Orogenic Belt (CAOB: Mossakovsky et al., 1994; Jahn et al., 2000, 2004) or the Altaids (Şengör et al., 1993; Şengör and Natal'in, 1996). The CAOB developed among the Siberian craton in the north, the Tarim craton in the south-west, and the North China craton in the south (Fig. 1.1a; Jahn et al., 2000). Tectonic evolution of the CAOB suggests that it probably represents a long-lived accretionary complex related to subduction of the North China oceanic plate beneath the Siberian craton, closure of the Palaeo-Asian ocean between the continents, and final collision of the Tarim and North China cratons during the Permian (Ao et al., 2010; Xiao et al., 2010, and references therein; Glorie et al., 2011; Rojas-Agramonte et al., 2011). Several tectonic models have been proposed for formation of the CAOB. These include presence of a long-lived single subduction system (Şengör and Natal'in, 1996), operation of several subduction systems with different polarities and collision of various microcontinents (Coleman, 1989; Mossakovsky et al., 1994; Xiao et al., 1994); involvement of a ridge-subduction system (Kovalenko et al., 1995; Windley et al., 2007), and occurrence of huge chains of double arc-backarc pairs (Yakubchuk, 2004). However, the detailed tectonic interpretation remains controversial.

Mongolia is traditionally subdivided into northern and southern domains. These domains are separated by a major fault, the Main Mongolian lineament (MML). The MML is a regional structural boundary separating mainly Precambrian and Lower Palaeozoic rocks in the north from Middle to Upper Palaeozoic rocks in the south (Badarch et al., 2002) (Figs. 1.1b and 1.2).

The western part of the northern domain contains a roughly 1,000 km long island arc terrane known as the Lake Zone. The arc is composed of several pre-Cambrian ophiolites, such as the Khantaishir ophiolites associated with the Dzabkhan-Baydrag basement block (Badarch et al., 2002) (Fig. 1.1b). Chandman district in the Lake Zone contains mainly of eclogite-bearing orthogneisses of the Alag Khadny metamorphic complex interleaving metacarbonate rocks with lenses of eclogite and garnet-chloritoid schist of the Maykhan Tsakhir Formation. Whole sequences associated with ophiolites of Khantaishir Formation in the north and basement block of Zamtyn Nuruu Formation in the south.

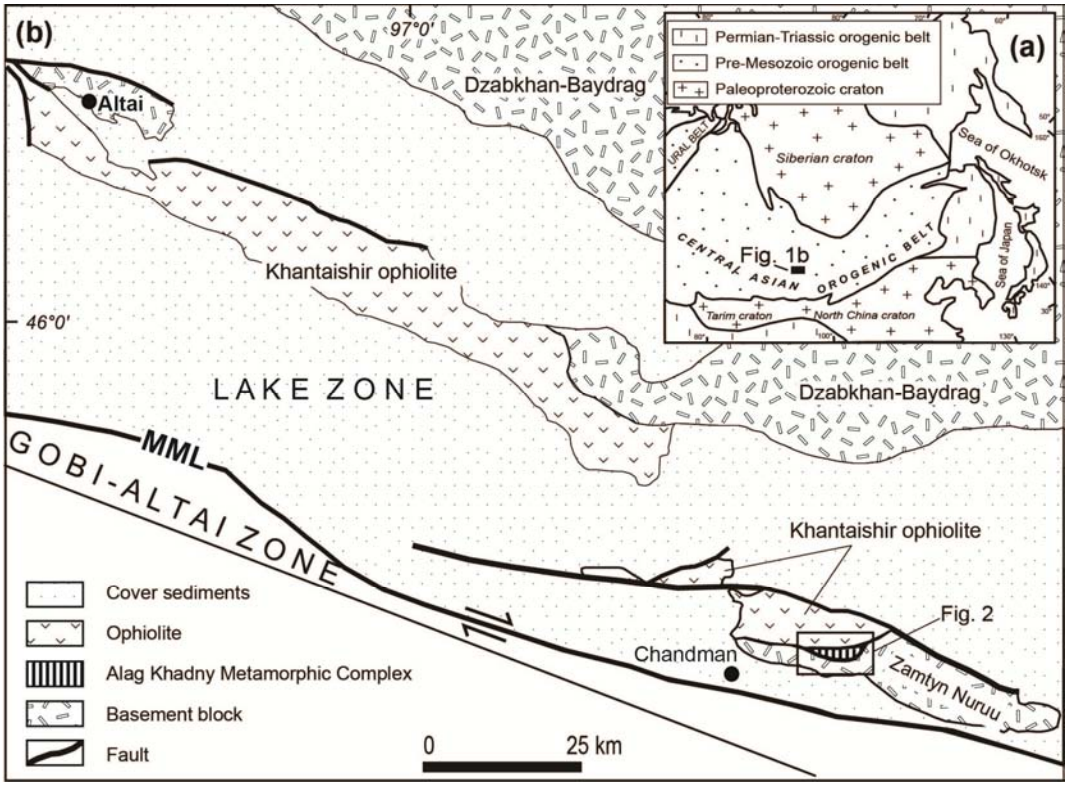

Fig. 1.1 (a) simplified tectonic map of the Central Asian Orogenic belt and adjacent cratons (modified after Jahn et al., 2000). (b) Simplified tectonic sketch map of the Lake Zone

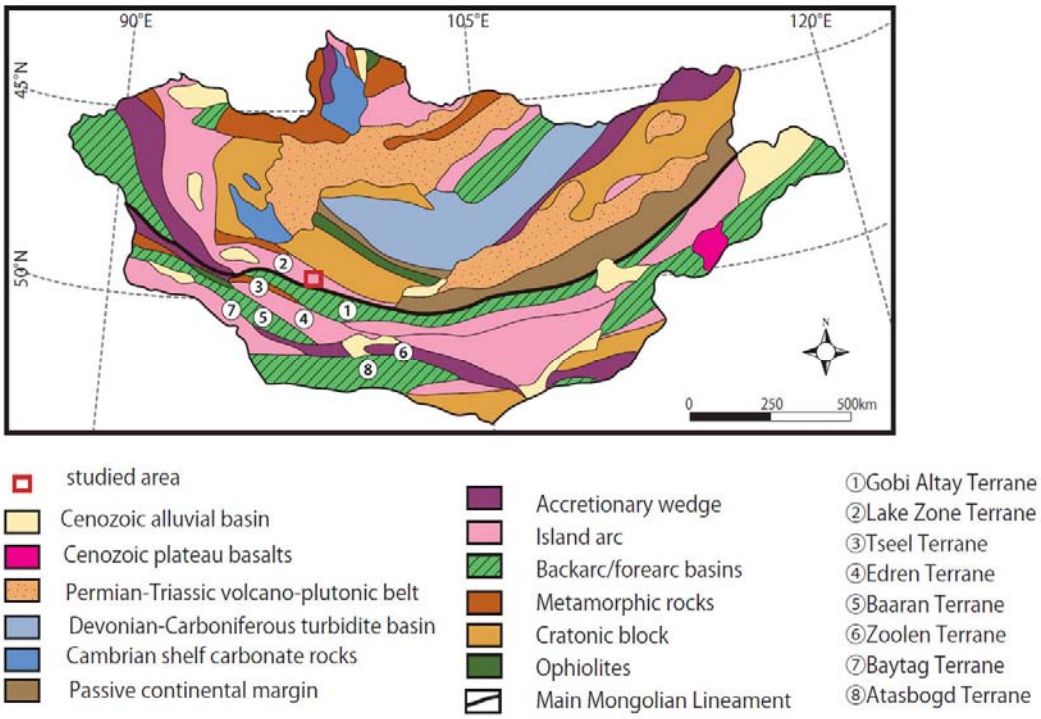

Fig. 1.2 Terrane map of Mongolia (Badarch et al., 2002)

1.2 Previous work

The general geology and tectonics of the Lake Zone have been investigated during regional geological mapping, studies of magmatism, metamorphism and geochronology.

Geological mapping works at 1:200,000 and 1:50,000 scales was completed (Rauzer et al., 1987 and Hanžl and Aichler, 2007, respectively) in the Chandman district. The geological maps revealed new systematic regional and stratigraphic classification of all geological formations occurring in the study area.

Hanžl and Aichler (2007) first time distinguished newly defined eclogites-bearing Alag Khadny metamorphic complex, Zamtyn Nuruu Formation and Maykhan Tsakhir Formation from the Khantaishir Formation.

Eclogites were first time reported (Hanžl and Aichler, 2007; Takasu et al., 2008). Štípská et al. (2010) determined the peak mineral assemblage of eclogite (garnet + omphacite + amphibole + rutile + quartz ± muscovite ± epidote) and amphiboles are zoned with winchite core and barroisite rim, but rarely reached tschermakitic composition at some of rim. The peak metamorphic conditions were estimated to be high P/T conditions of 590-610 °C and 20-22.5 kbar and decompressed at conditions of 600-630°C by peak eclogitic minerals and that of tschermakitic amphiboles, respectively (Štípská et al, 2010).

The whole rock composition of the eclogites represents an affinity to T-MORB of magmatic protolith. The protolith of the garnet-chloritoid schists is considered to have been sedimentary rocks derived from the continental crust, based on bulk rock compositions rich in K_2O (~3 wt%) and Al_2O_3 (~20 wt%) (Štípská et al., 2010).

$^{40}Ar/^{39}Ar$ muscovite plateau ages of the eclogite (543 ± 3.9 Ma), garnet-chloritoid schists (537 ± 2.7 Ma) (Štípská et al., 2010) and orthogneiss (573 ± 15 Ma) (Lehmann et al. 2010) have been reported, and are interpreted as the timing of cooling after their peak metamorphism.

Garnet-chloritoid schists were explained that they were formed together with eclogites by the subduction and exhumed simultaneously at c. 540 Ma (Štípská et al., 2010). Štípská et al. (2010) pointed out that the Alag Khadny eclogites record the presence in the CAOB of an Early Cambrian long-distance subduction system extending through the Gorny Altay (650-630 Ma; Buslov et al., 2001) and the Kokchetav subduction-collision zone (c.510 Ma; e.g. Katayama et al., 2001).

1.3 Aims and significance of the study

The following studies to aim for discuss metamorphism and tectonic relationships of eclogites and associated metamorphic rocks in the Chandman district, Lake Zone, SW Mongolia: (i) to clarify the metamorphism and timing evolutions of eclogites; (ii) to determine the precise metamorphic and timing evolutions of metamorphic rocks (such as orthogneisses and garnet-chloritoid schists) closely associated with eclogites bodies; (iii) to determine metamorphic and whole-rock compositions of ophiolite rocks of Khantaishir Formation and compare with eclogites of Alag Khadny metamorphic complex.

The determination of metamorphic and tectonic relationship of eclogites and associated metamorphic rocks are significant for providing better understanding of tectonic implications of the Chandman district and Lake Zone and understanding of subduction process and subsequent collisional metamorphism.

CHAPTER 2 GEOLOGICAL SETTING

2.1 General geology of Lake Zone

The Lake zone corresponds to the Lake terrane exhibiting island arc features in the terrane classification by Badarch et al., 2002 (Fig. 1.2). The Lake Zone is composed of slightly metamorphosed volcano-sedimentary sequences of Proterozoic to Lower Palaeozoic ages, which alternate in tectonic mosaic with highly metamorphosed rocks (such as eclogite) with relics of oceanic crusts (ophiolite). The Permian volcanic and volcano-sedimentary sequences cover the Lower Palaeozoic rocks. They are tectonically incorporated into the structure of the Lake Zone along its southern boundary (Hanžl and Aichler, 2007).

2.2 Geology of Chandman district

The Chandman district is located in the southeast part of the Lake Zone (Fig. 1.1b), and is composed of four major geologic units. Neoproterozoic ophiolites of the Khantaishir Formation occur in the north. High-pressure metamorphic rocks including eclogites of the Alag Khadny Metamorphic Complex are interleaved with Maykhan Tsakhir Formation marbles in the central part of the district, and the Zamtyn Nuruu Formation crops out in the south (Fig. 2.1).

The Zamtyn Nuruu Formation consists mainly of migmatized orthogneiss, amphibolites, metagabbro and paragneiss. Plutonic rocks intruded into the Zamtyn Nuruu Formation. Based on a concordia intercept age of 950 ± 16 Ma obtained from orthogneiss, the Zamtyn Nuruu Formation has been interpreted as a basement block (Kröner et al., 2010).

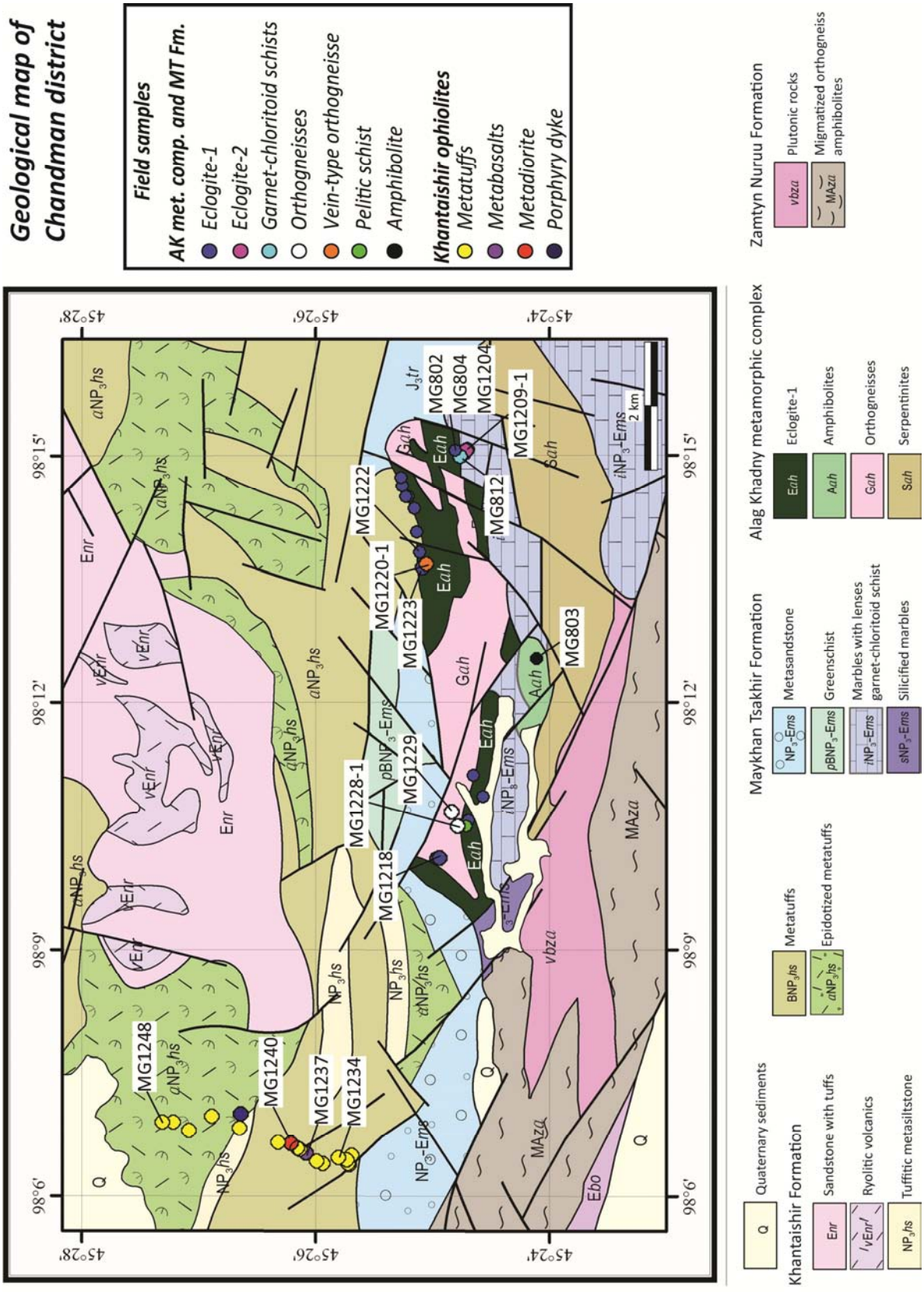

Fig. 2.1 Geology map of Chandman district (after Hanžl and Aichler, 2007). Field localities of samples collected from Alag Khadny metamorphic complex (AK met.comp.), Maykhan Tsakhir Formation (MT Fm.) and Khantaishir Formation (ophiolites). K-Ar ages obtained from samples of eclogites (MG1218 and MG1222) and orthogneisses (MG1220-1, MG1228-1 and MG1229). Sm-Nd analysis conducted in the eclogite sample of MG1223.

This age corresponding that U-Th-Pb dating from oscillatory zoned core of zircon age given 941 ± 11 Ma, whereas the coarse zoned overgrown rim given 514.4 ± 7.4 Ma. U-Th-Pb zircon ages of 542±4 Ma (diorite) and 517±7 Ma and 511 ± 5 Ma(granite), and monazite age of 513 ± 5 Ma have also been determined for plutonic rocks of the Zamtyn Nuruu Formation (Hanžl and Aichler, 2007; Hrdličková et al., 2010). The Zamtyn Nuruu Formation is over-thrusted by both the Alag Khadny Metamorphic Complex and the Maykhan Tsakhir Formation, which themselves are over-thrusted by the Khantaishir Formation (Fig. 2.1) (Lehmann et al., 2010).

The ophiolites of the Khantaishir Formation consists various types of metabasalts, greenschists and metatuffs with lenses of limestones. Ophiolites are originated as a supra-subduction island arc (Zonenshian and Kuzmin, 1978; Khain et al., 2003) or an intra-oceanic island arc complex (Matsumoto and Tomurtogoo, 2003), which was emplaced onto continental crust. Khantaishir plagiogranites have yielded concordia intercept age of 568±4 Ma (Gibsher et al., 2001). However, Jian et al. (2014) obtained distingtly young $^{206}Pb/^{238}U$ zircon ages of c. 520 Ma from the layered gabbro and the leucogabbro of ophiolitic Khantaishir Formation.

The Alag Khadny metamorphic complex consists of metamorphic rocks and ultramafic bodies, is exposed in a belt extending between the Ulaan Tsakhir Mountain and Alag Khadny Mountain (Fig. 2.1). It forms about 10 km long and up to 4 km wide, E-W oriented, belt between the Khantaishir Formation in the north and the Zamtyn Nuruu Formation and the maykhan Tsakhir Formation in the south. Contacts of all these units are tectonic or tectonized. A series of steep faults separates this complex from the Zamtyn Nuruu metamorphic complex, whereas the Khantaishir Formation is thrust over the Alag Khadny metamorphic complex. Maykhan Tsakhir Formation interleaving with Alag Khadny metamorphic complex

and both units are interpreted as a tectonic mélange (Hanžl and Aichler 2007) (Fig. 2.1). The Alag Khadny metamorphic complex subdivided into the three different parts, (i) orthogneisses with intercalations of pelitic schist. This sequence contains large boudins of eclogite. Some of orthogneisses are intruded into eclogite bodies as veins, (ii) amphibolites bodies tectonically incorporated in limestones of the Maykhan Tsakhir Formation and (iii) serpetinite bodies (Fig. 2.1).

The Maykhan Tsakhir Formation is predominately metacarbonate rocks (marble) accompanied by bodies of volcaniclastic rocks, and is interleaved with the Alag Khadny Metamorphic Complex (Hanžl and Aichler, 2007). Marbles in the Maykhan Tsakhir Formation is considered as former passive margin sediment (Rauzer et al., 1987) scontain lenses of garnet-chloritoid schists (1-2 m in length and ~0.5 m in width), located close to the contact with the eclogite body (Fig. 2.1).

2.3 Field relations of eclogites and associated rocks of Chandman district

Large lenticular-shaped (max. 2 km x 0.8 km) eclogitic bodies occur within orthogneisses and minor pelitic schists of the Alag Khadny metamorphic complex (Figs. 2.1 and 2.2). Marbles of the Maykhan Tsakhir Formation are intercalated some of the large eclogite boudins (Figs. 2.1 and 2.3). At the contact zone between marbles and large eclogite bodies, small lenses of eclogite occur within marbles. Most of bodies are strongly amphibolized, though; fresh massive eclogites are commonly preserved in the interiors of the amphibolized eclogitic bodies (Fig. 2.1). Various veins (from 1 mm to 40 cm in width) of amphibole-, calcite-, chlorite-, K-feldspar-rich veins and vein-type orthogneisses (Fig. 2.2) are developed in eclogite bodies. According to the field studies, eclogites thus have two modes of occurrences, i.e., large blocks of eclogites surrounded and intruded by orthogneisses (eclogites-1) (Fig.

2.2) and small lenses of (up to 0.5 m across) eclogites within marbles (eclogites-2) (Fig. 2.3).

Various types of low to high grade pelitic rocks occur within Alag Khadny metamorphic complex and Maykhan Tsakhir Formation. Orthogneisses surrounding eclogite bodies intercalate pelitic schists and some of pelitic schists enclosed eclogite bodies. Eclogite bodies are also locally intercalated thin layer (~ 40 cm) of garnet-phengite schists close to the contact zone with marbles (Fig. 2.3). Marbles itself contain lenses of garnet-chloritoid schists (1-2 m in length and ~0.5 m in width) which are close to the eclogite lenses within marbles (Fig. 2.3).

Large sequences of various types of metatuffs of the ophiolitic Khantaishir Formation which are strongly chloritized and epidotized occurred in the north. They are tectonically overlying on eclogites-bearing orthogneisses. Metatuffs locally contain metabasalts and metadiorite, intruded by porphyry dykes (Fig. 2.4).

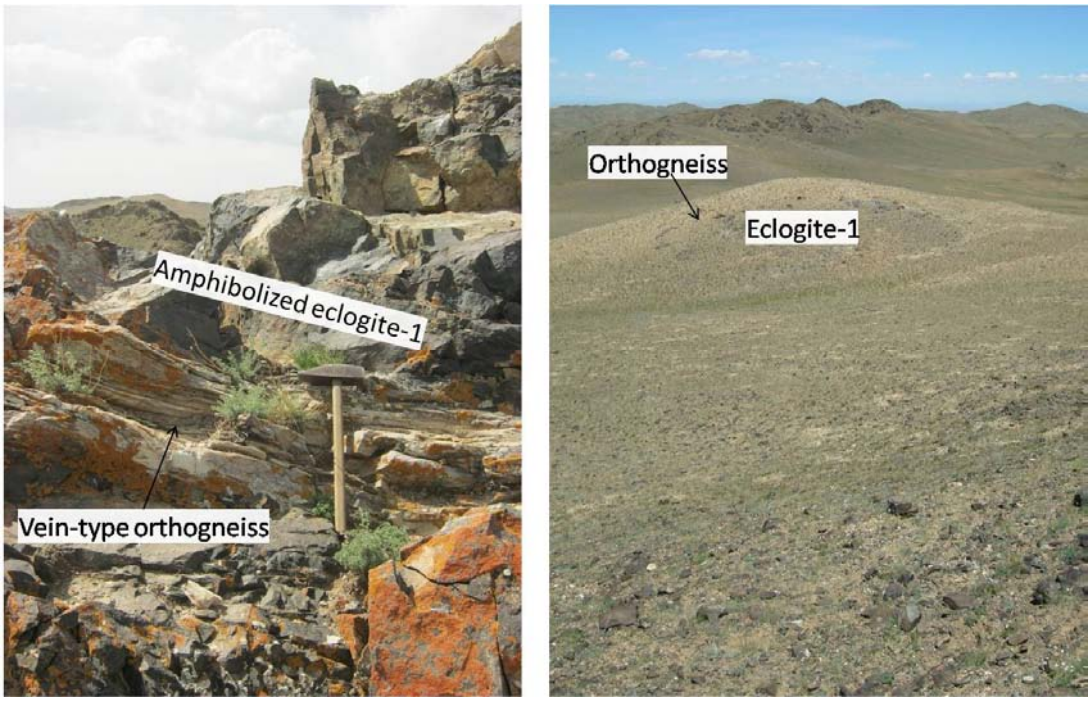

Fig. 2.2 (a) Orthogneiss vein outcrop in the eclogite body (MG1220-1) and (b) the orthogneiss surrounding eclogite body (MG1228-1) in the Alag Khadny metamorphic complex, Lake Zone.

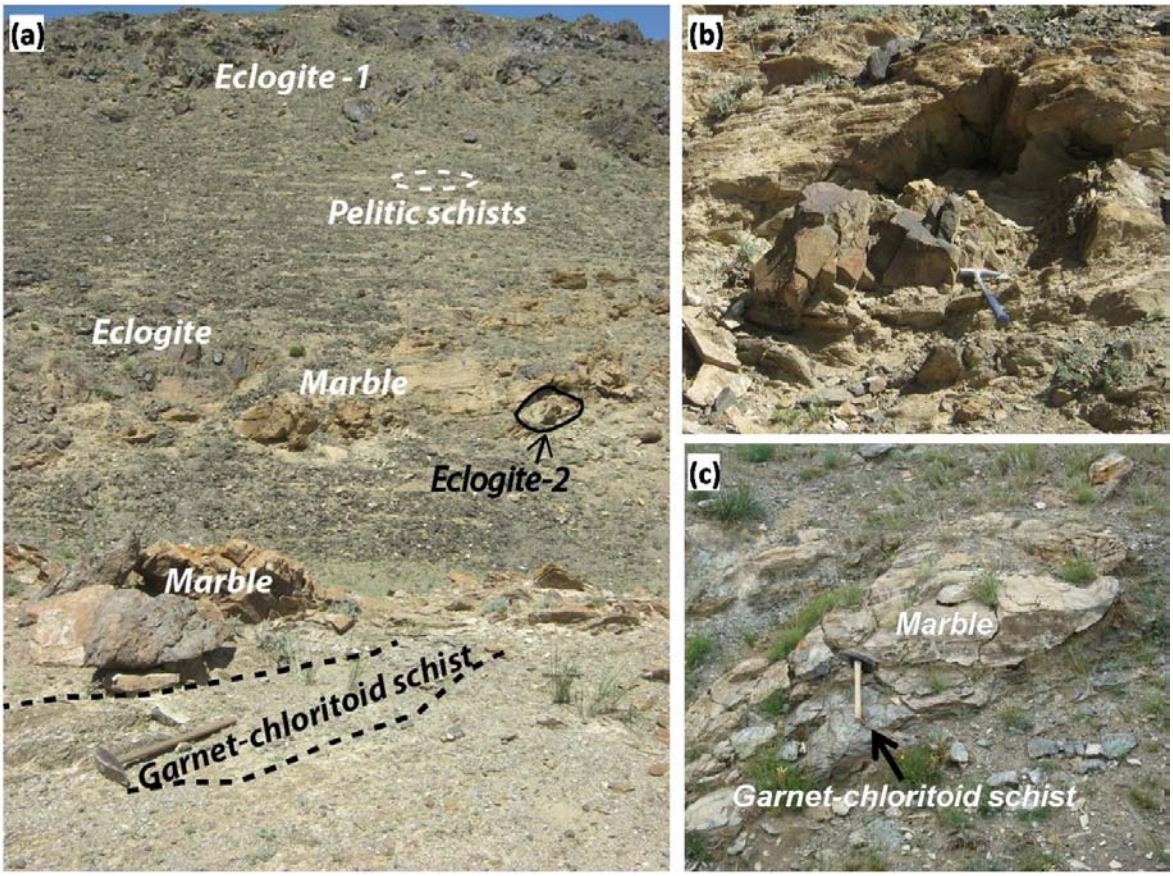

Fig. 2.3 Field photos of boundary zone between large eclogites boudin and intercalated marbles. (a) Intercalation of large boudin of eclogites-1 and marbles. Eclogite-1 intercalated with garnet-phengite schists (samples of MG1204 and MG1207 were collected). At the boundary zone marbles contain small lense of eclogites-2 (sample MG1209-2; zoomed photo shown at photo b) and lenses of garnet-chloritoid schists (samples of MG806 and MG812 were collected). (b) Small lense of eclogites-2 enclosed by marbles (sample MG1209-2). (c) Lens of garnet-chloritoid schist wihin marble (sample MG812).

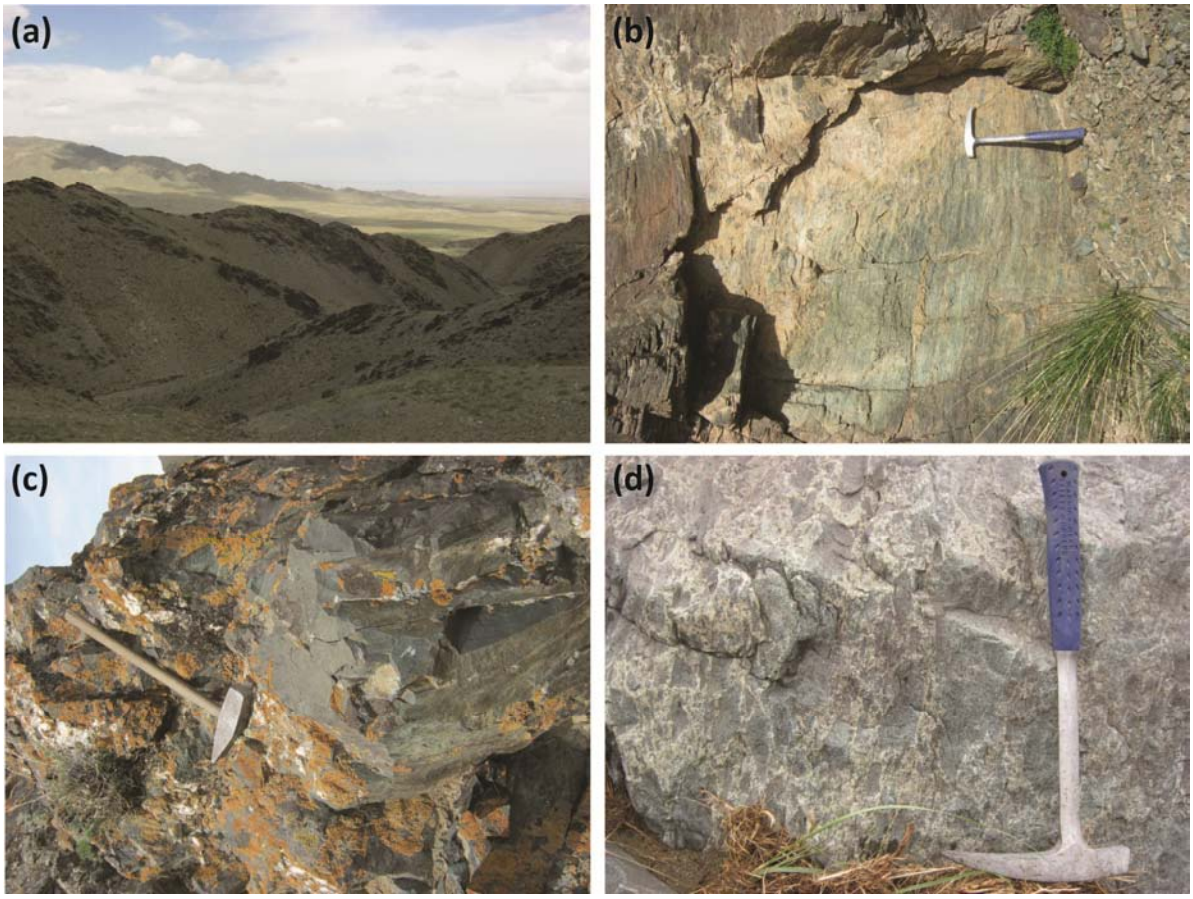

Fig. 2.4 Field photos of Khantaishir ophiolitic Formation. (a) View of the sequence of Khantaishir metatuffs with minor metabasalts and metadiorites looking north-northeast. The main section with sample collections was conducted along this valley. (b) The foliated metatuffs which are strongly chloritized and epidotized. (c) The massive metabasalt outcrop. (d) Volcanic breccia is created by fracturing existing rock during the intrusion of fresh magma.

2.4 Field sampling

Totally seventy one samples were collected from Alag Khadny metamorphic complex, Maykhan Tsakhir Formation and Khantaishir ophiolite Formation.

Fiftheen eclogite samples have been described petrologically. Fourteen samples collected from the large eclogite bodies (eclogite-1) within the orthogneisses and one sample described (eclogite-2) within marbles. Collected eclogite samples are slightly to intensely amphibolized. One amphibolite sample was collected from amphibolite body within marble. Two samples from orthogneisses surrounding eclogite bodies and one sample from the vein-type orthogneiss in the eclogite bodies. One samples of pelitic schist intercalated with orthogneisses were collected. Two samples of garnet-phengite schists intercalating with eclogites and two samples of garnet-chloritoid schist within marbles were collected. Twelve samples of metatuffs, two samples of metabasalts, three samples of metadiorite and two samples of porphyry dikes were collected from the Khantaishir ophiolitic complex. Representive samples with their numbers and localities shown in the Fig. 2.1.

CHAPTER 3 PETROGRAPHY

3.1 Eclogites

3.1.1 Eclogite-1 surrounded by orthogneisses

Eclogite-1 consists mainly of garnet, clinopyroxene, and sodic, sodic-calcic, and calcic amphiboles (glaucophane, taramite, barroisite, winchite, pargasite, tschermakite, hornblende, actinolite) with subordinate amounts of epidote, phengite, paragonite, plagioclase (An1-17), biotite, chlorite, K-feldspar, rutile, titanite, quartz, calcite, hematite, ilmenite, and zircon (Table. 3.1). Amphibole (barroisite, pargasite, tremolite) -rich veins (up to 0.3-5 mm in width) which are occur parallel or subparallel to the schistosity of the eclogite, and veins consisting of prehnite, albite, K-feldspar, calcite and quartz bearing veins are developed in eclogite bodies (Fig. 3.2).

Table 3.1. Representative mineral assemblage of eclogites-1 and eclogites-2. +++, rich; ++, common; +, poor.

Rock type	Eclogites-1 within orthogneisses													Eclogite-2 within marbles
Sample No.	MG801	MG802	MG804	MG818	MG821	MG822	MG823	MG829	MG1218	MG1220-2	MG1222	MG1223	MG1228-3	MG1209-2
Garnet	+++	+++	+++	+++	+++	+++	+++	+++	+++	++	+++	+++	+++	+++
Omphacite	+++	+++	+++	++	++	++	+++	++	++	+	+	+++	++	+++
Na-amphibole		+												
Na-Ca amphibole	+++	+++	+++	+++	+++	+++	+	+++	+++	+	++	+++	++	+
Ca amphibole	+++	+++	+++	+++	+++	+++	+	+++	+++	+++	+++	++	+++	+
Phengite	++	+	+	+	+	+	+	+	+			+		
Chlorite	++	++	++	++	++	++	+	++	++	++	++	++	++	+
Epidote	+	++	+	++	++	++	+	++	++	++	+	+	++	+
Paragonite														+
Plagioclase	++	++	++	++	++	++	++	++	++	+++	++	++	++	+
Biotite		+	+											+
K-feldspar	+	+	+	+	+	+	+	+	+			+		
Rutile	+	+	+	+	+	+	+	+	+	+	+	+	+	+
Titanite	+	+	+	+	+	+	+	+	+	+	+	+	+	+
Quartz	++	++	++	++	++	++	++	++	++	+	++	++	++	+
Hematite	+	+	+	+	+	+	+	+	+	+	+	+	+	+
Calcite	+	+	+	+	+	+	+	+			+	+	+	+
Ilmenite	+	+	+	+	+	+	+	+	+	+	+	+	+	+
Zircon	+	+	+	+	+	+	+	+	+	+	+	+	+	+
Apatite	+	+	+	+	+	+	+	+	+	+	+	+	+	+

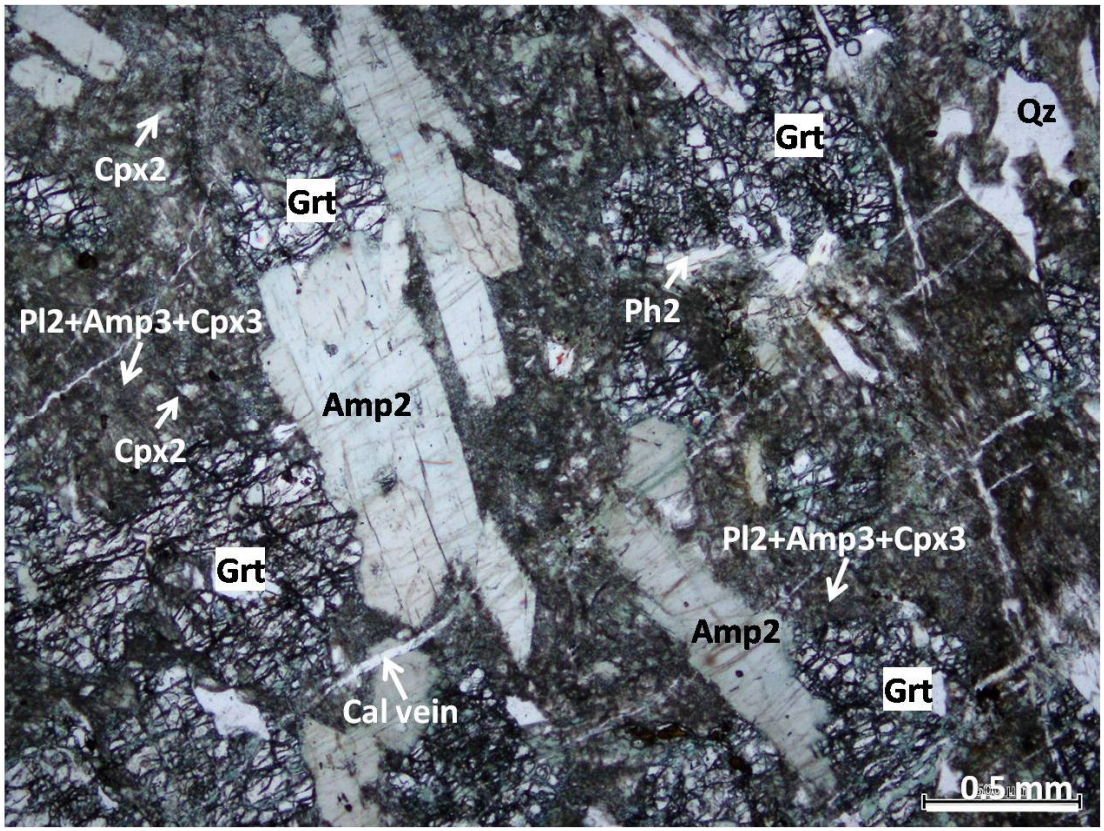

Fig. 3.1 Photomicrograph of eclogite-1 (MG1218). Garnet (brownish), Amp2 (barroisite), Ph2, Cpx2 (omphacite) and symplectite of Pl2+Amp3+Cpx3 after Cpx2. Most of Cpx2 consumed into symplectites. Cpx2 and Amp2 have a preferred orientation (S_e).

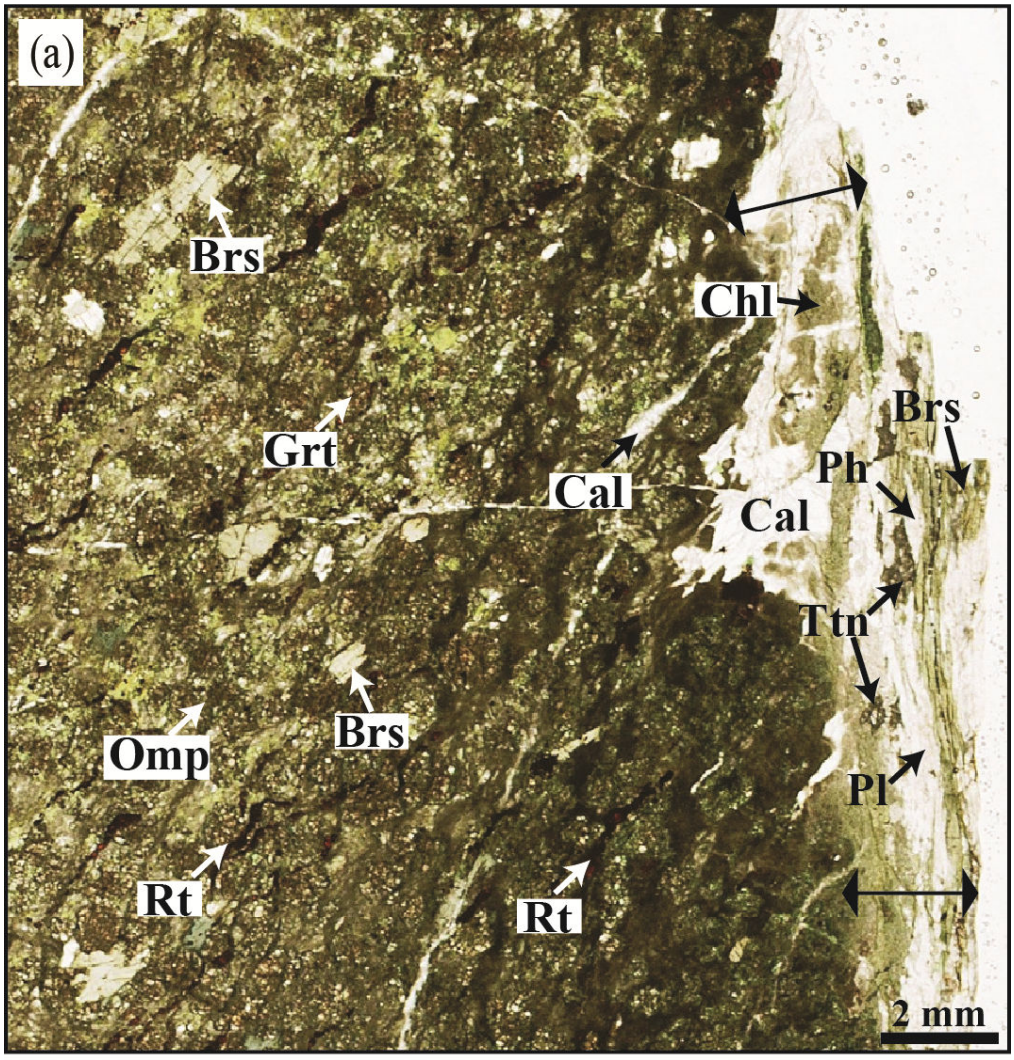
(a)
Brs
Chl
Brs
Grt
Cal
Ph
Cal
Ttn
Omp
Brs
Pl
Rt
Rt
2 mm

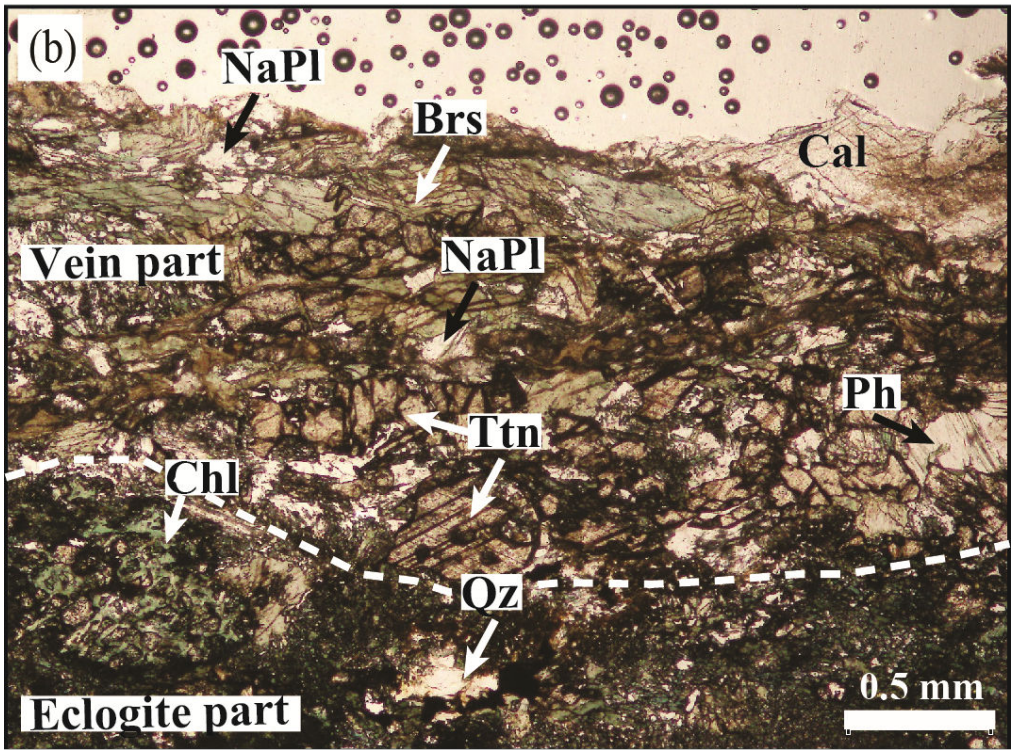
(b)
NaPl
Brs
Cal
Vein part
NaPl
Ph
Ttn
Chl
Qz
Eclogite part
0.5 mm

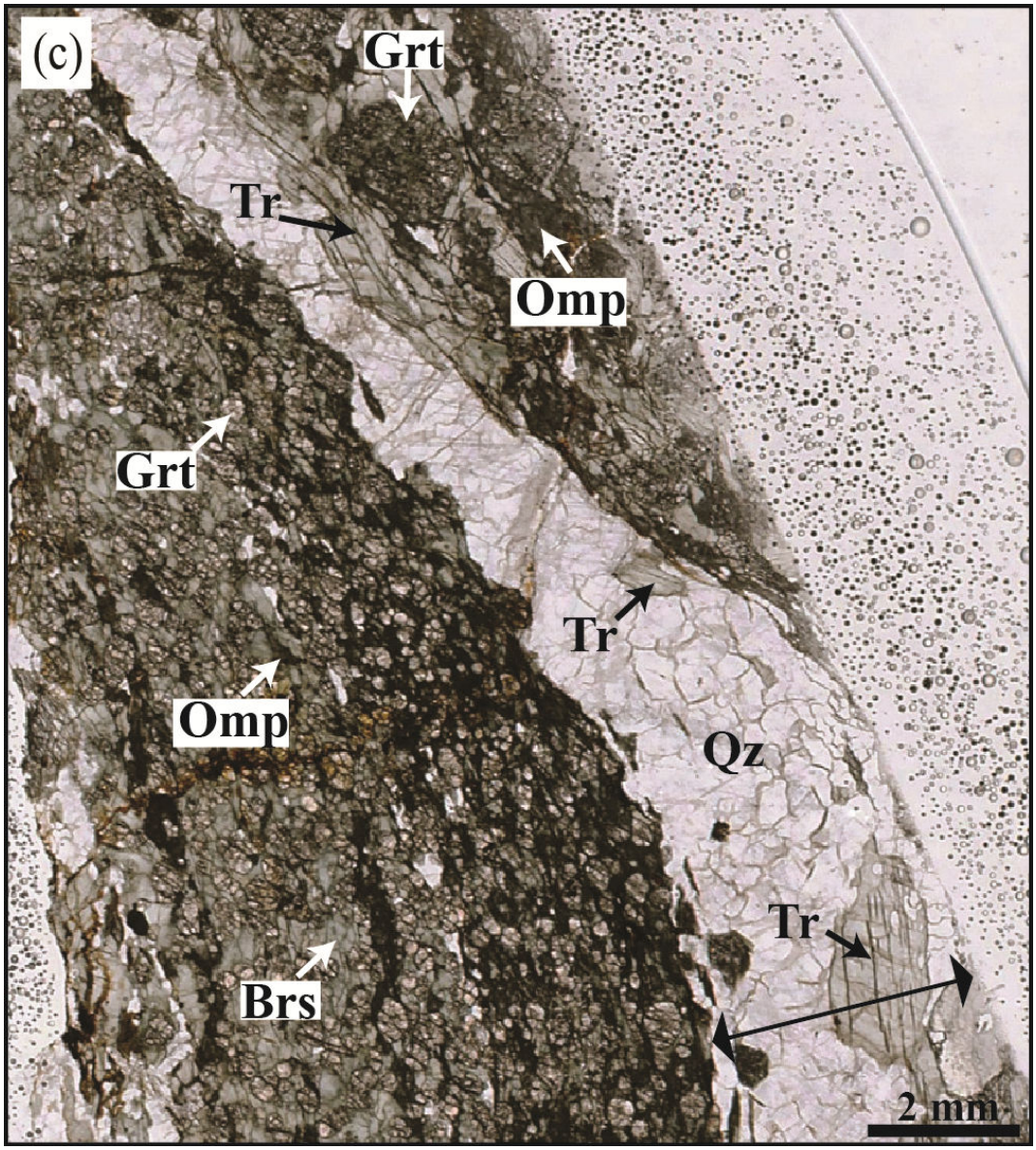

Fig. 3. 2 Microphotopgraph of amphibole-rich veins in the eclogite matrixes. Veins are indicated by double-headed arrows. (a) Amp-NaPl-Ph vein. The vein intruded slightly oblique to the schistosity of the host eclogites (MG1218). (b) Aggregates of barroisitic amphibole, na-plagioclase, phengite, titanite, and calcite in the Amp-NaPl-Ph vein part. In the eclogites part, chlorites strongly replaced garnet grain. Matrix part of eclogites mainly consists of small grain symplectites of plagioclase (Pl2) Amp3 and Cpx3 (MG1218). (c) amp-Qz vein (MG1222).

A schistosity (Se) is defined by preferred orientation of amphibole, epidote, and omphacite. The orientation of inclusions in the porphyroblastic garnet (Si) is oblique comparing to Se (Fig. 3.3).

Garnets occur as euhedral to subhedral porphyroblasts, and their maximum size up to 2 mm across. Sometimes along the fracture of garnet, it is filled by albite (An1-5), K-feldspar, epidote, and chlorite. Garnets consist of inclusion-rich core and inclusion-poor rim (Figs 3.3 and 3.4).

Garnets contain inclusions of polyphase and single grain inclusions in the core and the rim (Table 3.2). The core of the garnet contains polyphase inclusions of Na-Ca amphibole (taramite, Mg-taramite, Fe-barroisite, Fe-pargasite) +quartz ± rutile, Mg-taramite + actinolite + quartz, aegirine-augite (Jd13) + taramite+quartz, aegirine-augite (Jd=14-16) + omphacite (Jd=20-21) + plagioclase (An=1-2) + Fe-tschermakite, epidote+albite (An2-5), biotite + oligoclase (An<17) + epidote, epidote + quartz, albite (An4-5) + calcite and single grained inclusions of taramite, Fe-barroisite, Fe-pargasite, tschermakite, Fe-tschermakite, quartz, epidote, K-feldspar, rutile and titanite (Table. 3.2, Figs. 3.4, 3.5, 3.7, 3.8). The rim of the garnet contains as polyphase inclusions of taramite + Mg-taramite + omphacite (Jd40) + rutile + quartz, taramite + omphacite (Jd41) + rutile, barroisite + omphacite (Jd37), edenite + omphacite (Jd32) and single grained inclusions of taramite, barroisite, omphacite (Jd<39), phengite, quartz, epidote, rutile, and titanite (Table 3.2; Figs. 3.7 and 3.8).

Table 3.2. Polyphase and single grains of inclusions in the garnet and amphiboles of eclogite

<table>
<tr><th colspan="2">Garnet porphyroblast</th><th rowspan="2">Porphyroblastic amphibole (Amp4)</th></tr>
<tr><td>Core</td><td>Rim</td></tr>
<tr><td colspan="3">Polyphase inclusions</td></tr>
<tr><td>taramite + quartz
Mg-taramite + Fe-actinolite + quartz
Fe-barroisite + quartz
Fe-pargasite + quartz</td><td>taramite +Mg-taramite + omphacite (Jd_{40}) + rutile + quartz
taramite + omphacite (Jd_{41}) + rutile,
Edenite + omphacite (Jd_{32})
Mg-Katophorite + omphacite (Jd_{36})
Barroisite + omphacite (Jd_{35})</td><td rowspan="10">Omphacite (Jd_{30-42}) + symplectite of clinopyroxene (Jd_{2-12}) + plagioclase (An_{1-12})</td></tr>
<tr><td colspan="2">biotite+oligoclase (An_{2-17}) + epidote
biotite + titanite
biotite + rutile + quartz
aegirine-augite(Jd_{13}) + taramite + quartz
aegirine-augite (Jd_{14-16}) + omphacite (Jd_{20}) + Fe-tschermakite + albite (An_2)
oligoclase (An_{14}) + chlorite + titanite
albite (An_{3-5}) + calcite
Epidote + albite (An_{2-5})
epidote + quartz</td></tr>
<tr><td colspan="3">Single grain inclusions</td></tr>
<tr><td>Core</td><td>Rim</td><td>Porphyrblastic amphibole (Amp4)</td></tr>
<tr><td>taramite, Fe-barroisite, tschermakite, Fe-tschermakite, pargasite, Fe-pargasite, epidote, quartz, rutile, titanite, chlorite, K-feldspar</td><td>taramite, Fe-barroisite, barroisite, Fe-pargasite, phengite, omphacite (Jd_{35-40}), quartz, epidote, rutile, titanite,</td><td>garnet, omphacite (Jd_{33-35}), phengite, quartz, epidote, rutile</td></tr>
</table>

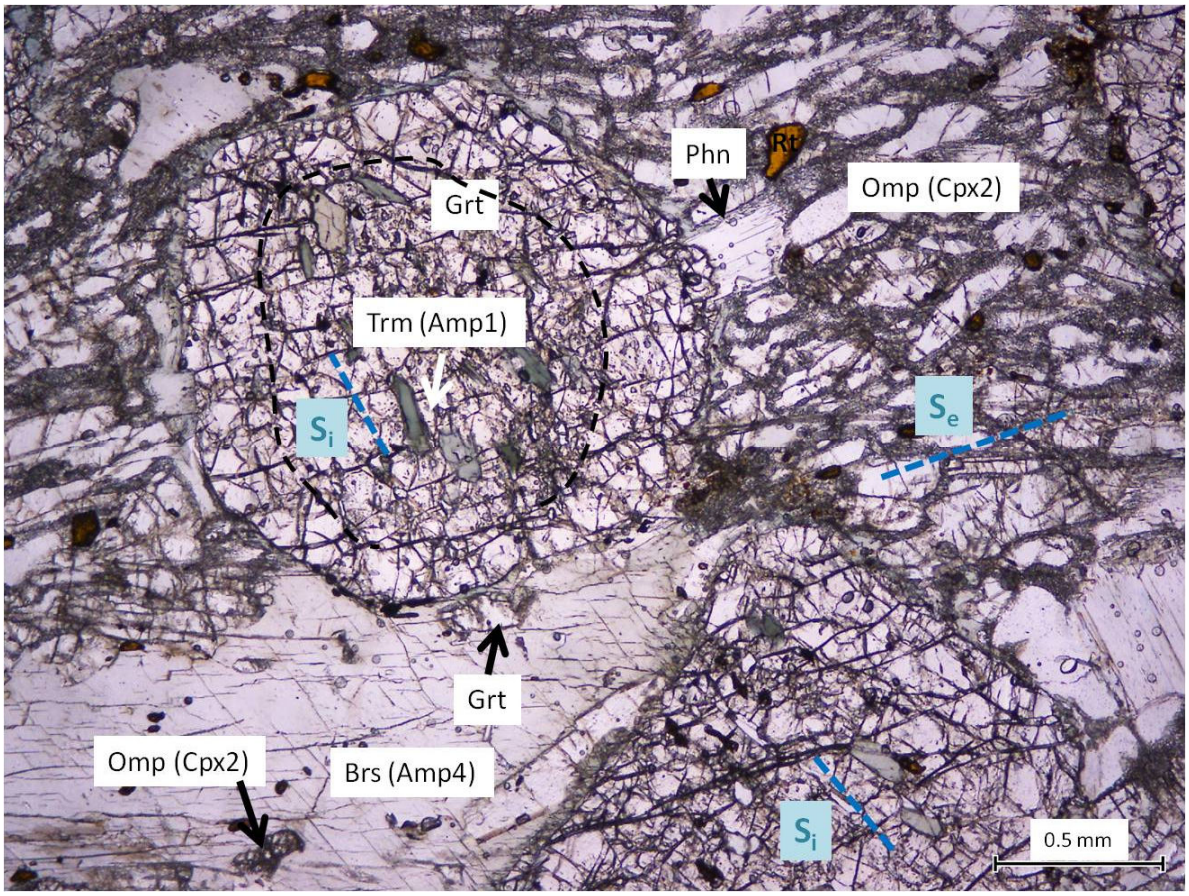

Fig. 3.3 Photomicrograph of eclogite-1 (MG829). Porphyroblastic garnet (brownish) consists of inclusion-rich core (prick-line) and inclusion-poor rim. Omphacites (Cpx2; grayish) and porphyroblastic barroisite (Amp4; greenish) have a preferred orientation (S_e) in the matrix. The orientation of inclusions in the core of garnet (S_i) is different comparing to the S_e. Phengite coexist with garnet and omphacite.

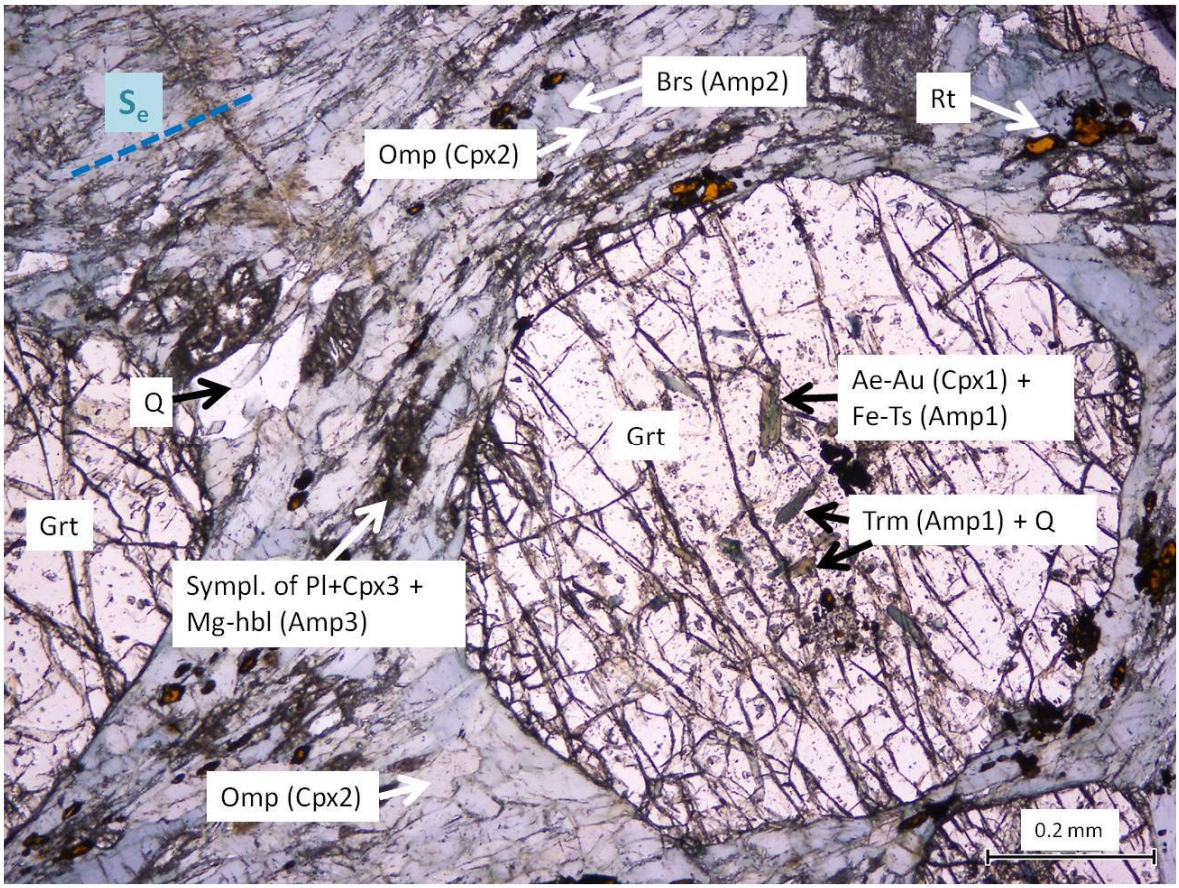

Fig. 3.4 Photomicrograph of eclogite-1 (MG802). Mineral assemblage of garnet, omphacite (Cpx2) barroisite (Amp2) and rutile in the matrix. Omphacties replaced by symplectite of plagioclase, clinopyroxene (Cpx3) and Mg-hornblende (Amp3). Garnet included polyphase inclusions of aegirine-augite (Cpx1) and Fe-tschermkaite (Amp1) and single grain inclusions of taramitess in the core. MG802, open nicol.

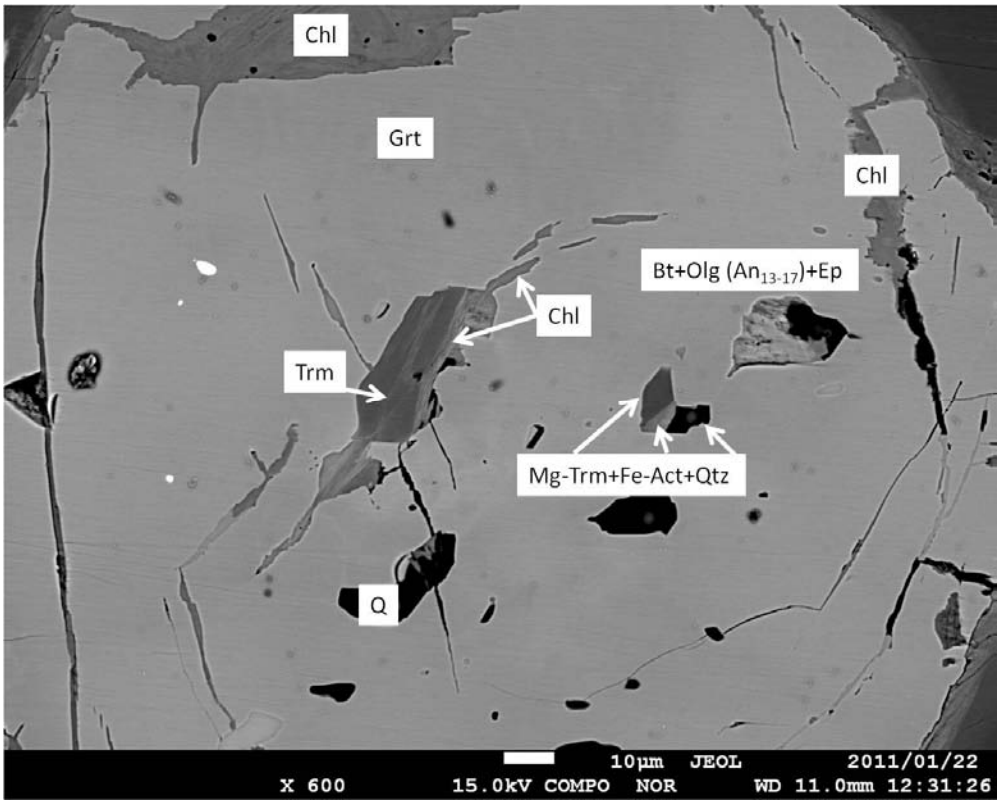

Fig. 3.5 Backscattered electron image (BEI) showing garnet includes polyphase inclusions of biotite+oligoclase ($An_{<17}$)+epidote, Mg-taramite+actinolite+quartz, single grain inclusions of quartz, and taramite. Inclusion of taramite replaced by chlorite of later stage (MG804).

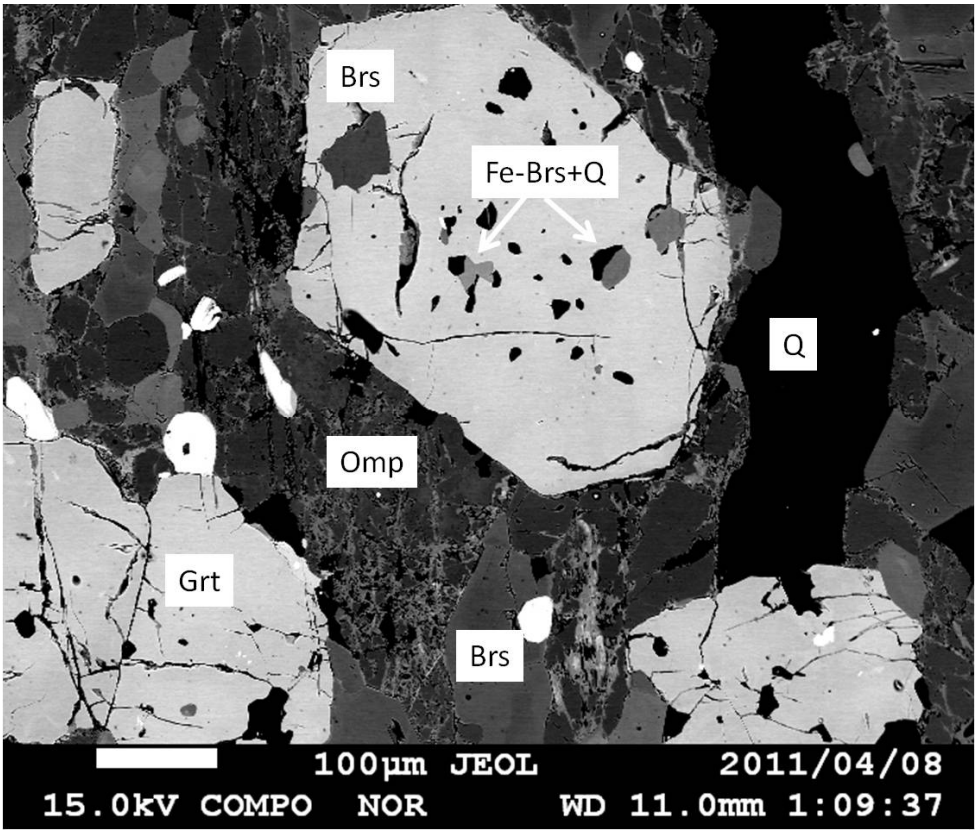

Fig. 3.6 Garnet includes polyphase inclusions of Fe-barroisite+quartz, single grain inclusions of barroisite and quartz (BEI; MG804).

Clinopyroxenes occur as three modes of occurrence, i.e. clinopyroxene inclusion in the rim of garnet (Cpx1), discrete grain in the matrix (Cpx2), and symplectitic clinopyroxenes (Cpx3) with plagioclase (An1-13) after Cpx2. Cpx2 and Cpx3 are sometimes enclosed by porphyroblastic amphiboles (Amp3). Cpx1 included in garnet occurs as anhedral to subhedral, up to 0.01 mm long (Figs. 3.7, and 3.8). They are mainly classified as omphacite, and rarely as aegirine-augite. Discrete grains of omphacite (Cpx2) occur in the matrix as euhedral to subhedral prismatic crystals. It is up to 1 mm long and pale grey in color (Figs. 3.9 and 3.10). Cpx2 contains quartz, epidote and rutile as inclusion. Cpx3 occurs as symplectite. It is fine-grained (~0.02 mm) and is classified into mainly diopsite, rarely aegirine-augite and omphacite (Figs. 3.9 and 3.10).

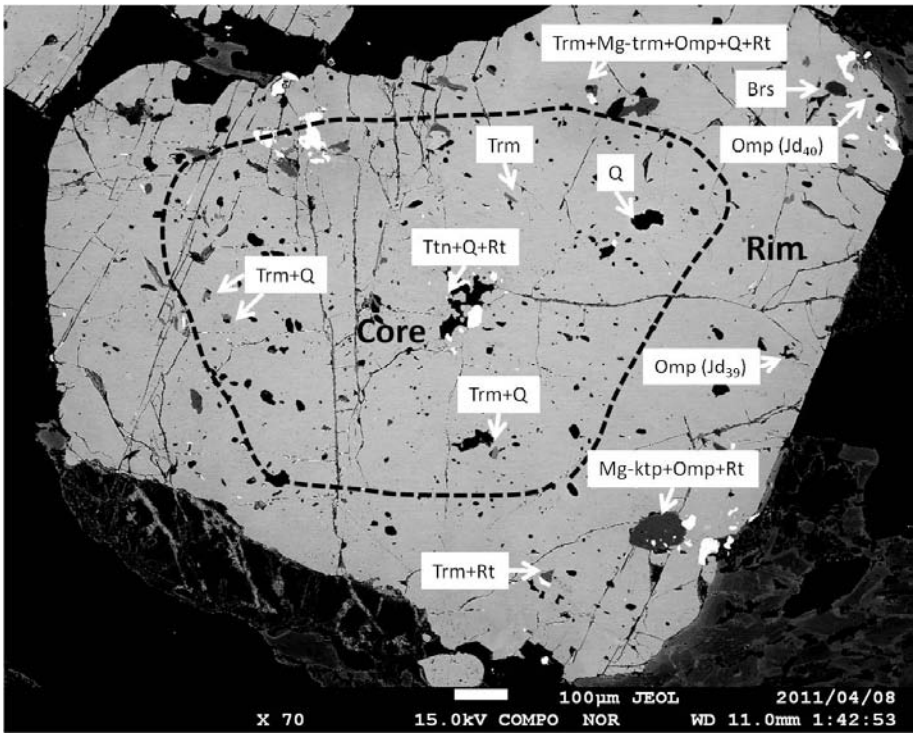

Fig. 3.7 The core of garnet includes mainly polyphase and single grained inclusions of taramite, quartz and rutile. Whereas the rim of garnet includes a omphacite (Cpx1), barroisite, Mg-katophorite as well as a taramite (BEI; MG802). Broken line indicates the boundary of inclusion rich-core and inclusion poor-rim of garnet

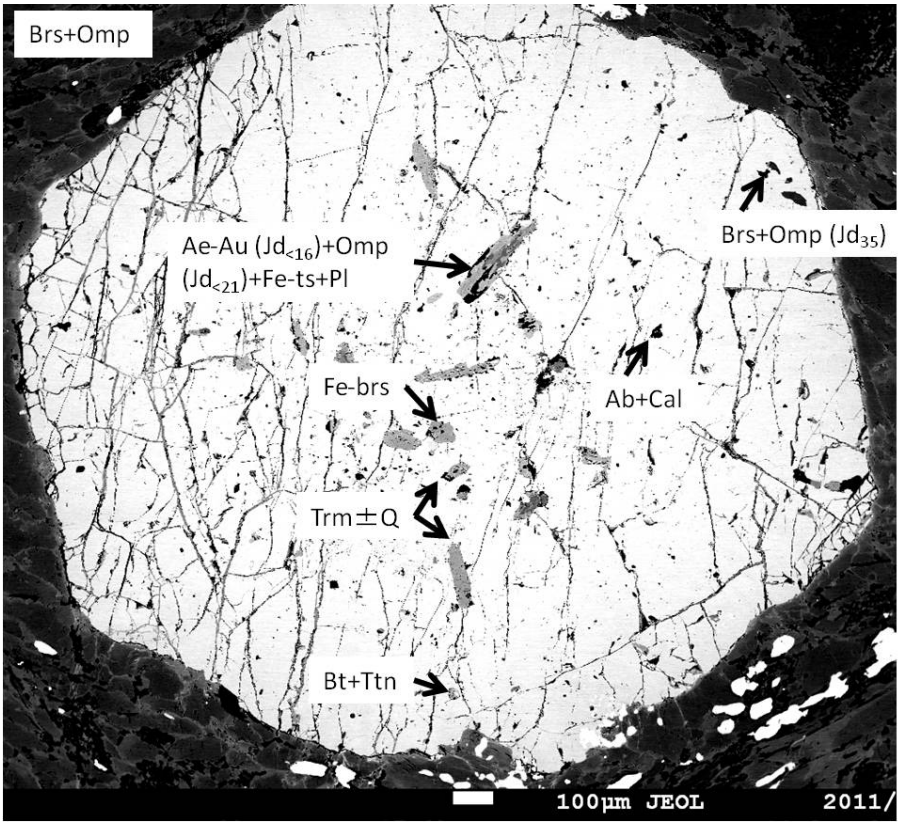

Fig. 3.8 The core of garnet includes polyphase inclusion of aegirine-augite (Jd<16), jadeite-poor omphacite (<21) (Cpx1), Fe-tschermakite and plagioclase as well as taramite and bitotie. Polyphase inclusions of barroisite (Amp1)+omphacite (Jd_{35}) (Cpx1) included in the rim of garnet (BEI; MG802).

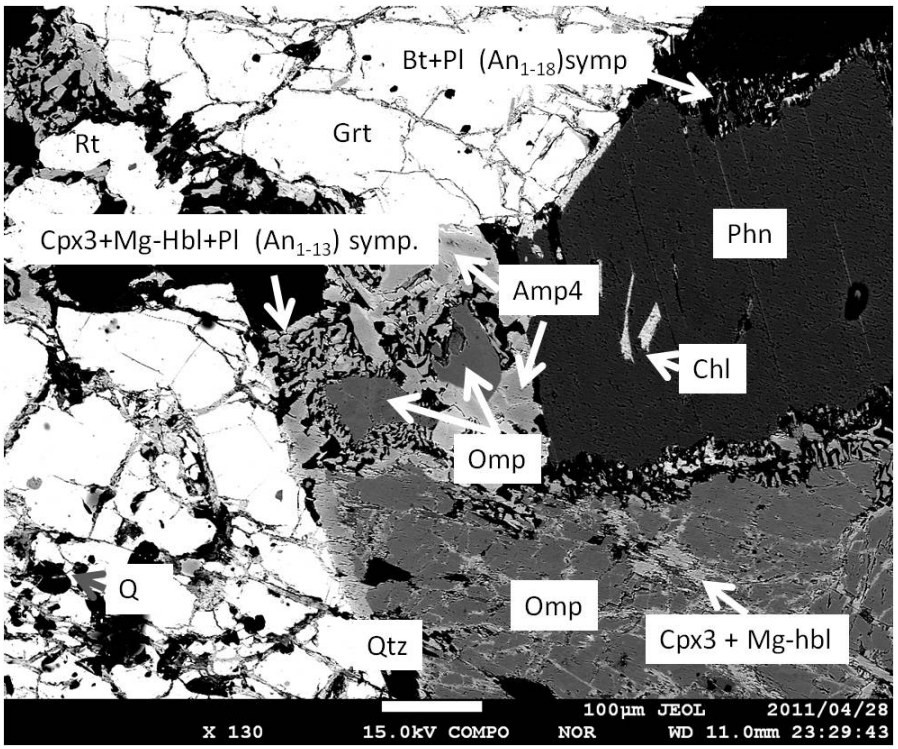

Fig. 3.9 Mineral assemblage of garnet, omphacite (Cpx2) and phengite. Omphacite replaced by symplectite of clinopyroxene (Cpx3), Mg-hornblende (Amp3) and plagioclase. Phegite replaced by biotite and plagioclase symplectite. Amphiboles (barroisite/Mg-katophorite; Amp4) grown among the garnet omphacite and phengite (BEI; MG801).

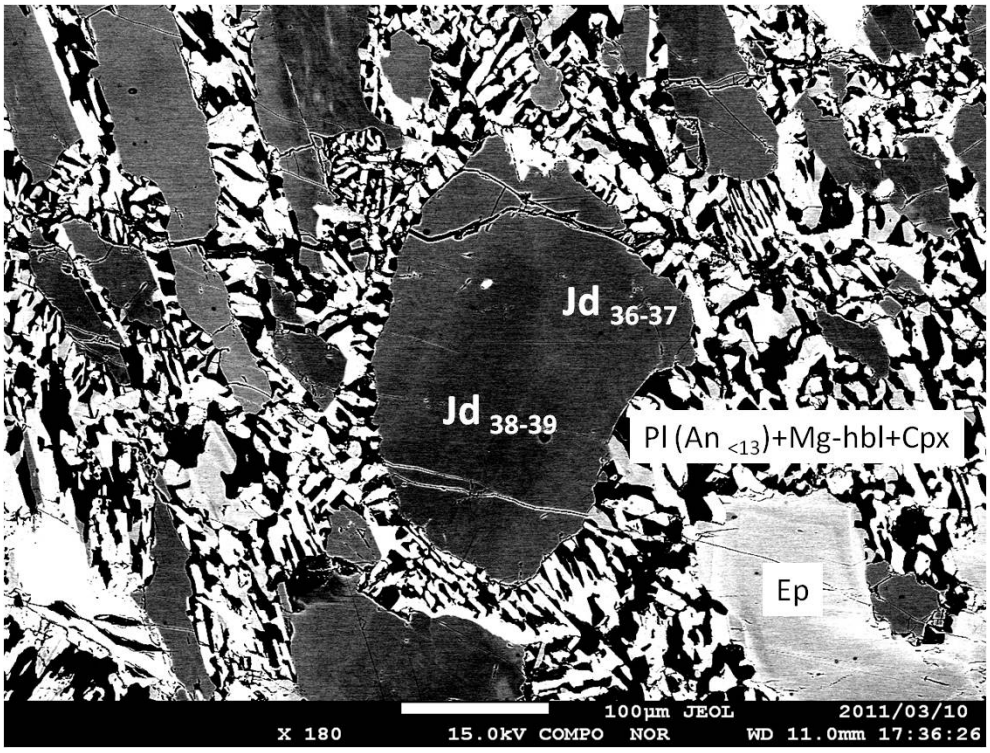

Fig. 3.10 BEI (MG829) is showing omphacite (Cpx2) replaced by symplectite of plagioclase (An_{1-13})+Mg-hornblende (Amp3)+Na-poor clinopyroxene (Cpx3; $Jd_{<13}$) and Ep3 in the matrix. Jadeite component in omphacite slightly is decreasing from the core (Jd_{38-39}) to the rim (Jd_{36-37}).

Amphiboles occur as six modes of occurrence: (1) Inclusion (Amp1) in the garnet, (2) discrete grained in the matrix (Amp2) coexisting with omphacite (Cpx2), (3) symplectitic amphibole (Amp3) with plagioclase (An1-13) after omphacite (Cpx2), (4) amphiboles (Amp4) containing inclusions of garnet, omphacite (Cpx2) and symplectite of plagioclase, Mg-hornblende (Amp3) and clinopyroxene (Cpx3), (5) amphiboles surrounding garnet (Amp5), and (6) amphiboles in amphibole-rich vein (Amp6). Amp1 (taramite, Fe-barroisite, barroisite, Fe-pargasite, pargasite, Fe-tschermakite, tschermakite, actinolite, Mg-hornblende) is euhedral to subhedral, up to 0.2 mm long. It is pleochroic with x‘=pale yellowish green and z’= green or deep green (Figs 3.3-3.8). Amp2 (glaucophane, barroisite, Mg-hornblende) occurs as subhedral, up to 0.3 mm long. It is forming a schistosity texture and it is coexisting with omphacite (Cpx2) in the matrix (Figs. 3.1, 3.11 and 3.12). Amp2 have a zoning

with glaucophane core, barroisite mantle, and Mg-hornblende rim and actinolite outermost rim (Fig. 3.12). It is pleochroic with x'=pale blue and z'=blue in the core, x'=pale green z'=bluish green in the mantle, x'=pale yellowish green and z'=pale green in the rim and x'=pale yellow and z'=pale green outermost rim. Amp3 (Mg-hornblende, actinolite) is, of anhedral to subhedral crystal, fine grained (~0.03 mm) in the symplectite (Fig. 3.10).

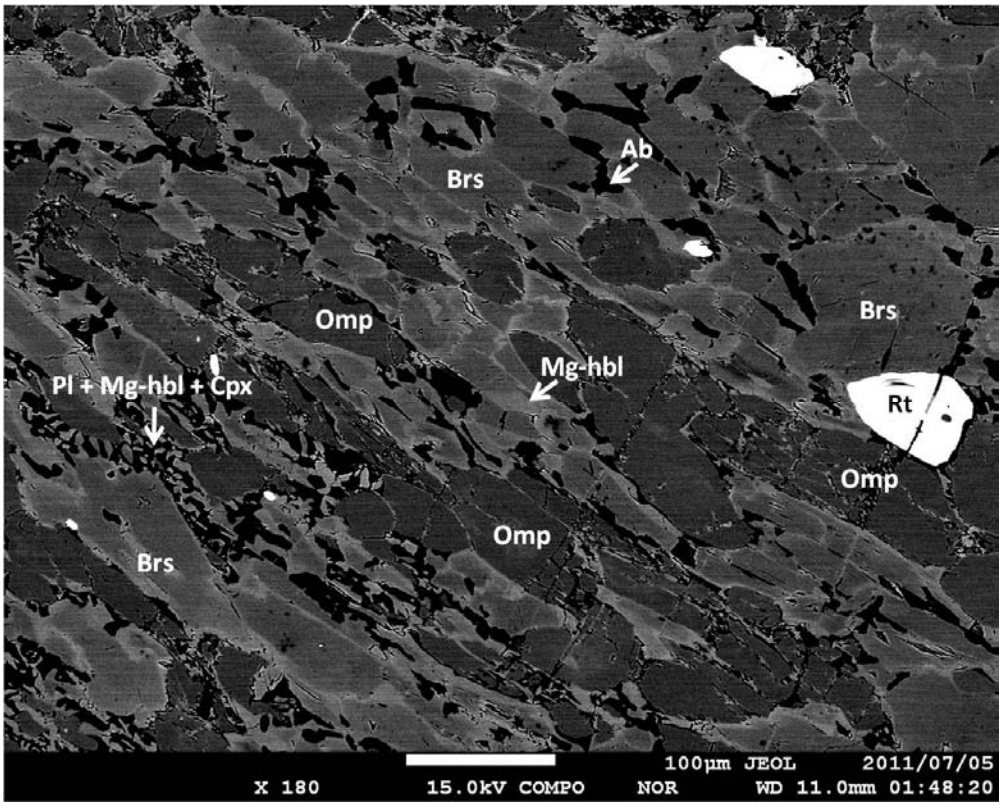

Fig. 3.11 Barroisite (Amp2) and omphacite (Cpx2) coexisting together, they are forming a schistosity texture. Cpx2 replaced by symplectite of clinopyroxene (Cpx3), plagioclase and Mg-hornblende (Amp3). Amp2 have have a retrograde zoning, barroisite core (dark grey) with Mg-hornblende rim (grey).

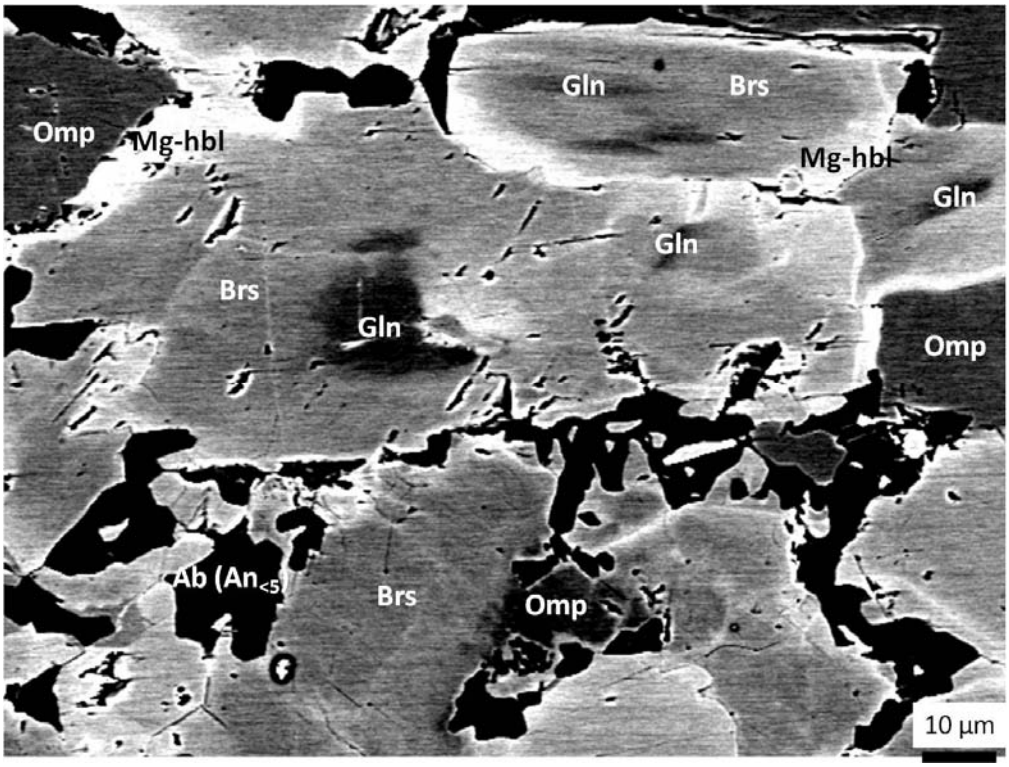

Fig. 3.12 BEI shown the prograde (glaucophane core with barroisite mantle) and retrograde (barroisite mantle with Mg-hornblende rim) zoning in the Amp2, coexisting omphacite (Cpx2).

Amp4 (barroisite, Mg-katophorite, winchite, actinolite, Fe/Mg-hornblende) is, of euhedral to subhedral in the matrix (Figs. 3.13 and 3.14). Some Amp4 are porphyroblastic sized up to 2.5 mm long. They have a actinolite or winchite core, barroisite mantle and Mg-hornblende rim (Fig. 3.15). It is pleochroic with x'= pale yellowish green, z'=pale green in the core; x'=pale green, z'=green in the rim. The rim of Amp4 includes garnet, omphacite (Cpx2), symplectitic aggregate of clinopyroxene (Cpx3) with plagioclase (Fig. 3.13-3.15), quartz, epidote, rutile and titanite. Amp4 coexists with albite (An2-7) and epidote (Fig. 3.16). Some of eclogites-1 (samples MG1218 and MG1222) does not have an evidence of Amp4 crystallization.

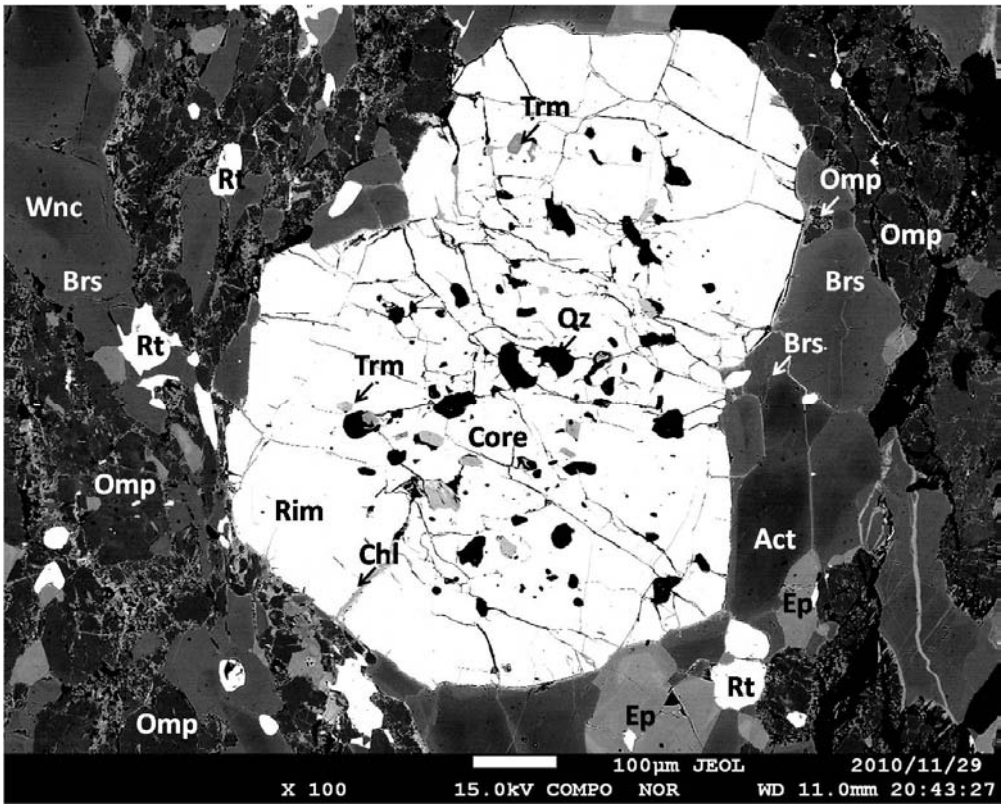

Fig. 3.13 Amp4 (zoned with Act and/or Wnc core with Brs rim) and Epidote (Ep4) in the matrix. Amp4 and Ep4 formed in between grain boundary of Omp (Cpx2) and in the pressure shadow of garnet. Amp4 contain inclusions of Omp (Cpx2) at the contact zone of garnet and Amp4 (top right site of figure).

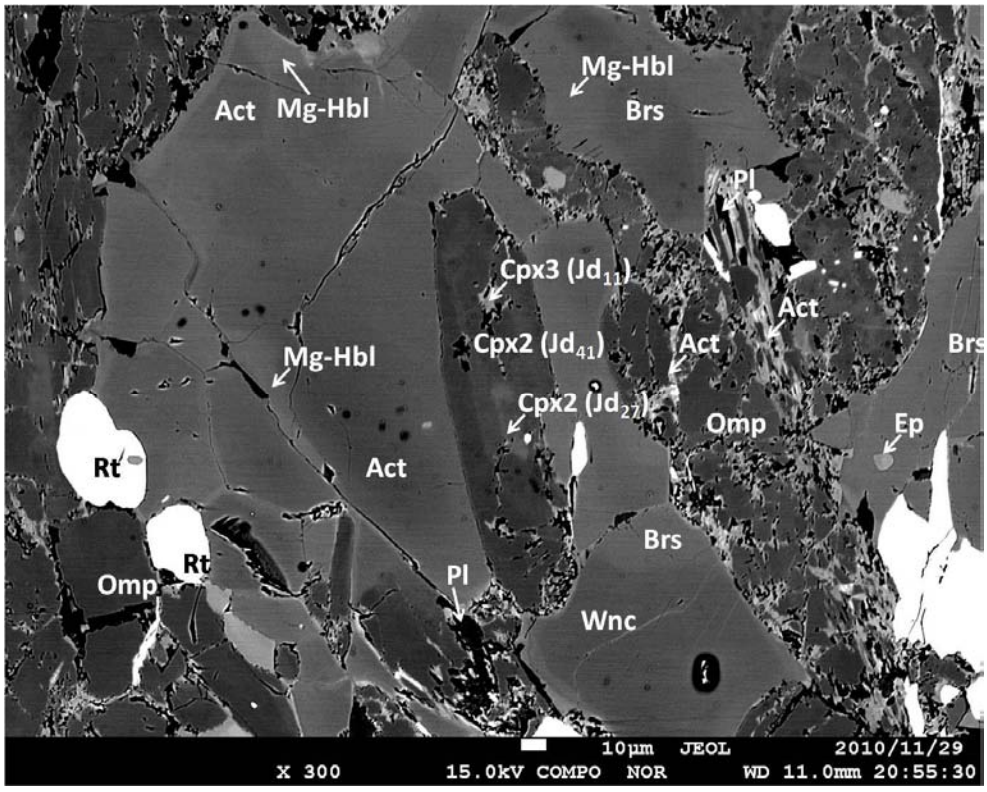

Fig. 3.14 Amp4 (zoned with Act and/or Wnc core with Brs mantle and Mg-Hbl rim) contain inclusions of zoned Omp (Cpx2). Micro fracture developed in the inclusion of zoned Omp (Cpx2) and Cpx3 crystallized within Cpx2.

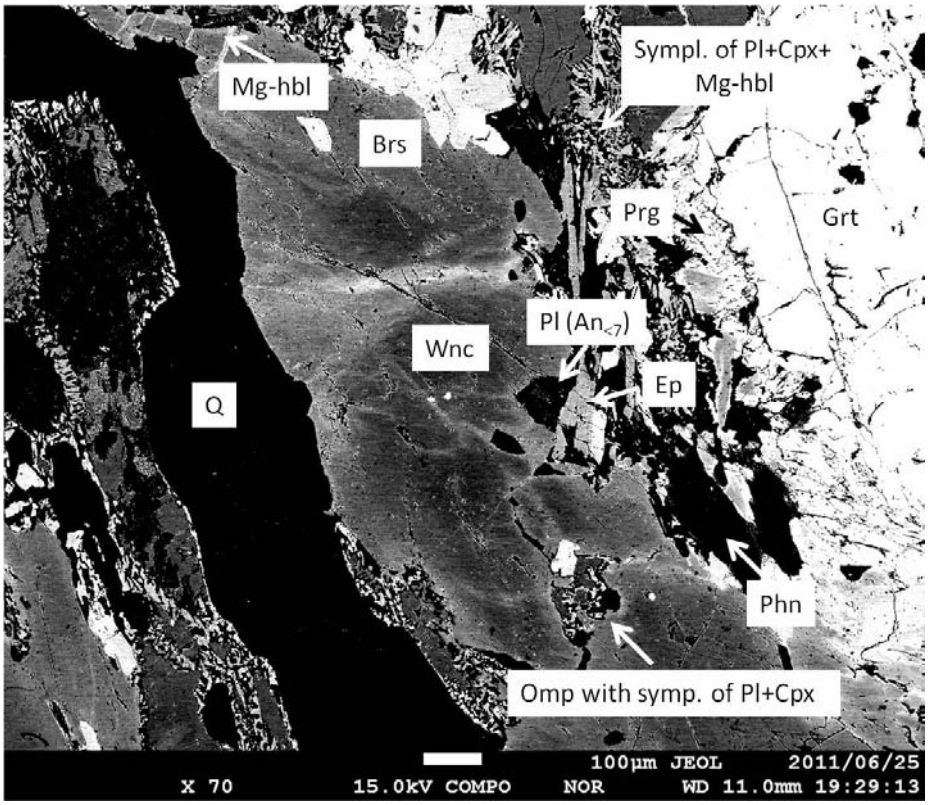

Fig. 3.15 Prograde and retrograde zoning of porphyroblastic amphibole (Amp4) in the matrix: Winchite core with barroisite mantle and Mg-hornblende rim. It coexist with albite (An<7) and epidote. Garnet surrounded by pargasite (Amp5). Omphacite surrounded by symplectite of plagioclase, clinopyroxene, and Mg-hornblende (Amp3). BEI; MG829

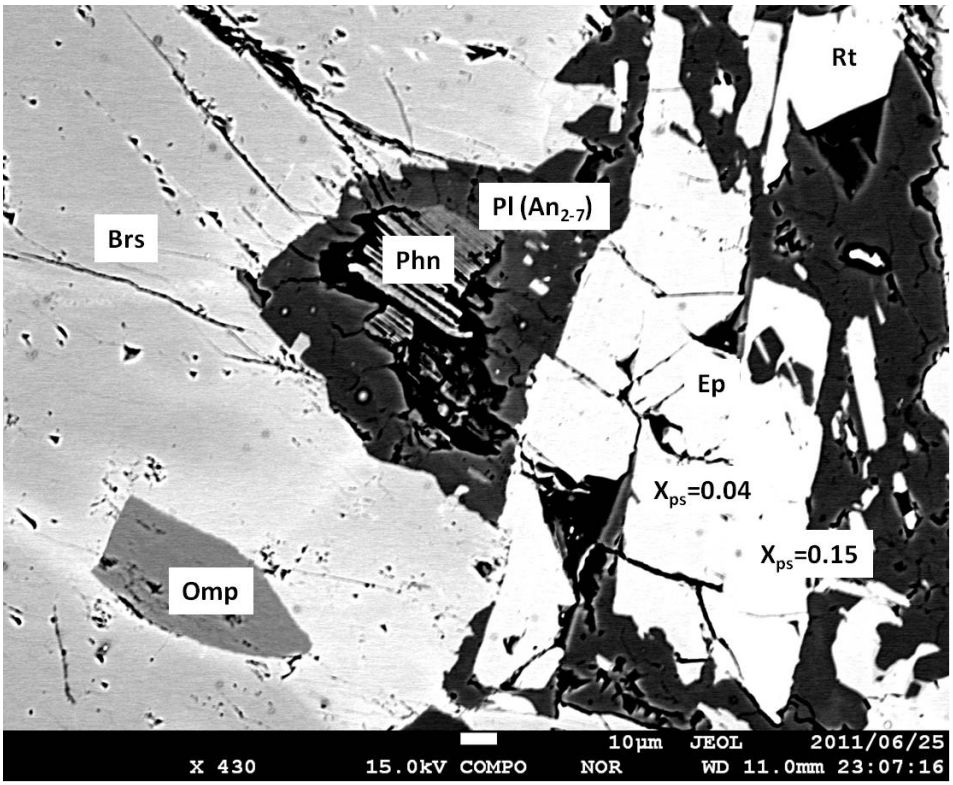

Fig. 3.16 Barroisite (Amp4), plagioclase (An_{2-7}) and epidote (Ep4) coexist together. Phengite surrounded by a plagioclase. Omphacite (Cpx2) included by barroisite (BEI; MG829).

Amp5 (pargasite, Fe-pargasite, Mg-hornblende) occurs as anhedral, up to 0.2 mm long, surrounding garnet (Fig. 3.15). Amp6 (barroisite, tremolite, pargasite, Fe-pargasite, Mg-hornblende, actinolite) occurs as subhedral prismatic crystal in the vein (up to 5 mm in width) (Figs. 3.2 and 3.16). Amp6 has a zoning with barroisite, Mg-hornblende and tremolite cores, with pargasite, Mg-hornblende rims and actinolite outermost-rims (Fig. 3.17).

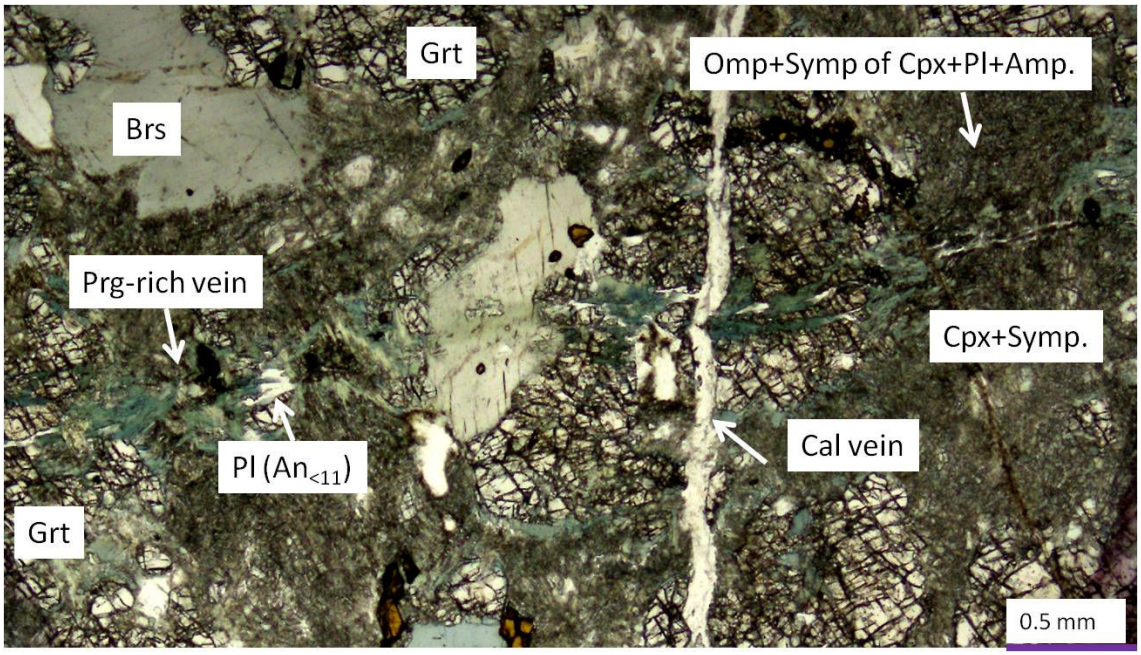

Fig. 3.17 Pargasite-rich vein cut the omphacite, eclogite, and porphyroblastic amphibole (Amp4). The vein mainly consist of pargasite (Amp6), and minor plagioclase ($An_{<11}$). Later calcite vein cut the pargasite-rich vein (MG823).

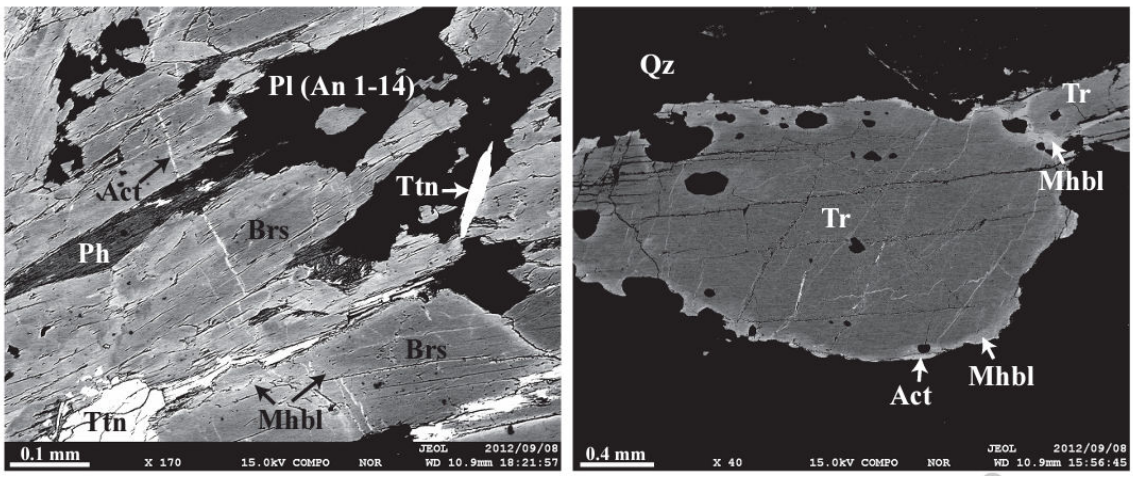

Fig. 3.18 BEI images of amphibole-rich veins. (a) The amphoble of Amp-NaPl-Ph vein is zoned, with barroisite core and Mg-hornblende and/or edenite rim. Fractures filled by actinolitic amphiboles are developed in some amphiboles (MG1218). (b) Amphibole in the Amp-Qz vein, zoned from tremolite core to Mg-hornblende rim, with rare actinolite outermost rim (MG1222).

Phengites occur as two modes of occurrence: Inclusion (phn1) in the garnet rim and discrete grain in the matrix (Phn2). Phn1 occurs as subhedral, and up to 0.1 mm across. Phn2 is euhedral to subhedral, and it is up to 0.5 mm across. It is replaced by symplectite of plagioclase (An2-18) and biotite (Fig. 3.9).

Epidote has four modes of occurrence: Inclusion in garnet (Ep1), symplectitic epidote with Amp3, Cpx3 and plagioclase after the omphacite (Ep2), discrete grain in the matrix (Ep3) coexisting with Amp4 and in the fracture zone in the porphyroblastic garnet (Ep4). Ep1 occurs as anhedral to subhedral, and up to 0.1 mm long. Ep2 occurs as in the symplectite with Amp3, plagioclase and Cpx3; it is up to 0.1 mm long. Ep3 occurs as subhedral crystal, and its size is up to 0.5 mm long (Fig. 3.16). It contains quartz as inclusion.

Plagioclase has three modes of occurrence: polyphase and discrete grain inclusions of plagioclase (Pl1; An=1-17) in the garnet, symplectitic plagioclase (Pl2; An=1-18) with Amp3, Cpx3 after the omphacite (Cpx2) and with biotite after the phengite (Ph2), dicrete grains of plagioclase (Pl3) coexisting with Amp4. Pl1 is

anhedral, up to 0.02 mm across. Pl2 occurs as discrete anhedral grains and its size up to 0.2 mm across. Pl3 occurs as anhedral up to 0.03 mm across. Paragonite occurs as inclusions in the garnet, anhedral, up to 0.02 mm across. Biotite has two modes of occurrence: inclusions of biotite in the garnet (anhedral, up to 0.01 mm across) and symplectitic bioite with Pl3 after the Ph2. K-feldspar occur locally as symplectitic together with Cpx3, Pl3, Amp3, and its size is up to 0.02 mm across.

Chlorites have three modes of occurrence, i.e. chlorite as inclusions in the garnet (Chl1) and occur as filling fractures of garnet grains (Chl2), anhedral, and pale green to green in one nicol. Hematite occurs in the matrix, it is anhedral, up to 0.8 mm across. Rutile occurs in the garnet, clinopyroxene (Cpx2), and amphibole (Amp2 and Amp4) as inclusion and in the matrix. Its size is up to 0.5 mm across. Titanite occurs in the matrix, usually replacing rutile. Titanite also occurs in the garnet as inclusion. Ilmenite often occurs replacing rutile and as anhedral discrete grain in the matrix.

Amphibolized eclogite-1 intruded by vein-type orthogneiss

Amphibolized eclogite-1 consist mainly of calcic amphiboles (Fe-pargasite, tschermakite, Fe-tschermakite Fe/Mg-hornblende, actinolite), plagioclase (An1-9), with minor amounts of garnet, sodic-calcic amphibole (barroisite), epidote, chlorite, K-feldspar, rutile, titanite, quartz, apatite, hematite, and zircon (Fig. 3.19) (Table. 3.1.1). Chlorite veins are locally cross-cut the rock (Fig. 3.19).

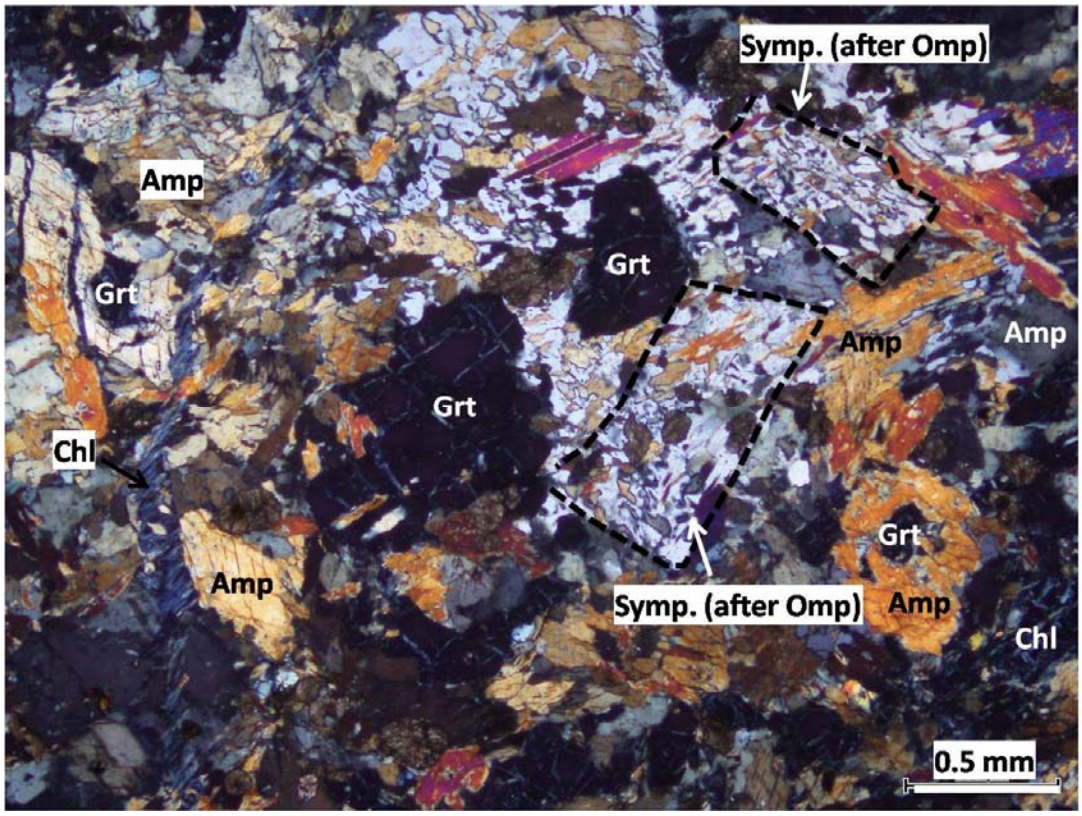

Fig. 3.19 Microphotograph of the amphibolized eclogites-1 intruded by orthogneiss vein. Subhedral to euhedral amphiboles replacing eclogitic garnets are dominant in the amphibolized eclogites-1. Smaller grains of amphiboles and plagioclase preserved rectangular shaped symplectitic texture (shown by dashed lines). Some of garnets are included by the euhedral shaped amphiboles. Chlorite vein cross-cut the rock.

Garnets occur as four modes of occurrence, i.e. (1) resorbed garnet (Grt1) which are strongly replaced by chlorites and sometimes included by amphibole (actinolite and barroisite), (2) garnets (Grt2) replacing Grt1 and coexisting with calcic amphibole (tschermakite, Fe-tschermakite, Fe-pargasite and Fe/Mg-hornblende), (3) fracture filling garnets (Grt3) partially developed in the Grt1 and Grt2, and (4) Mn-rich films of garnet (Grt4) rimming Grt1 and Grt2 (Fig. 3.20). Grt1 are anhedral to subhedral, and they are up to 0.7 mm across (Fig. 3.20a). Grt1are rarely contain inclusions of omphacite and quartz (Fig. 3.21). Grt2 are anhedral to subhedral replacing Grt1 (Fig. 3.20c), and their maximum size up to 0.2 mm across, relatively lesser replaced by chlorites. Grt3 are anhedral filling fractures of Grt1 and Grt2 (Fig. 3.20b), up to 0.01

mm in width. Grt4 occur as anhedral thin film, rimming Grt1 and Grt2 (Fig. 3.20 b-d), and they are up to 0.03 mm in width.

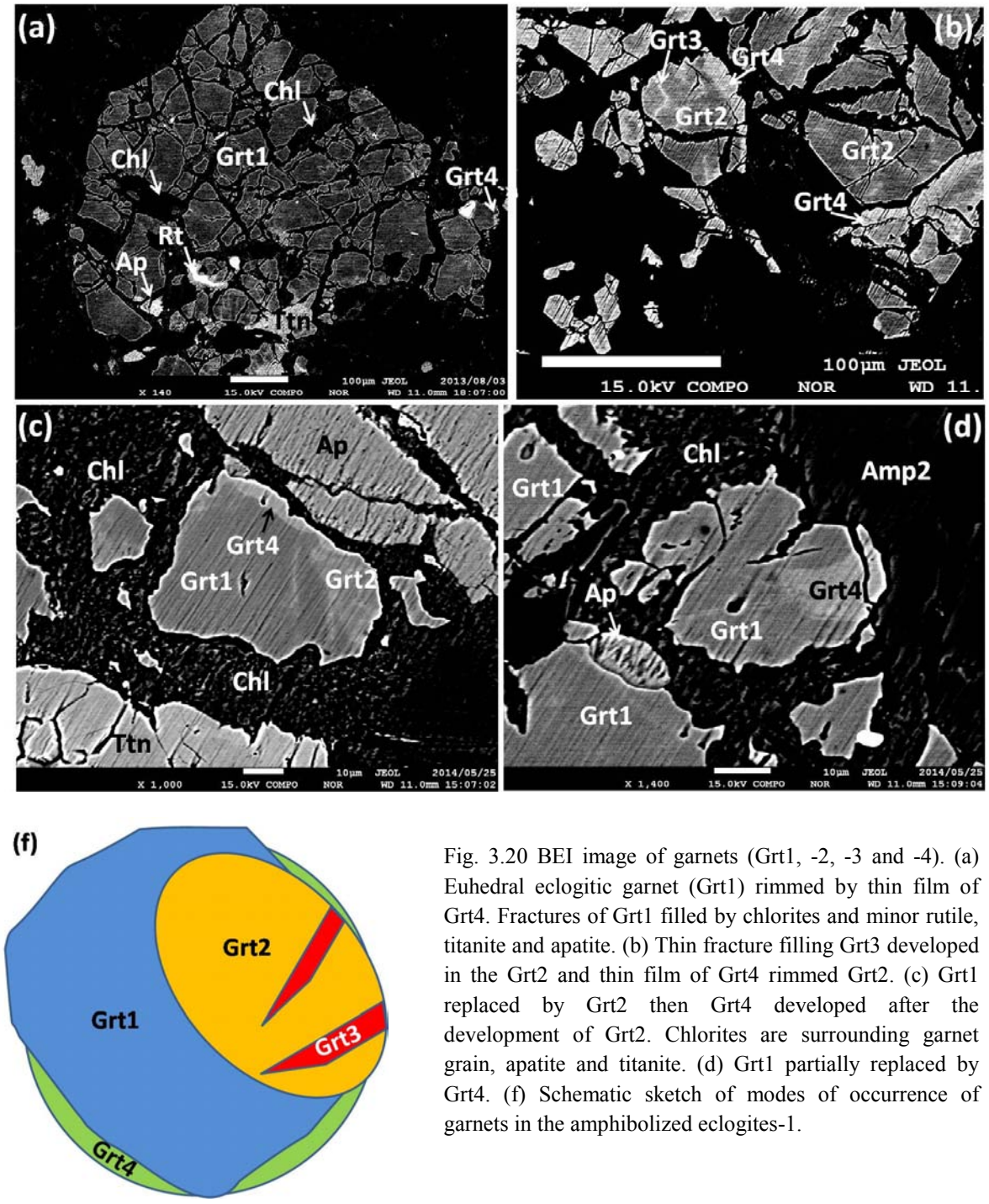

Fig. 3.20 BEI image of garnets (Grt1, -2, -3 and -4). (a) Euhedral eclogitic garnet (Grt1) rimmed by thin film of Grt4. Fractures of Grt1 filled by chlorites and minor rutile, titanite and apatite. (b) Thin fracture filling Grt3 developed in the Grt2 and thin film of Grt4 rimmed Grt2. (c) Grt1 replaced by Grt2 then Grt4 developed after the development of Grt2. Chlorites are surrounding garnet grain, apatite and titanite. (d) Grt1 partially replaced by Grt4. (f) Schematic sketch of modes of occurrence of garnets in the amphibolized eclogites-1.

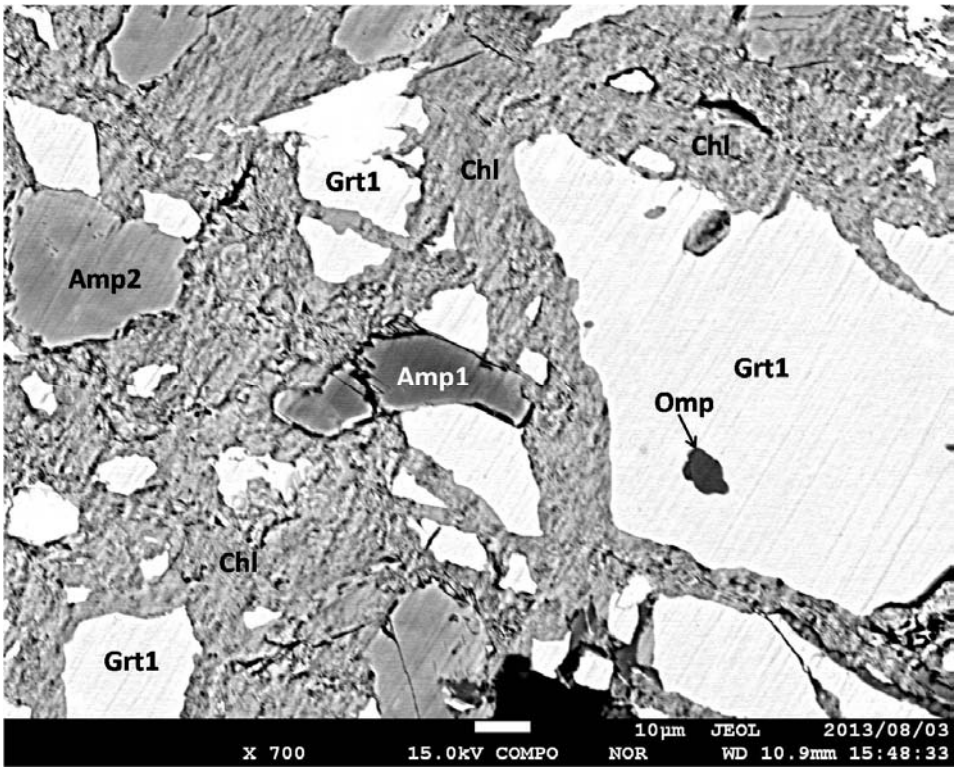

Fig. 3.21 Aggregates of Grt1, Amp1 (barroisite) and Amp2 (Mg-hornblende) are surrounded by chlorite. Grt1 contain inclusion of omphacite.

Amphiboles occur as three modes of occurrence: (1) relic amphibole (Amp1; actinolite core with barroisite rim), (2) calcic amphibole (Amp2; Mg-hornblende core with tschermakite/pargasite rim) replacing Amp1, and coexisting with Grt2, (3) thin actinolite micro-vein cross-cutting Amp1 and Amp2.

Amp1 (actinolite and barroisite) is euhedral to subhedral, up to 0.5 mm across, pleochroic with x‘=pale yellowish green to pale green and z’= pale green to pale bluish green. Amp1 are overgrown by Amp2. They have a zoning with actinolite core with barroisite rim (Fig. 3.22). Amp1 locally contain Grt1 and fine-grained symplectites of amphibole and plagioclase as inclusions (Figs. 3.23 and Fig. 3.24).

Amp2 (Fe-pargasite, tschermakite, Fe-tschermakite Fe/Mg-hornblende) occurs as euhedral to subhedral, up to 0.3 mm long. They are pleochroic with x’=pale green to green and z’=green to deep green. Amp2 are overgrown Amp1 and formed

as discrete grains with plagioclase and epidote, and they have a zoning with Fe/Mg-hornblend cores with tschermakite, Fe-tschermakite, Fe-pargasite rims (Fig. 3.22). Anhedral Grt2 are crystallized with Amp2 replacing Amp1, indicating they were formed at a same time (Figs. 3.22 - 3.25). Smaller grains of Amp2 and plagioclase are preserved symplectitic texture indicating they were formed after the consummations of omphacites (Figs. 3.19 and 3.22).

Amp3 (actinolite) occur as thin micro-vein (up to 0.2 mm thickness) cross-cutting Amp1 and Amp2 (Fig. 3.23).

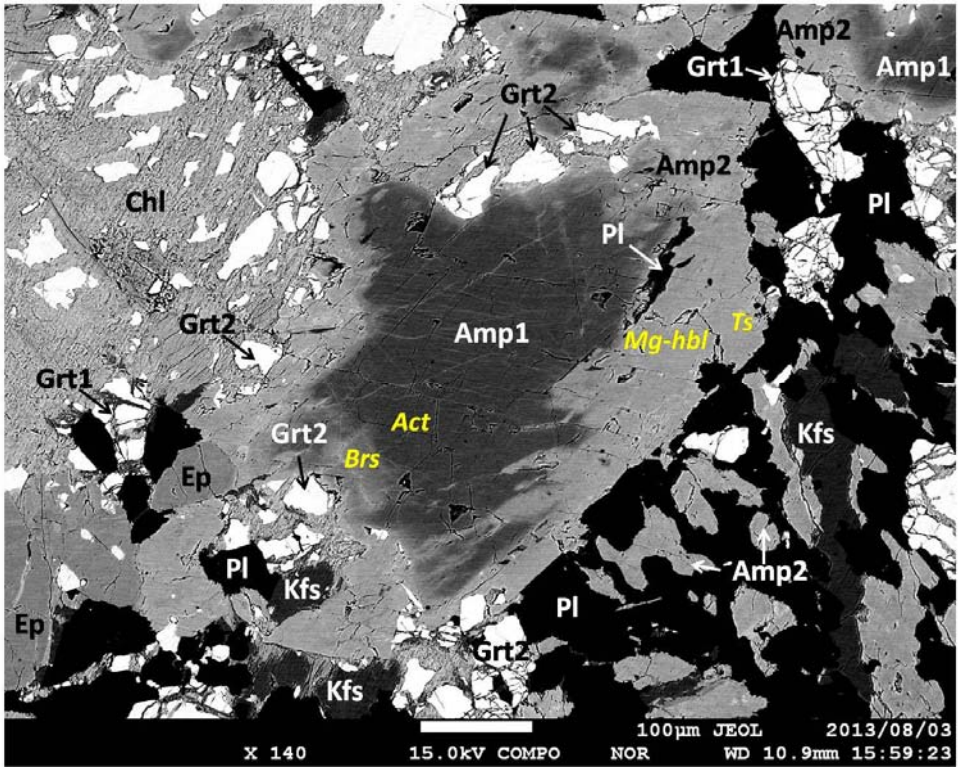

Fig. 3.22 Resorbed Amp1 overgrown by Amp2, Grt2 and plagioclase (Pl). Amp1 have a zoning with actinolite core and barroisite rim. Amp2 have a zoning with Mg-hornblende core with tschermakite rim. Aggregates of Grt1 surrounded by plagioclase, epidote and Amp2. Discrete anhedral and subhedral smaller Amp2 with plagioclase and K-feldspar forming symplectite texture.

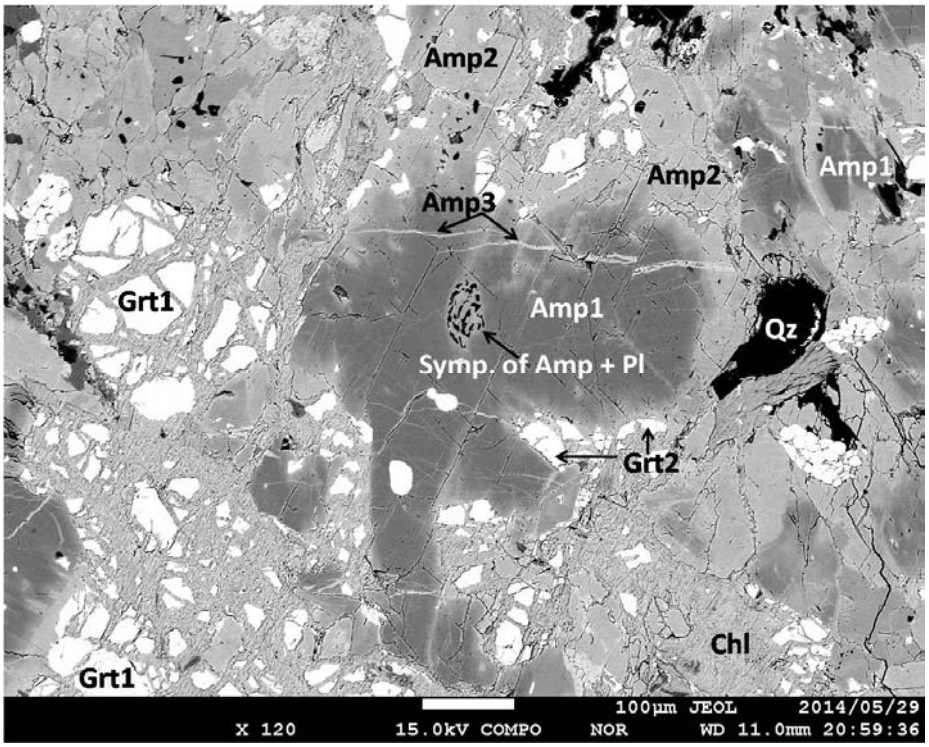

Fig. 3.23 Resorbed Amp1 overgrown by Amp2, Grt2 and Grt1 partially replaced by chlorite. Amp1(actinolite and barroisite) contain symplectitic polyphase inclusion of amphibole and plagioclase, indicating former omphacite inclusion was replaced by amphibole and plagioclase.

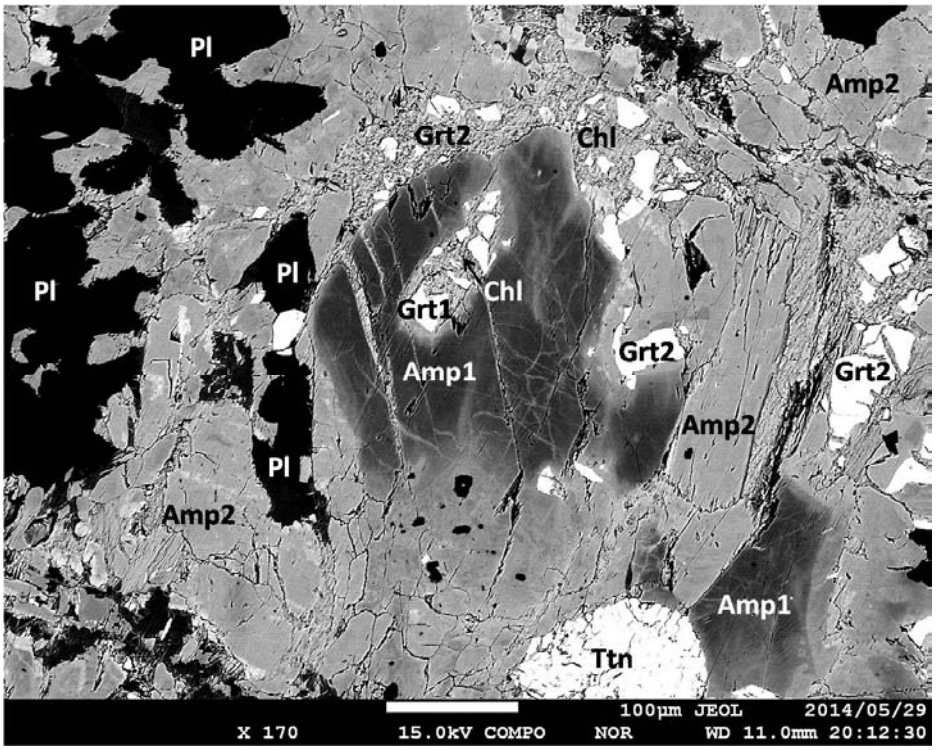

Fig. 3.24 Resorbed Amp1 overgrown by Amp2, plagioclase and Grt2. Amp1contain inclusion of Grt1 partially replaced by chlorite. Chlorite partially surrounding Amp2 and Grt2.

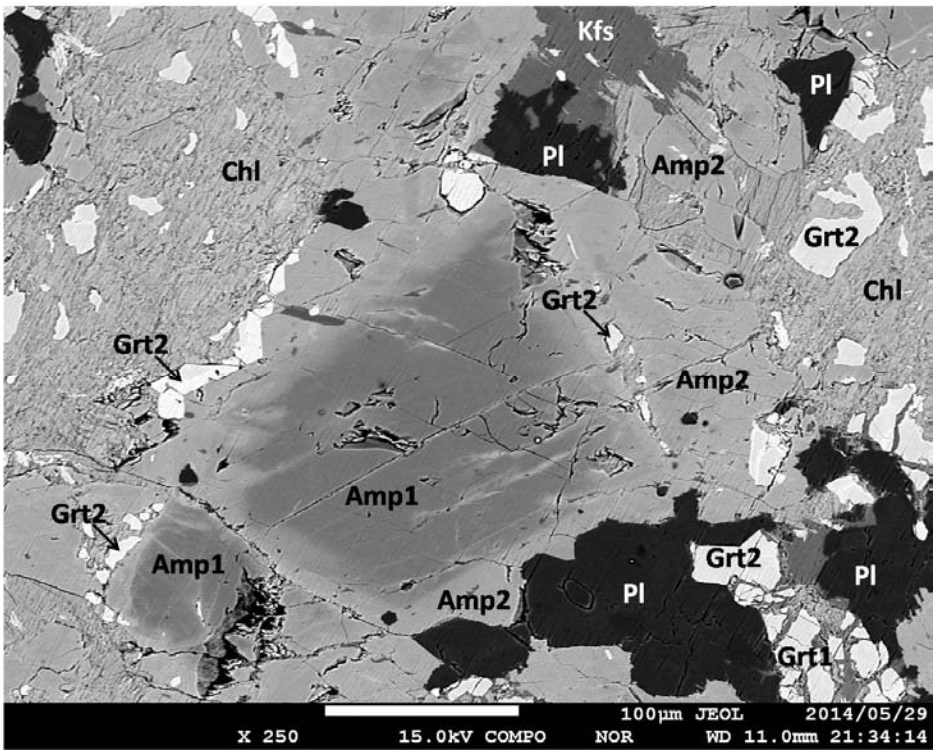

Fig. 3.25 Resorbed Amp1 overgrown by Amp2 and anhedral Grt2. Plagioclase and K-feldspar crystallized with Amp2 and Grt2.

Plagioclases occur as anhedral and up to 0.1 mm across. They occur as symplectitic with Amp2 and sometimes replacing Amp1 together with Amp2 (Figs. 3.19). They have a zoning with core (An=4-5), mantle (An=8-9) and rim (An=1-2) (Fig. 3.26)

K-feldspars occur as anhedral and up to 0.1 mm across, coexist with plagioclase and Amp2 (Figs. 3.22 and 3.25).

Epidotes occur as discrete grains often crystallized with Mg-hornblende (Amp1). They are anhedral to subhedral crystal, and its size is up to 0.1 mm across (Fig. 3.22).

Chlorites occur as anhedral, replacing garnets (Grt1 and Grt2) and surrounding amphiboles (Amp1 and Amp2) and plagioclase (Figs. 3.21 - 3.25).

Apatites occur as anhedral and they up to 0.5 mm across. They coexist with Amp2, plagioclase and Grt2. Hematite occurs in the matrix, it is anhedral, up to 0.1 mm across. Rutiles are up to 0.2 mm across surrounded by titanite. Titanite oftern occur as discrete grains and they are up to 0.3 mm across (Fig. 3.24).

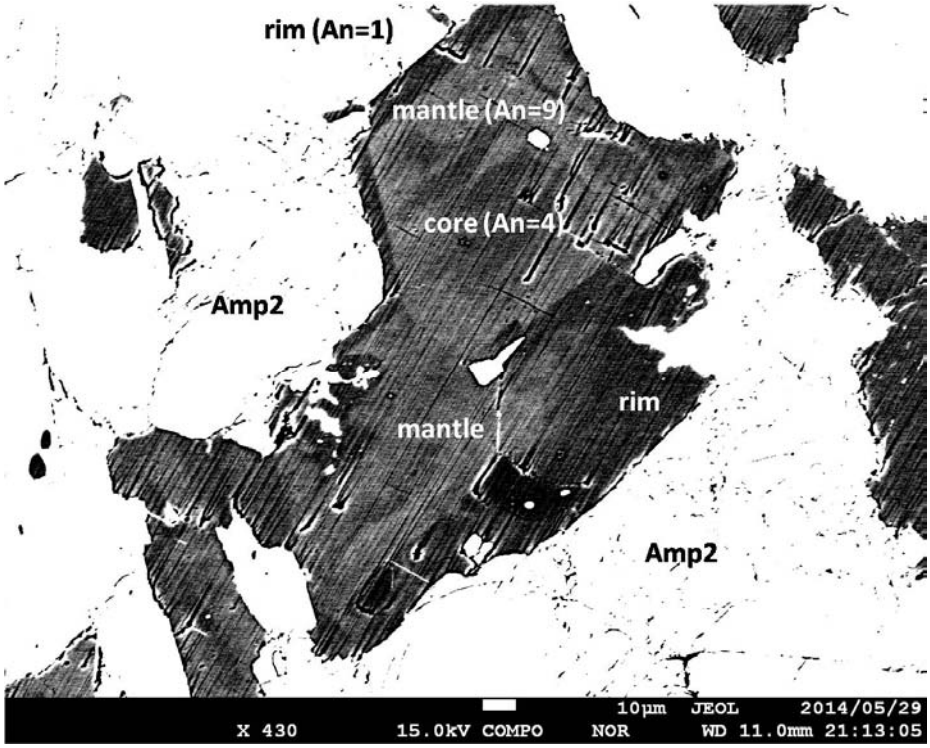

Fig. 3.26 Symplectitic plagioclase have a zoning with anorthite content increase from the core (An=4) to the mantle (An=9) and decrease from the mantle to the rim (An=1).

3.1.2 Eclogite-2 within marbles

Eclogite-2 in marbles consists of small grains of garnet (<0.1 mm) and omphacite (XJd=0.34-0.48) with minor amounts of amphibole, epidote, paragonite, plagioclase, chlorite, calcite, biotite, quartz, titanite and rutile (Table. 3.1.1). The matrix of eclogite-2 shows a pseudomorpous texture, where small grains of garnet crowd cemented by titanite forming isomorphic round shape. Some of cores of garnet grain contain relics of garnet indicating previous mineral were larger porphyroblastic garnet. In addition, small grains of omphacite forming rectangular prismatic nature surrounded by garnet grains (Fig. 3.27). Poikiloblastic amphiboles which contain garnet, omphacite, epidote, and symplectites of plagioclase and amphibole are developed (Fig. 3.28).

Garnet grains occur as subhedral to euhedral, and up to 0.3 mm across. Garnets have a zoning with core, mantle and rim. Sometimes rims of garnet crystallized as discrete grains next to the mantles of garnet (Fig. 3.27). Garnets contain rare inclusions of quartz and omphacite.

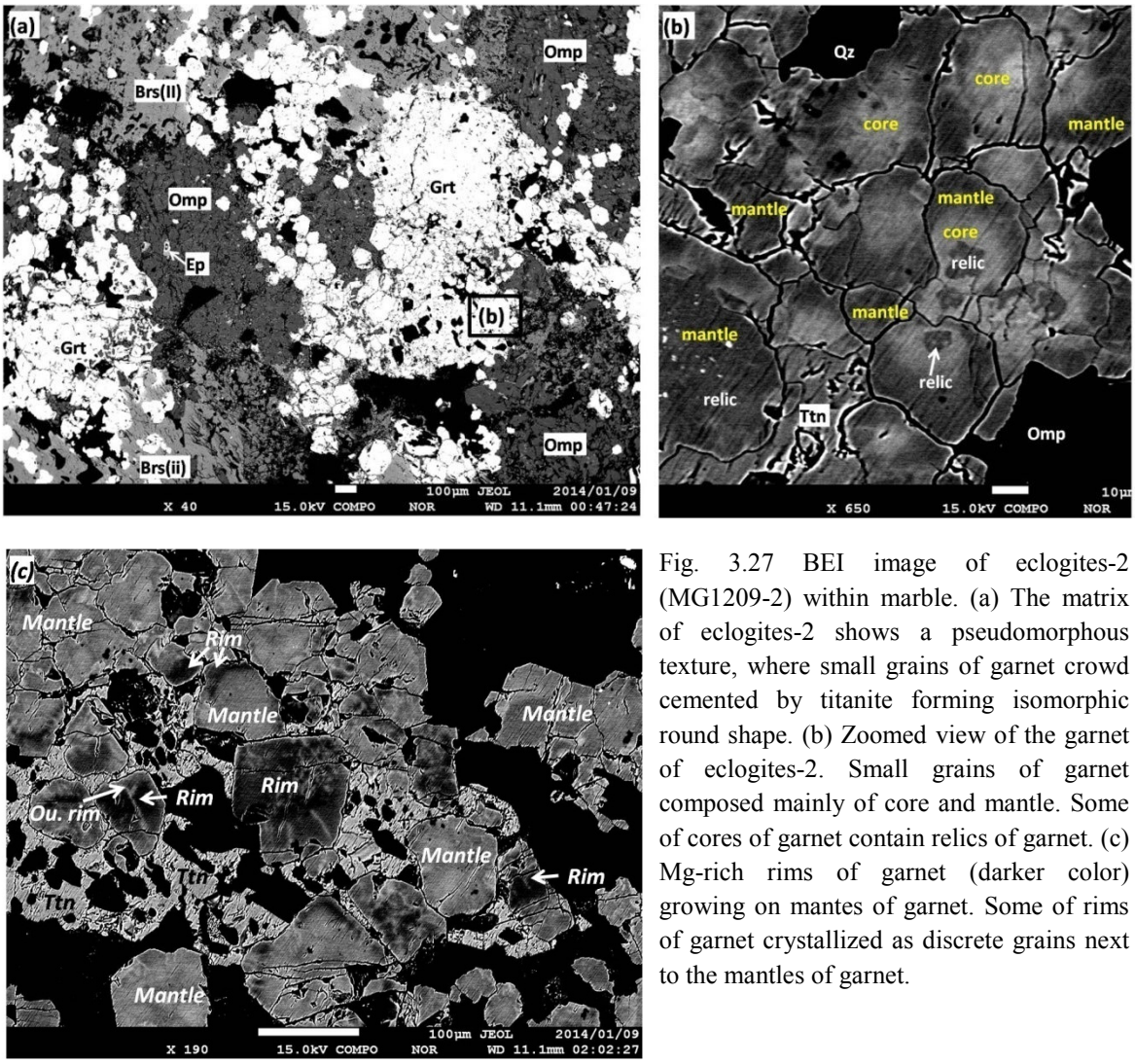

Fig. 3.27 BEI image of eclogites-2 (MG1209-2) within marble. (a) The matrix of eclogites-2 shows a pseudomorphous texture, where small grains of garnet crowd cemented by titanite forming isomorphic round shape. (b) Zoomed view of the garnet of eclogites-2. Small grains of garnet composed mainly of core and mantle. Some of cores of garnet contain relics of garnet. (c) Mg-rich rims of garnet (darker color) growing on mantes of garnet. Some of rims of garnet crystallized as discrete grains next to the mantles of garnet.

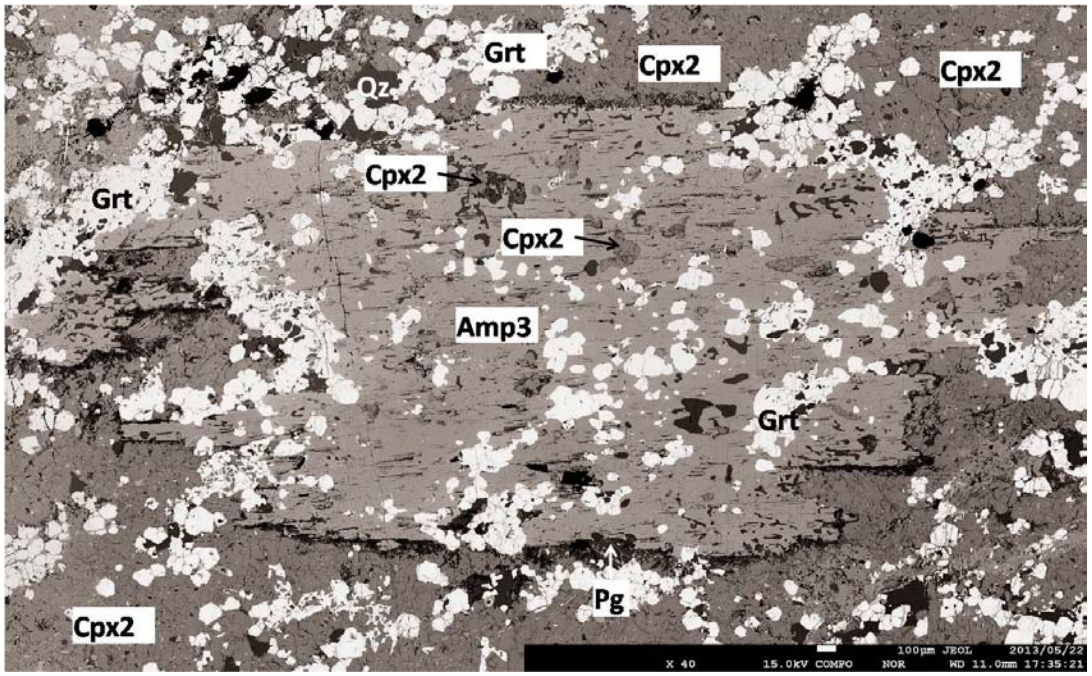

Fig.3.28 BEI image of poikiloblastic barroisitic amphibole (Amp3) containing eclogitic minerals of garnet and omphacite with symplectite of Amp2 and plagioclase in the eclogites-2 within marble. The preferred orientation of inclusions of eclogitic garnet and omphacite (Cpx2) are same as preffered orientation of matrix garnet and omphacite (Cpx2).

Omphacites occur as two modes of occurrence, i.e. clinopyroxene inclusion in the garnet (Cpx1) and discrete grain in the matrix (Cpx2). Cpx1 included in garnet occurs as anhedral, and up to 0.01 mm long (Fig. 3.29). Discrete grains of clinopyroxene (Cpx2) occurs in the matrix as subhedral prismatic crystals. It is up to 0.1 mm long and pale grey in color (Fig. 3.27 and 3.29). Cpx2 also occur as inclusion in the poikiloblastic amphibole (Amp3) often surrounded by symplectitic assemblage of plagioclase (An=1-17) and amphibole (actinolite, Mg-hornblende, edenite) (Fig. 3.30). Cpx2 contains quartz, amphibole (barroisite, Mg-hornblende and actinolite) as inclusions (Fig. 3.29).

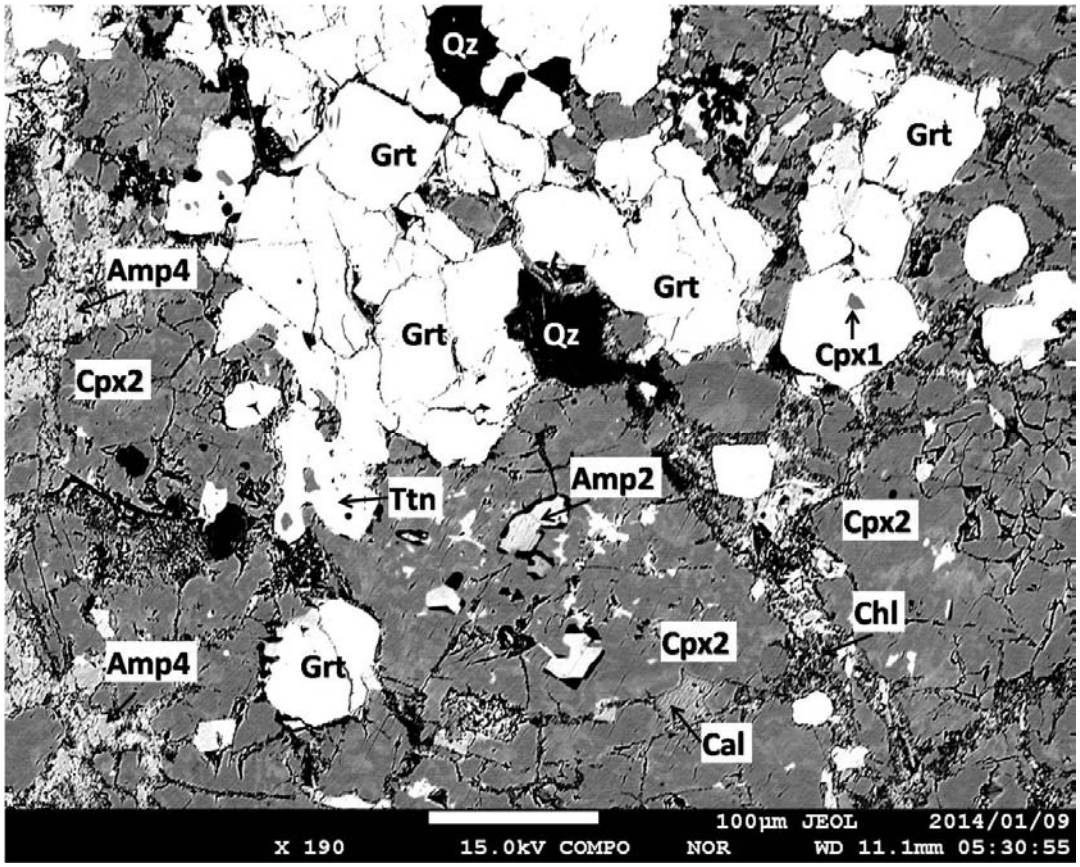

Fig.3.29 BEI image of garnet, Cpx2 (omphacite). Garnet contain inclusions of Cpx1 (omphacite). Amp2 (pargasite) rimmed by quartz formed within Cpx2 indicating that Amp2were formed after the fluid infiltrated into Cpx2. Amp4 (actinolite) toghether with chlorite and calcite are filling grain boundaries of Cpx2.

Four modes of occurrence of amphibole are distinguished. Amphibole (Amp1) (zoned with actinolite core, barroisite mantle and rims of tschermakite, pargasite, Mg-taramite, Mg-hornblende) coexisting with garnet and omphacite (Fig. 3.30), symplectitic amphibole (Amp2) (pargasite, actinolite, Mg-hornblende), poikiloblastic barroisitic amphibole (Amp3) containing eclogitic minerals of garnet and omphacite with symplectitic Amp2, plagioclase and epidote, and finally actinolitic amphiboles (Amp4) partially filling grain boundaries of omphacite and garnet.

Amp1 occurs as subhedral, up to 0.1 mm long. It is forming a schistosity texture and it is coexisting with omphacite (Cpx2) and garnet (Fig. 3.30). It is

pleochroic with x'=pale green, yellowish green z'=bluish green, green. Amp2 is, of anhedral to subhedral crystal, and fine grained (~0.03 mm) in the symplectite (Fig. 3.31).

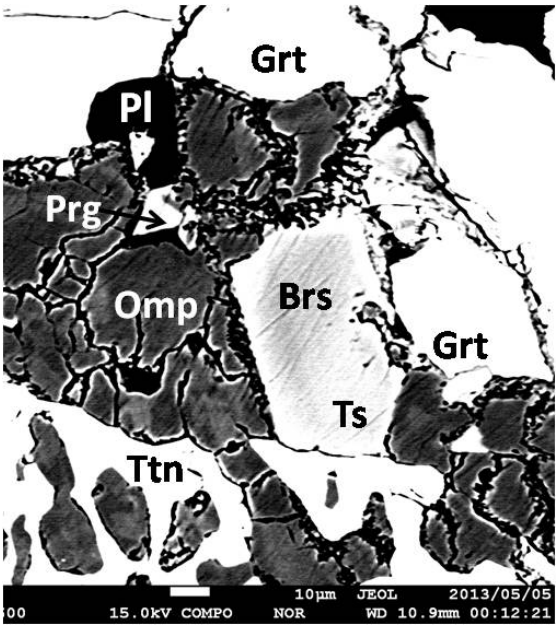

Fig.3.30 BEI image of garnet, omphacite (Cpx2) and barroisite (Amp1). Amp1 has zoning with barroisite core and tschermakite rim. Titanite, pargasite (Amp2) and plagioclase (An=8) crystallized between the grain boundaries.

Amp3 occurs as subhedral poikiloblastic, up to 3 mm long. Garnet and omphacite and symplectites of Amp2, plagioclase and epidote are contained as inclusions and their internal orientation is same as preferred orientation of matrix garnet and omphacite (Fig. 3.28). Amp4 (actinolite) are filled grain boundaries of Cpx2 and garnet grains and partially replaced poikiloblastic Amp3 (Fig. 3.32).

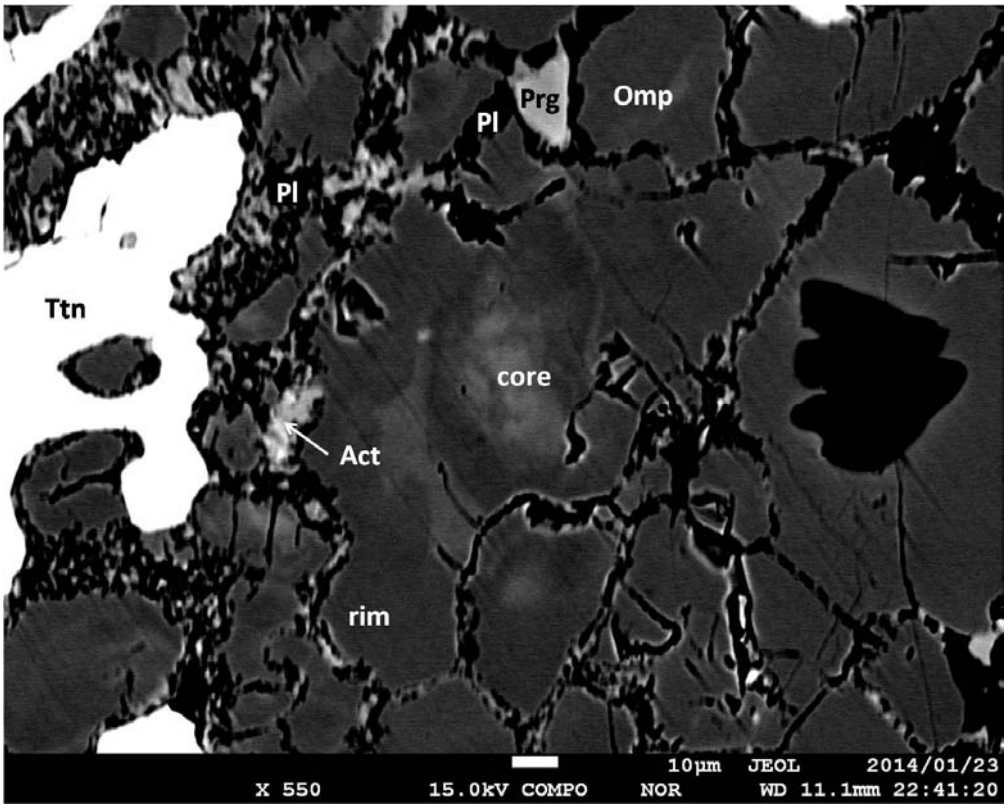

Fig.3.31 BEI image of zoned omphacite (Cpx2). Cpx2 has zoning with core (Jd=27-31%) and rim (Jd=34-42%). Jadeite component is fluctuated in the rim. actinolite, pargasite (Amp2) plagioclase and titanite are filling grain boundaries of Cpx2.

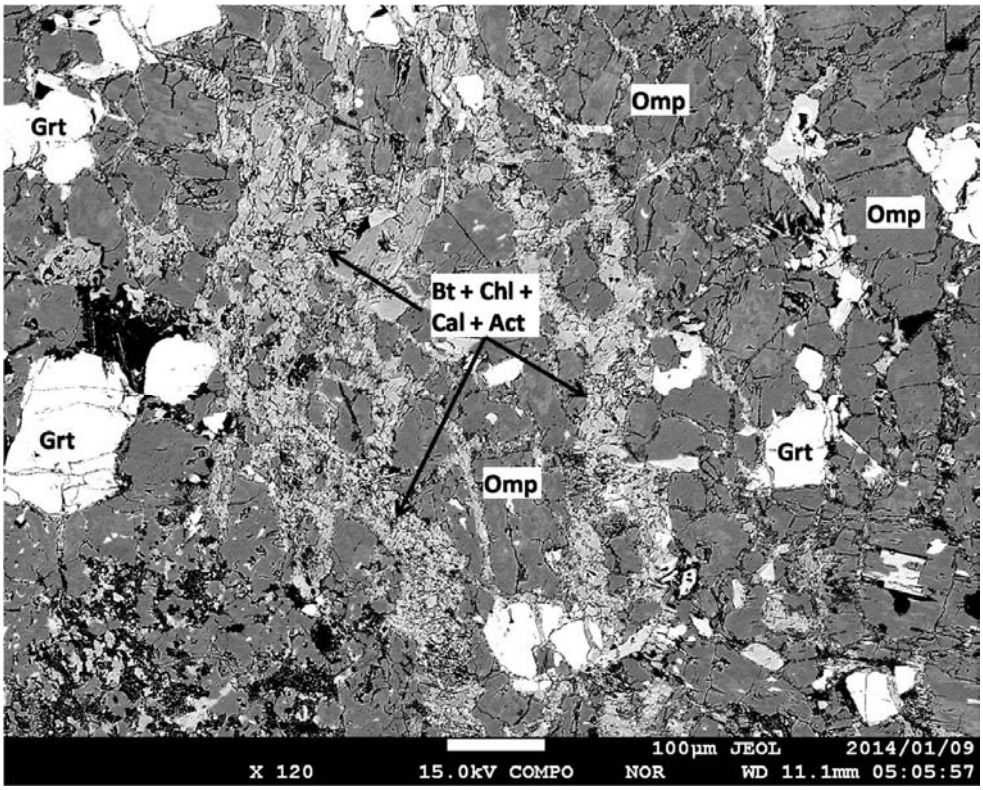

Fig.3.32 BEI image of zoned omphacite (Cpx2). Cpx2 has zoning with core (Jd=27-31%) and rim (Jd=34-42%). Jadeite component is fluctuated in the rim. Actinolite, pargasite (Amp2) plagioclase and titanite are filling grain boundaries of Cpx2.

Epidote has three modes of occurrence: epidote (Ep1) occurs as resorbed core of discrete grains of epidote (Ep2) in the matrix. Epidote (Ep3) occurs as symplectitic with plagioclase and Amp2 (Ep3). Discrete grain epidotes (Ep1 + Ep2) occur as anhedral to subhedral crystal, and its size is up to 0.5 mm long (Fig. 3.33).

Paragonites occur as discrete grains in the matrix, and subhedral up to 0.1 mm across. They sometimes replaced by plagioclase (An=2-28) and Ep3 (Fig. 3.34).

Plagioclase occurs as two modes of occurrence: plagioclase (Pl1) symplectitic plagioclase (An1-17) with Amp2 and Ep3; and discrete grains of plagioclase (An=2-28) in the matrix (Figs. 3.33 and 3.34).

Chlorite occurs as filling grain boundaries of Cpx2 and garnet together with biotite and calcite. Hematite occurs in the matrix, it is anhedral, up to 0.03 mm across. Rutile occurs among the garnet crowd, surrounded by titanite.

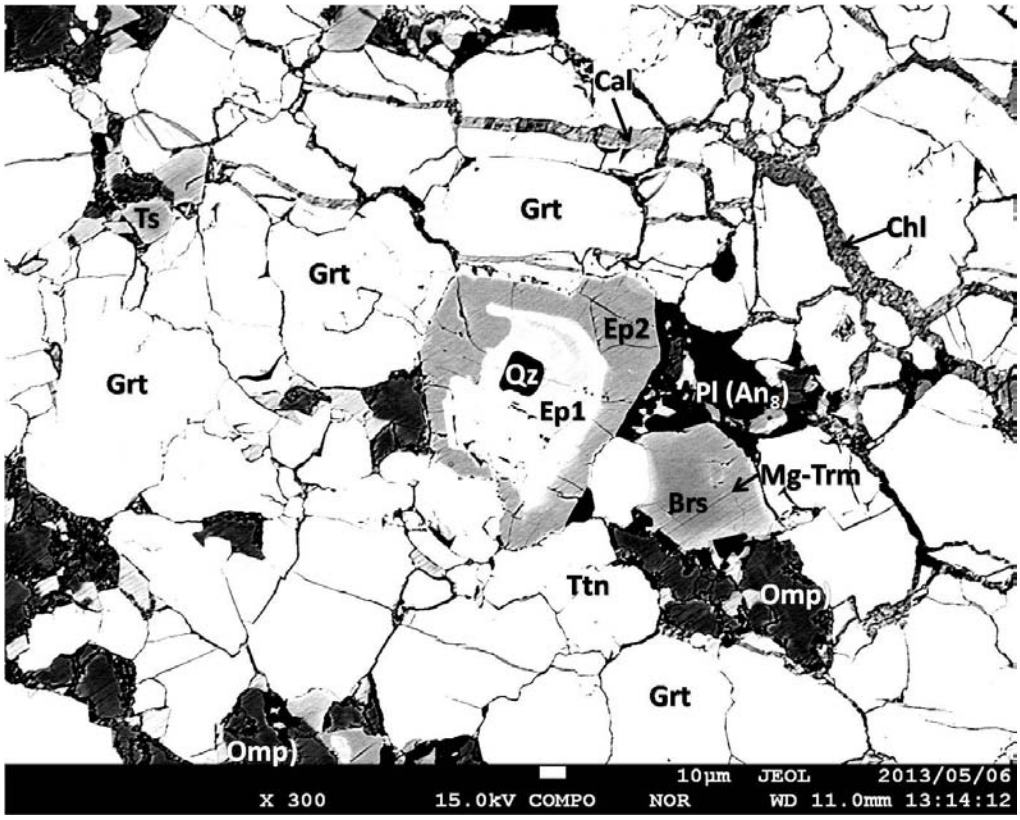

Fig.3.33 BEI image of garnet, epidote (Ep1 and Ep2), amphibole (Amp1 with barroisite core and Mg-taramite rim) and omphacite (Cpx2). Fractures of garnet filled by chlorites. Tschermakite (Amp2) and plagioclase are formed between grain boundaries.

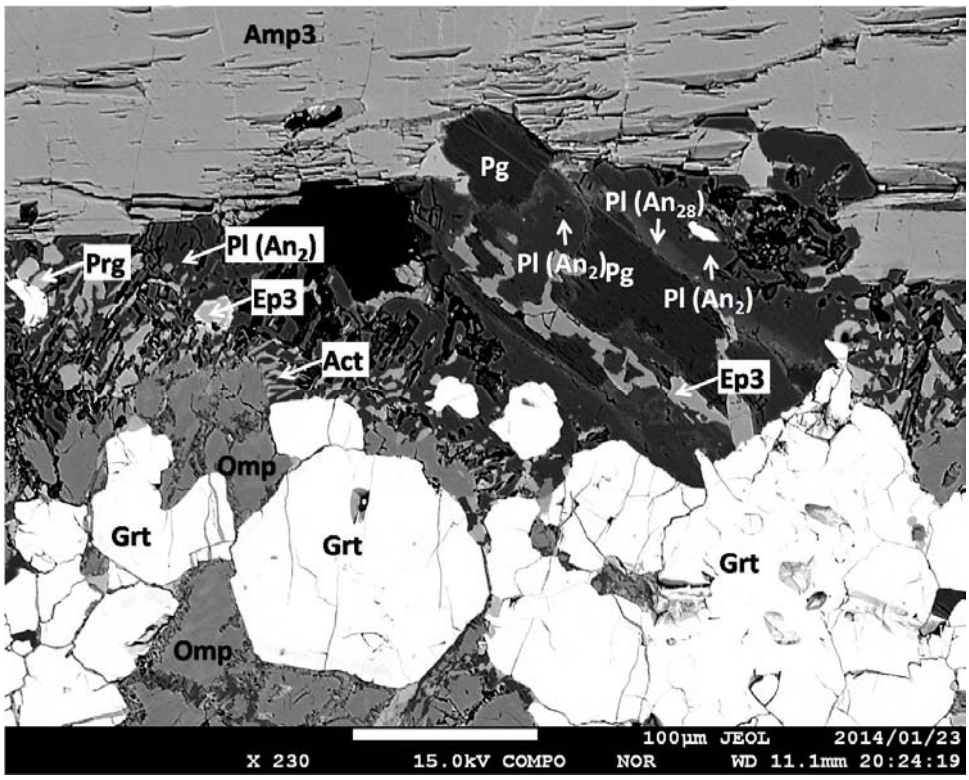

Fig.3.34 BEI image of garnet, omphacite (Cpx2), paragonite symplectite of pargasite (Amp2) and epdiote (Ep3) and poikiloblastic Amp3. Omphacite consumed into symplectite of pargasite (Amp2), plagioclase (Pl) and epidote(Ep3). Paragonite partially replaced by symplectitic Ep3 and Pl ($An_{2\text{-}28}$).

3.2 Amphibolite within marbles

Amphibolite within marbles of Maykhan Tsakhir Formation consists mainly of calcic amphibole and plagioclase with minor garnet, K-feldspar, rutile, titanite, epidote, paragonite, and quartz (Fig. 3.35) (Table 3.2). They have a preferred orientation of amphiboles.

Amphibole has two modes of occurrence. Amphibole (Fe-pargasite, tschermakite, Mg-hornblende; Amp1) occurs as inclusion in garnet rim (Fig. 3.36). It occurs as subhedral prismatic crystal, up to 0.1 mm long, and it is pleochroic with x'=pale green and z'=green. Discrete grained amphiboles (Amp2) occur in the matrix and they occur as euhedral to anhedral, up to 1 mm long. They have a zoning, Mg-hornblende core to Fe-pargasite or tschermakite rim (Fig. 3.36). They are pleochroic with x'=pale yellowish green, z'=pale green in the core and x'=pale green, z'=green to deep green in the rim. Plagioclase has two modes of occurrence, i.e. polyphase inclusions of plagioclase (An9-12; albite, oligoclase) with Amp1 occur in the rim of garnet and plagioclase (An5-8), coexisting amphibole (Amp2) surrounding a garnet (Fig. 3.36). Garnet is anhedral, and it is up to 0.5 mm across. It includes chlorite, ilmenite, epidote, K-feldspar, quartz and paragonite in the core; polyphase inclusions of plagioclase (An9-12) and Amp1 (Fe-pargasite, Fe-tschermakite and Fe-edenite) are included in the rim (Fig. 3.36). Epidote occurs as inclusion in garnet and in Amp2 (Fig. 3.36). Epidote inclusions in garnet occur as anhedral crystal, up to 0.02 mm across. Epidote inclusions in amphibole occur as subhedral grains up to 0.03 mm long. Rutile occurs as inclusion (0.03 mm) in garnet and in the matrix (0.2 mm); it is sometimes fully replaced by titanite. Paragonite occurs only as inclusion (up to 0.01 mm) in garnet core.

Rock type	Amphibolite	Garnet-phengite schists		Garnet-chloritoid schist		Orthogneisses (Vein-type)	Orthogneisses		Metapelites
Sample No.	MG803	MG1204	MG1207	MG806	MG812	MG1220-1	MG1228-1	MG1229	MG827
Garnet	+	+++	++	+++	+++	+			+++
Ca amphibole	+++								
Phengite		+++		+	+	++	++	++	+++
Muscovite				+++	+++	+	+		
Chlorite		+	+	++	++	+	+		++
Chloritoid				++	++				
Epidote	+					+	+		++
Paragonite	+	+	+	+	+				+
Plagioclase	+++	++	++			+++	+++	+++	
K-feldspar	+					+++	+++	+++	
Rutile	+	+	+	+	+	+	+	+	+
Titanite	+		+	+	+	+	+	+	
Quartz	++	+++	+++	+++	+++	+++	+++	+++	+++
Hematite	+	+	+	+	+				+
Calcite				+	+	+	+	+	+
Ilmenite	+			+	+				+
Zircon	+	+	+	+	+				+
Tourmaline		+	+						
Apatite	+	+	+	+	+	+	+	+	+

Table 3.2. Representative mineral assemblage of amphibole, garnet-phengite schists, garnet-chloritoid schists, orthogneisses and metapelites. +++, rich; ++, common; +,

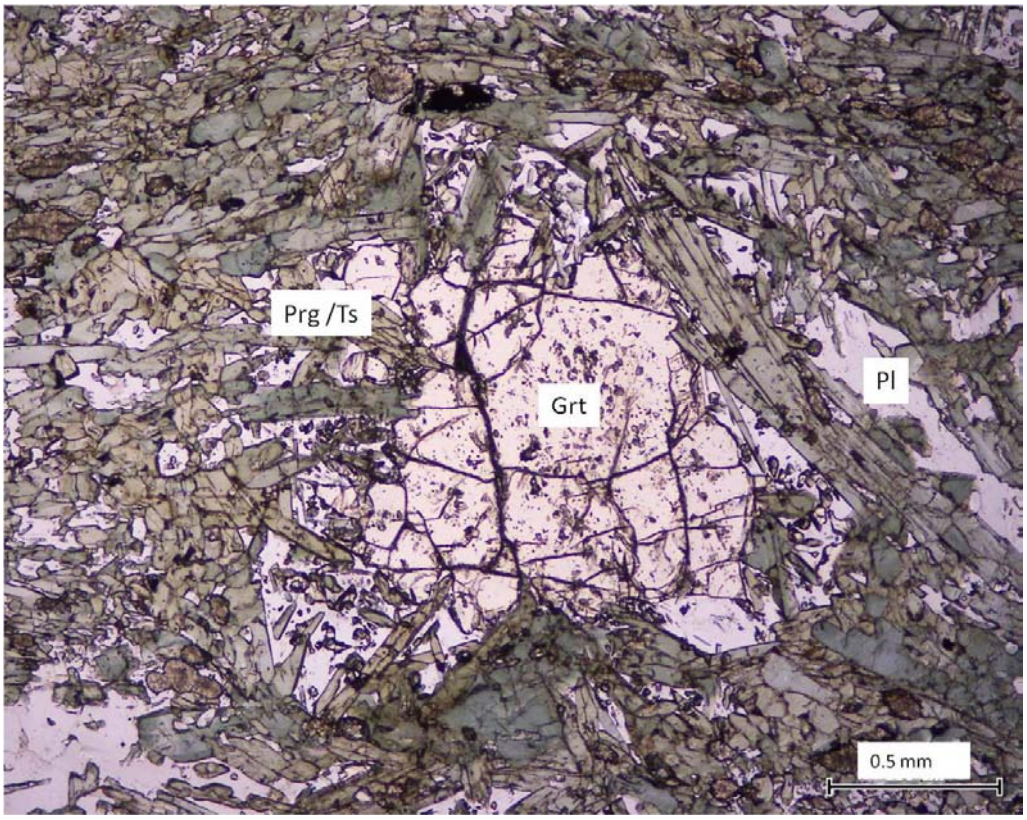

Fig.3.35 Microphotograph is showing amphibolites. Subhedral garnet surrounded by prismatic pargasite or tschermakites (Amp2) with plagioclase ($An_{<12}$) and quartz (open nicol; MG803).

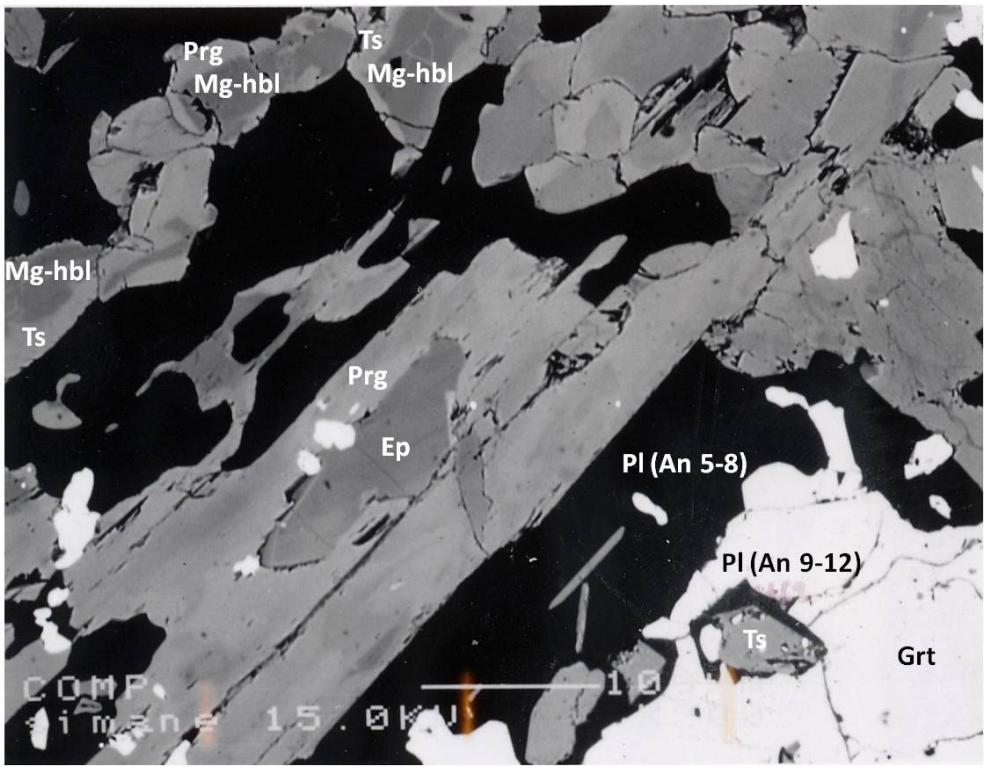

Fig.3.36 BEI is showing a zoning of amphiboles in the amphibolites. Amphiboles have a prograde zoning, Mg-hornblende core with pargasite or tschermakite rim (Amp2) coexist with plagioclase (An_{5-8}). Garnet include tschermakite (Amp1) and plagioclase (An_{9-12}) in the rim (MG803).

3.3 Garnet-phengite schists intercalating with eclogite-1

Garnet-phengite schists consist mainly of garnet, phengite and quartz, with minor chlorite, turmaline, rutile, and paragonite. Preferred orientation of phengite, paragonite and quartz defines a schistosity, however there are randomly oriented grains of phengite, plagioclase (An=12-13) and chlorites (Fig. 3.37) (Table 3.3).

Garnets occur as euhedral to subhedral porphyroblasts, and their maximum size is up to 4 mm across. Garnets in the garnet-phengite schists intercalating with eclogites bodies display a compositional zoning and divided as Grt1, Grt2 and Grt3. Grt1 has a zoning with core and mantle and both core and mantle of Grt1 partially replaced by relatively Fe-rich Grt2. Then both Grt1 and Grt2 partially replaced by overgrown Grt3. (Fig. 3.39). Sometimes the fracture of garnet is filled by albite, K-

feldspar and chlorite. Garnets contain inclusions of phengite (Ph1), paragonite, and chlorite (Chl1) (Fig. 3.38 and 3.40).

Phengite has three modes of occurrence: inclusions of phengite (Ph1), discrete grains of phengite along schistosity (Ph2) and randomly oriented phengite (Ph3) in the matrix. Ph1 inclusions occur as anhedral, and their maximum size up to 0.03 mm across. Ph2 in matrix occur as subhedral, and their maximum size up to 0.2 mm across. Ph3 in matrix occur as subhedral, and their maximum size up to 0.4 mm across. Chlorite has two modes of occurrence, i.e. inclusions of chlorite (Chl1) in the garnet (anhedral, maximum size up to 0.01 mm), discrete grains of chlorite (Chl2) which are anhedral, up to 0.1 mm across, mostly they are intercalated with Ph2 and occur in the pressure shadows of garnet. Plagioclase in matrix are subhedral, up 1 mm across intercalating with Ph2. Paragonite occur as subhedral, up to 0.02 mm across, intercalating with Ph1. Tourmaline occur as euhedral to subhedral, yellow brown in one nicol, up to 0.3 mm across. Rutile occur as anhedral, up to 0.1 mm in across.

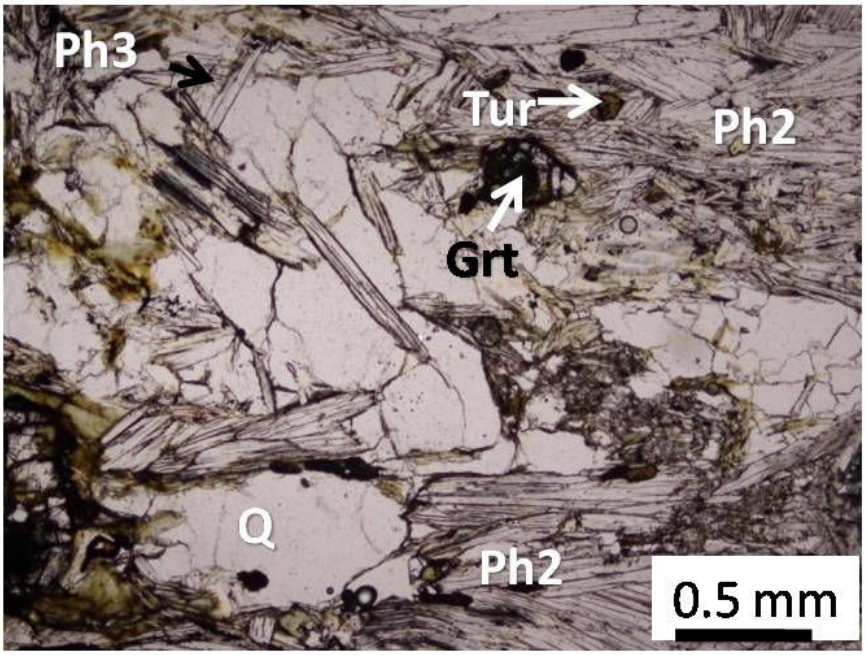

Fig.3.37 Microphotograph of garnet-phengite schist intercalating with eclogites. Schistosity forming phengites (Ph2) and quartz and randomly oriented phengite (Ph3).

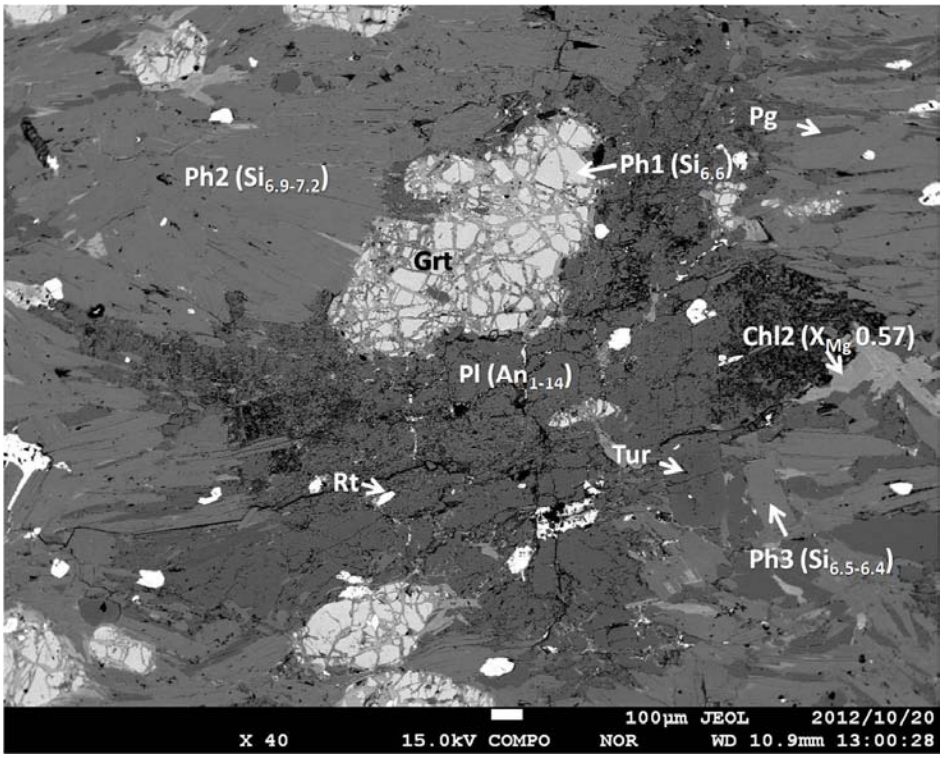

Fig.3.38 BEI image of garnet-phengite schist intercalating with eclogites. Garnet contains inclusions of Ph1. Paragonite (Pg) intercalating with Ph2. Chl2, Tur and Ph3 are randomly oriented.

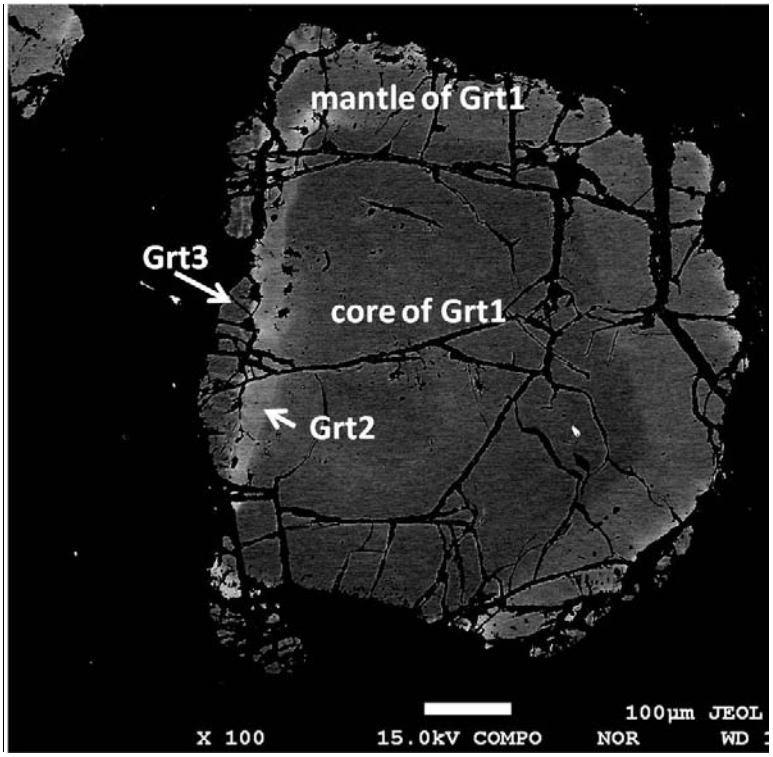

Fig.3.39 Garnet grain in the garnet-phengite schist. Resorbed Grt1 (zoned with core and mantle) partially replaced by Grt2 and overgrown by Grt3.

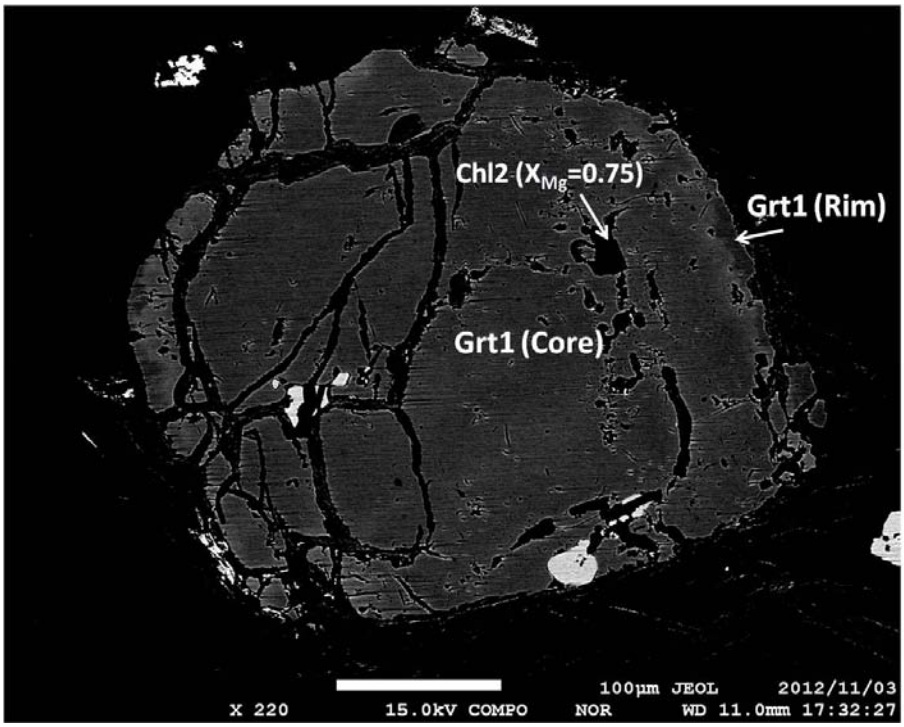

Fig.3.40 Inclusion of Mg-rich chlorite (X_{Mg}=0.75) in the Grt1.

3.4 Garnet-chloritoid schists within marble

Javkhlan et al. (2013) already described the petrographic description of garnet-chloritoid schists. The garnet-chloritoid schists consist mainly of garnet, chloritoid, white mica (phengite, muscovite and paragonite), chlorite and quartz, along with minor amounts of rutile, ilmenite, zircon and carbonaceous matter. Garnet grains occur as porphyroblasts, and occasionally contain inclusions of kyanite. Preferred orientation of chloritoid, chlorite and white micas define a schistosity (Fig. 3.41) (Table 3.3).

Subhedral to anhedral garnet porphyroblasts up to 6 mm across are typically zoned, with pale orange inclusion-rich core, and colorless inclusion-poor rim (Figs. 3.41 and 3.42). The core of the garnet contains inclusions of muscovite (Si=6.06-6.38 cations per formula unit, pfu), paragonite, chlorite (Fe-rich), chloritoid, and quartz

(Fig. 3.42). The core also contains polyphase inclusions of paragonite + chlorite ± phengitic muscovite ± quartz (Fig. 3.43c). The rim of the garnet contains inclusions of phengite (Si=6.38-6.63 pfu), chloritoid, chlorite (Fe-rich), quartz, and occasional kyanite and Mg-rich chlorite (X_{Mg}=0.38-0.42) (Figs. 3.42 and 3.43). Most garnet grains are intensely fractured, with the fractures filled by chlorite (Fe-rich) and muscovite (Si=6.15-6.23 pfu) (Fig. 3.44d).

Chloritoid occurs in the matrix as subhedral crystals up to 1.5 mm across (Fig. 3.44c), containing inclusions of phengite, paragonite, phengitic muscovite, rutile, and quartz. Chloritoid in the matrix is occasionally replaced by Fe-rich chlorite along the rim (Fig. 3.44c). Chloritoid inclusions up to 0.04 mm in diameter also occur within the garnet (Figs. 3.41 and 3.42).

Phengite in the matrix occurs as subhedral to anhedral crystals up to 1 mm across (Fig. 3.41). Paragonite occurs as inclusions in the core of the porphyroblastic garnet (<0.05 mm), and as inclusions within chloritoid (<0.1 mm). Paragonite grains are also found in the matrix as subhedral to anhedral grains about 1.5 mm across, intercalated with phengitic muscovite (Fig. 3.43c).

Chlorite in the matrix consists of subhedral to anhedral grains up to 3 mm across, with zoning from pale green core (Mg-rich) to greenish rim (Fe-rich) (Fig. 3.43b).

Kyanite is occasionally present as inclusions in the rim of the porphyroblastic garnet, as tiny anhedral grain up to 0.03 mm across (Figs. 3.42 and 3.43a).

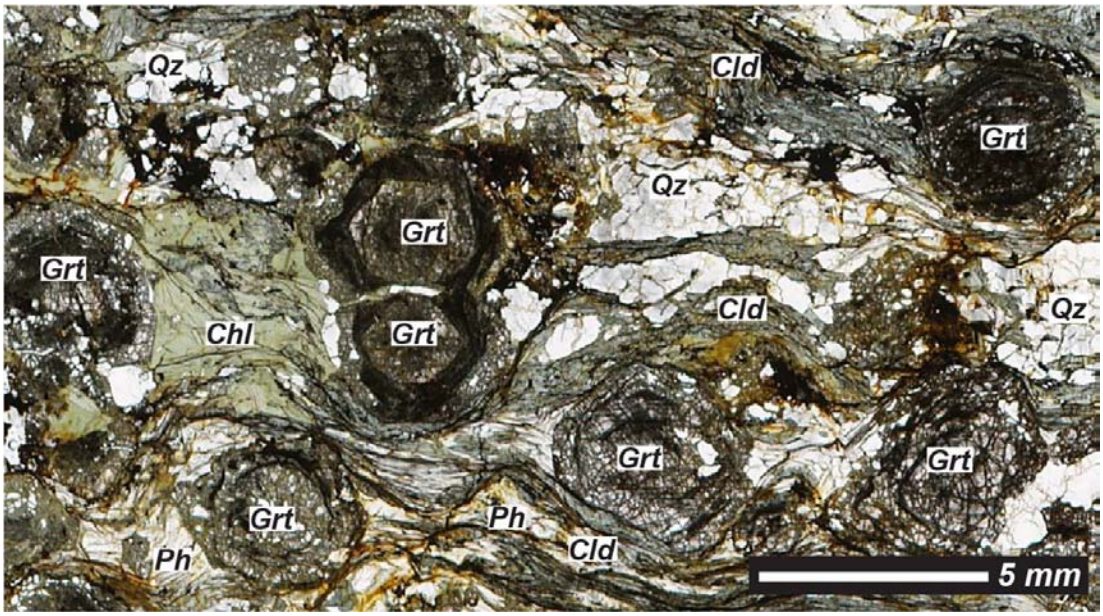

Fig.3.41 Microphotograph is showing garnet-chloritoid schist (after Javkhlan et al., 2013). Porphyroblastic garnet includes chloritoid, paragonite and chlorite. Muscovite, hematite, and quartz occur among the garnet grains (open nicol; MG812).

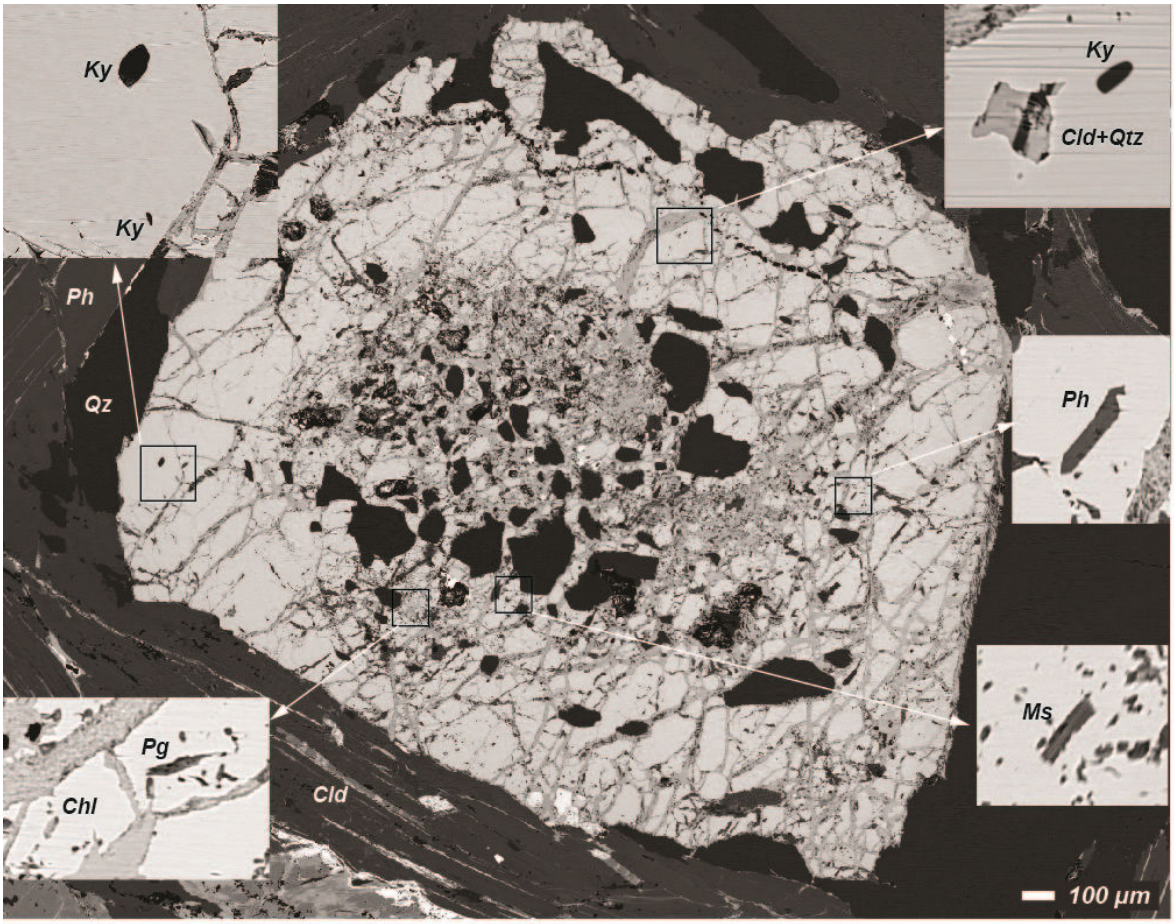

Fig.3.42 BEI images of a porphyroblastic garnet in garnet-chloritoid schist from the Maykhan tsakhir Formation (after Javkhlan et al., 2013). The garnet is zoned, with inclusion-rich core and inclusion-poor rim. The core contains muscovite, paragonite and chlorite, and the rim contains kyanite, chloritoid, phengite and quartz.

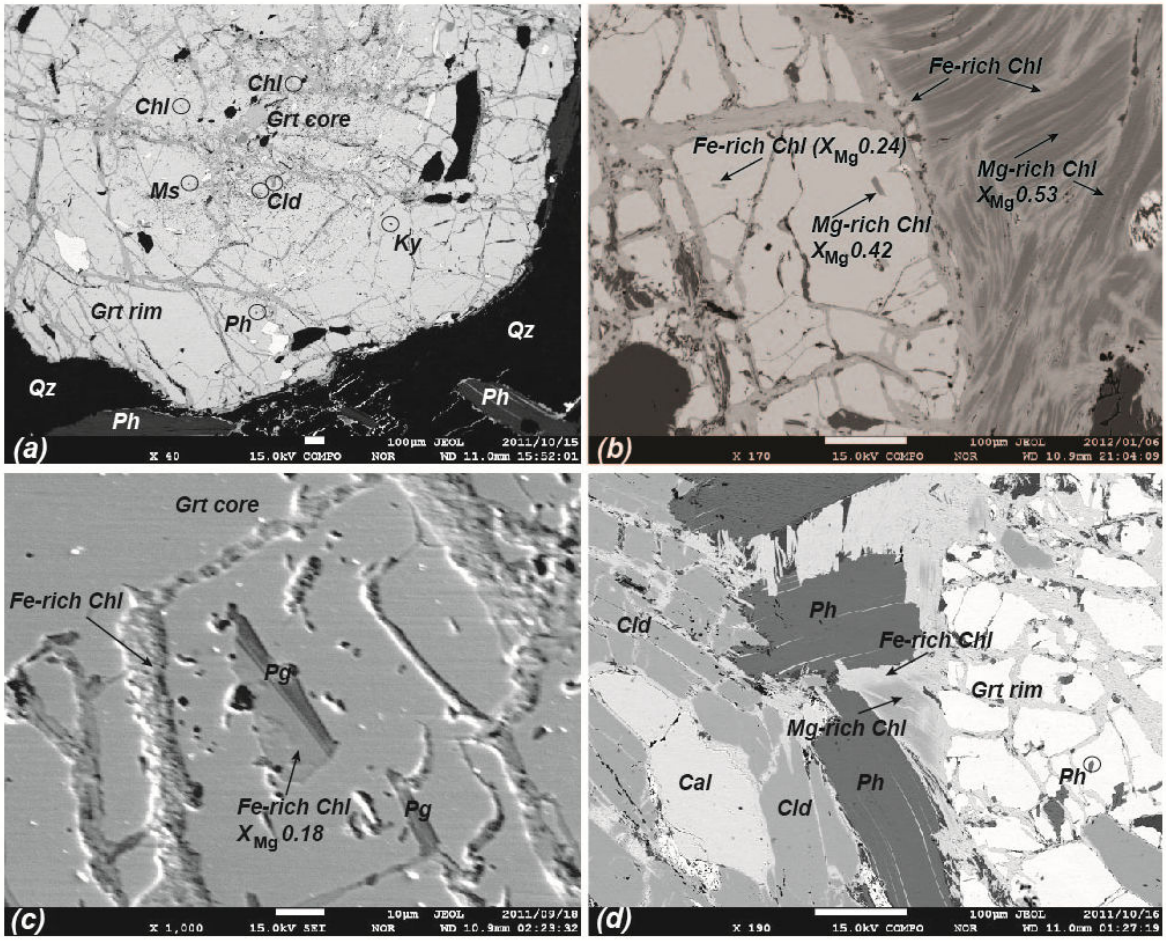

Fig.3.43 BEI images of kyanite-garnet-chloritoid schists from the Maykhan Tsakhir Formation (after Javkhlan et al., 2013). (a) Inclusion-rich core and inclusion-poor rim of porphyroblastic garnet. Porphyroblastic garnet contains inclusions of chlorite, muscovite and chloritoid in the core and kyanite and phengite in the rim. (b) Rim of the garnet containing inclusions of Mg-rich chlorite; Mg-rich chlorite in the matrix is rimmed by Fe-rich chlorite. (c) Polyphase inclusions of paragonite + chlorite in the core of a garnet. (d) Coexisting garnet, phengite, chlorite and chloritoid; Mg-rich cores of chlorites are rimmed by Fe-rich chlorite.

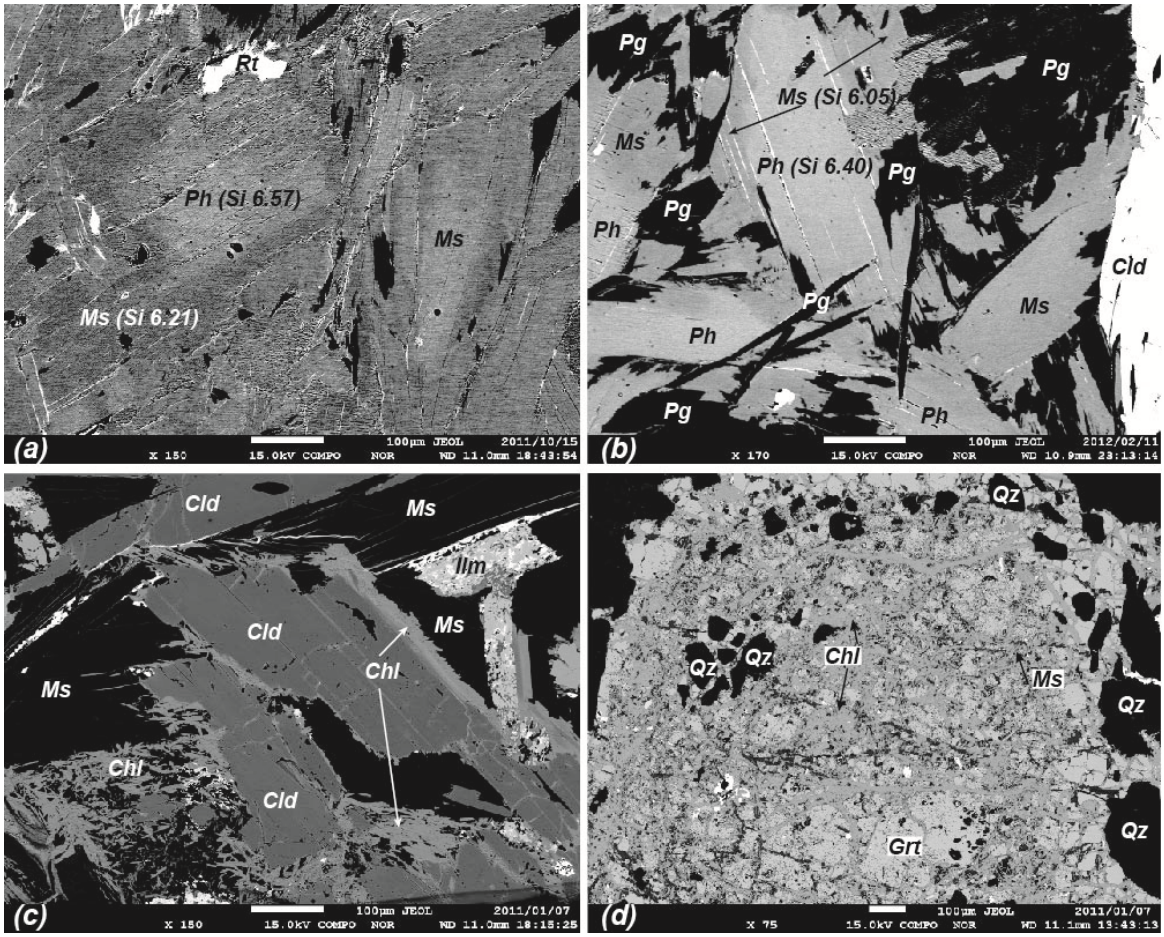

Fig.3.44 BEI images of the garnet-chloritoid schists (after Javkhlan et al., 2013). (a) Phengites in the matrix rimmed by muscovite. (b) Paragonites coexisting with muscovites rimming phengites. (c) Chloritoids in the matrix rimmed by chlorites. (d) Strongly fractured porphyroblastic garnet; fractures are filled by chlorite and muscovite.

3.5 Pelitic schist intercalating with orthogneisses

Pelitic schists consist mainly of garnet, quartz, and phengite with minor epidote, rutile, ilmenite, chlorite, and hematite (Fig. 3.45) (Table 3.3). Schistosity defined by phengites, quartz and epidotes. Garnets occur as porphyroblast and they are subhedral grain up to 6 mm across. They are intensely fractured. Quartz and rutile are included in garnet as inclusion.

Phengite occurs in the matrix, and it is of subhedral crystal up to 1 mm across. They are sometimes rimmed by muscovite. Epidote occurs as subhedral porphyroblastic, up to 2 mm long. It includes rutile as inclusion. Rutile occurs as inclusion in the garnet and as discrete grain in the matrix. It is usually rimmed by ilmenite. Hematite rarely occurs in the matrix. Chlorite occurs in the matrix often replacing phengite.

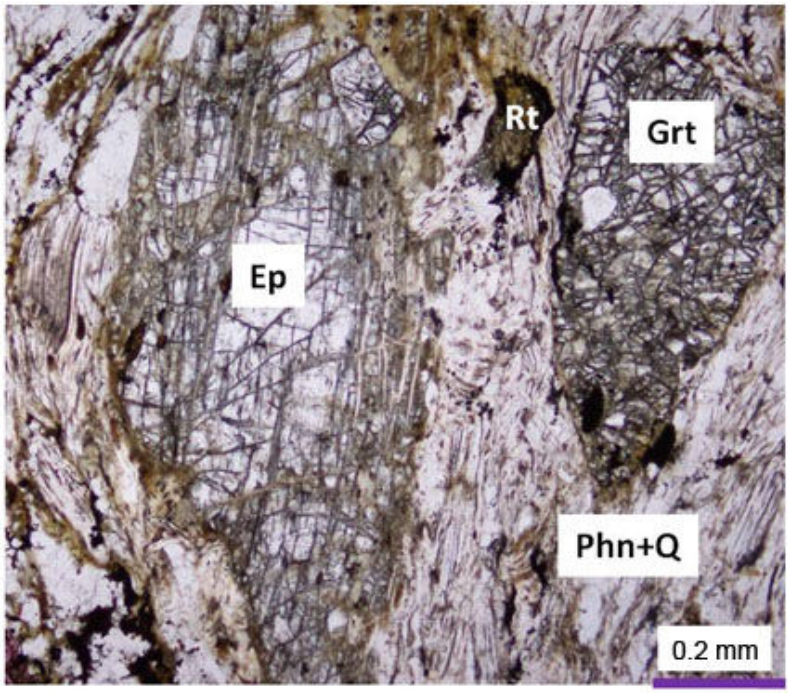

Fig.3.45 Microphotograph is showing garnet-phengite schist. Phengite, quartz, and rutiles occur among the porphyroblastic garnet and epidote (open nicol; MG827).

3.6 Orthogneisses

3.6.1 Vein-type orthogneiss

The vein-type orthogneiss (sample MG1220-1) consists mainly of quartz, albite (An=0-1) with minor amounts of K-feldspar, phengite, epidote and chlorite. Accessory minerals are garnet, calcite, zoisite, rutile, titanite, zircon, monazite, apatite and hematite. Textures are fine-grained, granular (Fig. 3.46) (Table 3.3).

The vein-type orthogneiss can be divided as (i) albite-quartz rich part and phengite-rich compositional layer. Albite-quartz rich part consists mainly of quartz and albite with minor phengite, epidote, K-feldspar and garnet; and (ii) phengite-rich layer consist mainly of phengite with minor epidote, chlorite, K-feldspar, albite and quartz (Fig. 3.46).

Quartz and albite are anhedral and up to 0.5 mm across.

Phengite occurs as two modes of occurrence, i.e., relict grains of phengite 1 (Ph1) (subhedral up to 0.5 mm across) overgrown by phengite (Ph2) (subhedral up 0.1 mm across) in the albite-quartz rich part (Fig. 3.46 and 3.47). Phengite-rich layers composed mainly of Ph2 (subhedral up 0.1 mm across) with minor chlorites, epidotes and K-feldspars (Fig. 3.46 and 3.47). Relics of Ph1 occasionally preserved in the Ph2 in the phengite-rich layer (Fig. 3.48).

Chlorites occur as four modes of occurrence i.e., chlorite 1 (Chl1) rarely occur as small (up to 0.02 mm long) aggregate with epidotes in the albite-quartz rich part, chlorite 2 (Chl2) (up to 0.2 mm long, anhedral.) intercalating Ph2 (Fig. 3.46 and 3.47), and chlorite 3 (Chl3) filling fractures of garnet grains (Fig. 3.50). K-feldspars occur as anhedral to subhedral, up to 0.2 mm across (Fig. 3.48).

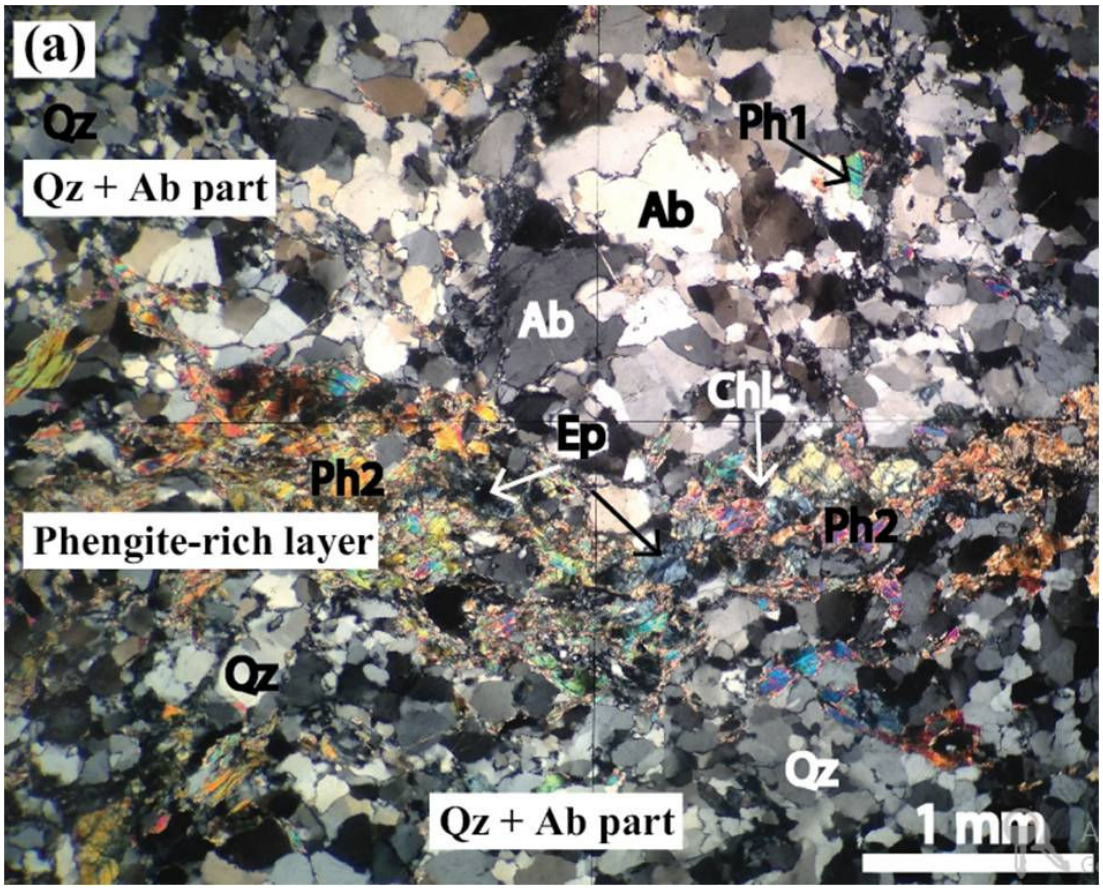

Fig.3.46The vein-type orthogneiss (MG1220-1) which consist of mainly of quartz + albite assemblage and minor phengite-rich layer.

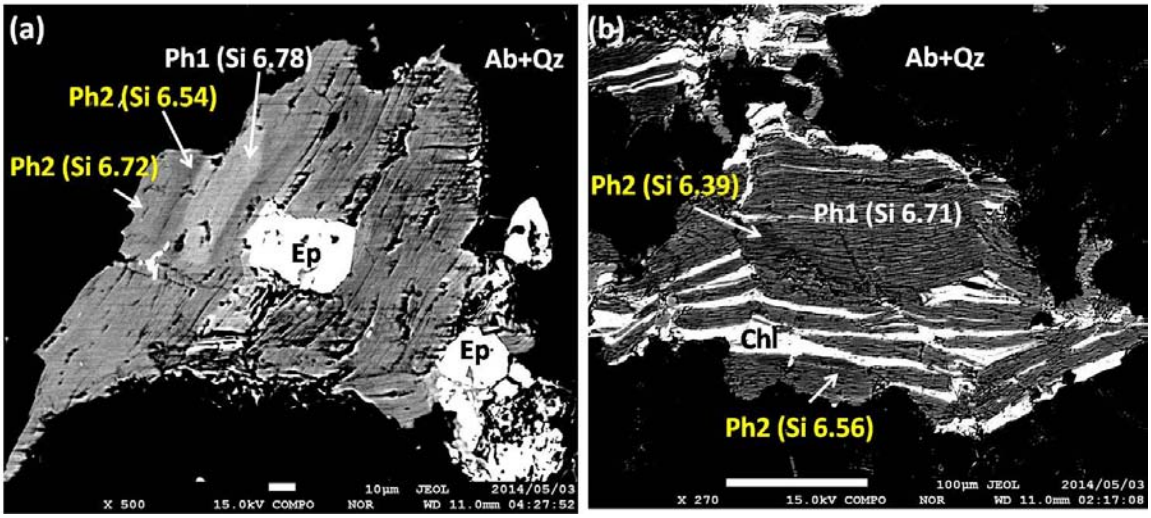

Fig.3.47BEI image of vein-type orthogneiss. (a) Resorbed Ph1 rimmed by muscovite (Ms) and overgrown Ph2 in the albite-quartz rich part of vein-type orthogneiss. (b) Resorbed Ph1 rimmed by Ms and overgrown Ph2 intercalated with Chl (Chl2).

Epidotes occur as two modes of occurrence i.e., relict grains of epidote (Ep1) overgrown by secondary epidote (Ep2) (Fig. 3.49). Ep1 is of anhedral to subhedral, up to 0.05 mm across. Ep2 coexisting with garnet and phengite in the albite-quartz rich part (Fig. 3.50) and in the phengite-rich layer with Ph2, Chl2 and K-feldspar (Figs. 3.48 and 3.49). Ep2 locally contains relict grains of Ep1 in the albite-quartz rich domain (Fig. 3.49). Some of Ep2 grains are partially replaced by albite and quartz. Rarely, fine grained, anhedral zoisite grains occur as inclusions in the K-feldspar.

Subhedral to euhedral garnet is up to 0.5 mm across. It is optically zoned from pale green core to colorless rim. Cores of garnet are resorbed and overgrown by colorless rims. Occationally, relic garnets are observed in the cores of garnet (Fig. 3.50 and 3.51). Inclusions of quartz and phengite are occasionally. Fractures are intensely developed in garnet and are mainly filled by chlorite (Chl3), K-feldspar and quartz (Fig. 3.50 and 3.51). Rutile is entirely or partially replaced by titanite.

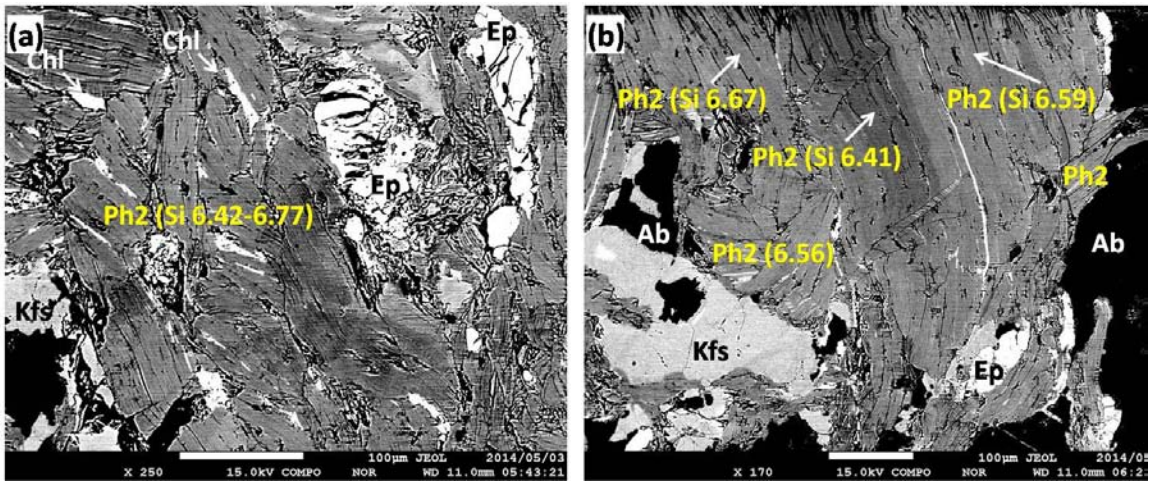

Fig.3.48 BEI image of vein-type orthogneiss. (a) Ph2 and chlorite (Chl2), epidote (Ep2) and K-feldspar in the phengite-rich layer. (b) Ms surrounded by Ph2, K-feldspar and epidote (Ep2) in the phengite-rich layer.

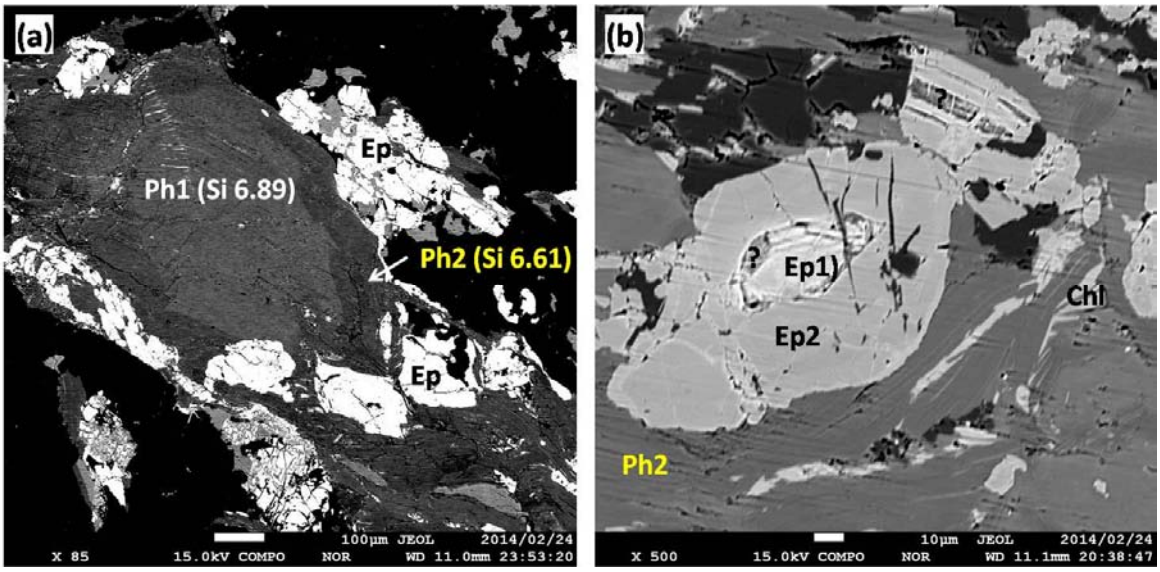

Fig.3.49 BEI image of vein-type orthogneiss. (a) Resorbed Ph1 and surrounding Ph2 and Ep2 in the phengite-rich layer. (b) Core of resorbed Ep1 with rim of Ep2 in the phengite-rich layer.

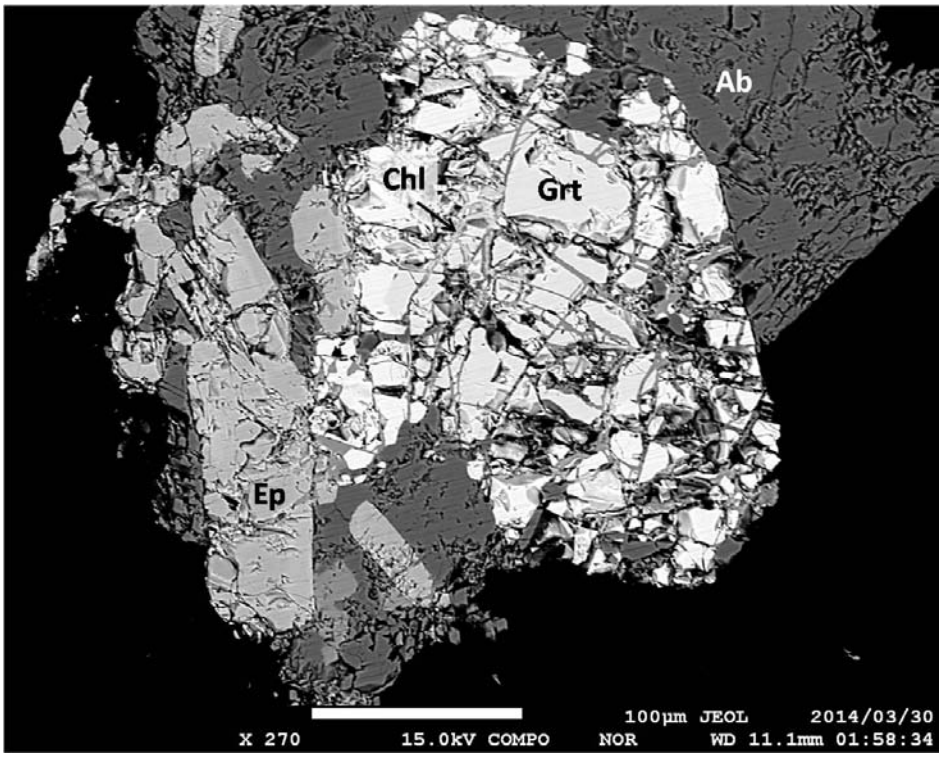

Fig.3.50 BEI image of vein-type orthogneiss. Garnet and epidote (Ep2) in the albite-quartz rich part. Garnet is intensely fractured and fractures filled by chlorite (Chl3) and K-feldspar.

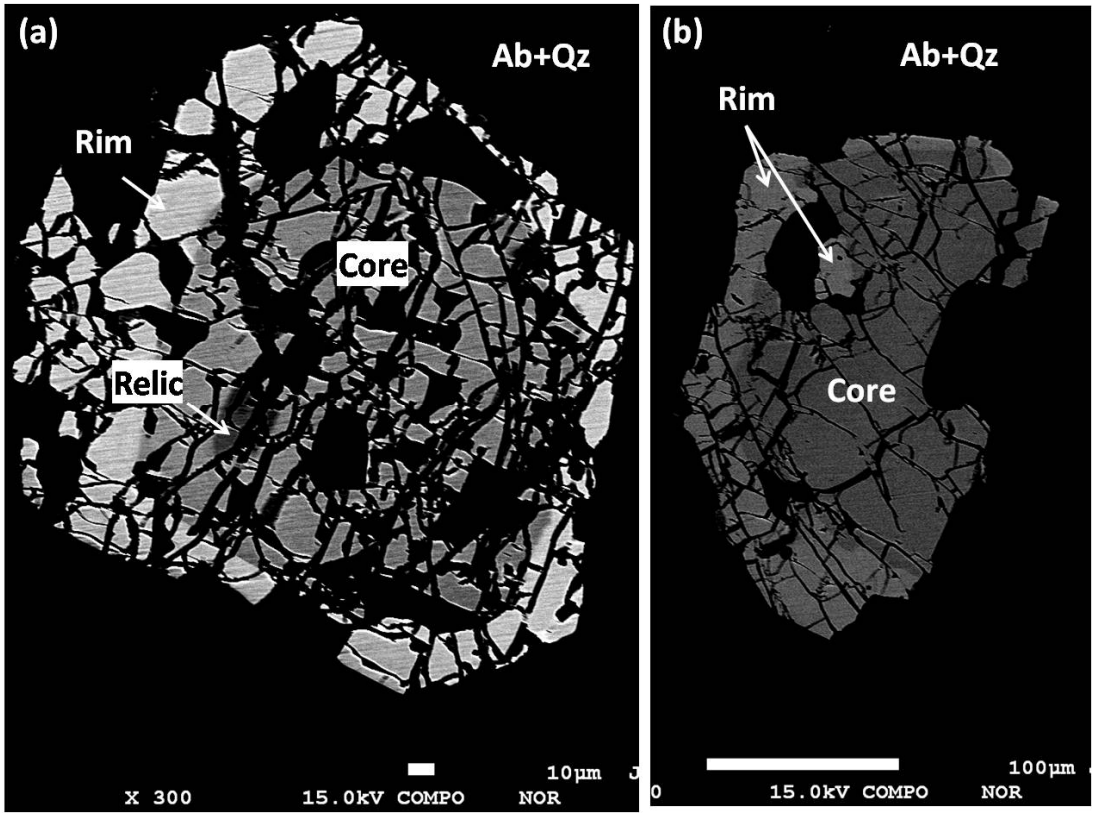

Fig.3.51 BEI images of garnets in the vein-type orthogneiss. (a) Garnet composed of core, mantle and rim. (b) Mantle of garnet has been resorbed and early stage of fracture formed. When rim of garnet overgrown on mantle, some part of rim of garnet overgrown on the fracture site.

3.6.2 Orthongeisses surrounding eclogite bodies

Orthogneiss surrounding eclogite bodies (MG1228-1 and MG1229) consists mainly of quartz and albite with minor amounts of phengite and K-feldspar in the both samples (MG1228-1 and MG1229), except epidote, dolomite, chlorite, calcite, muscovite present in the sample MG1228-1 (Figs. 3.52 and 3.53). Accessory minerals of rutile, zircon, and apatite are present in the both sample (Table 3.3). Orthogneiss shows fine- to medium-grained and granular texture. In the sample MG1228-1, calcite, plagioclase, quartz and dolomite aggregates are sometimes formed large rectangular shape, indicating previous mineral were probably magmatic in origin (Fig. 3.52). In the sample MG1229, large K-feldspar and plagioclase (up to 1.5 mm across) with twin-interface regarded as also magmatic in origin and they are partially replaced by phengite and albite assemblage (Fig. 3.53). Dolomite-rich micro-veins with up to 0.3 mm in thickness intensely developed in the orthogneiss of MG1228-1 (Fig. 3.52).

Quartz and albite are replaced by fine-grained chlorites, dolomite and K-feldspar in the sample MG1228-1 (Fig. 3.54) whereas in the sample MG1229 are not (Fig. 3.55).

Phengite in the sample MG1228-1 occur as subhedral crystal up to 1 mm across intercalated with fine-grained chlorite and K-feldspar. Resorbtion texture preserved in the phengite grains that phengite with slightly higher Si content (6.76-6.84) (Ph1) overgrown by phengite with lower Si content (6.69-6.73) (Ph2) (Fig. 3.54a). Dolomite-rich micro-vein locally infiltrated into phengites.

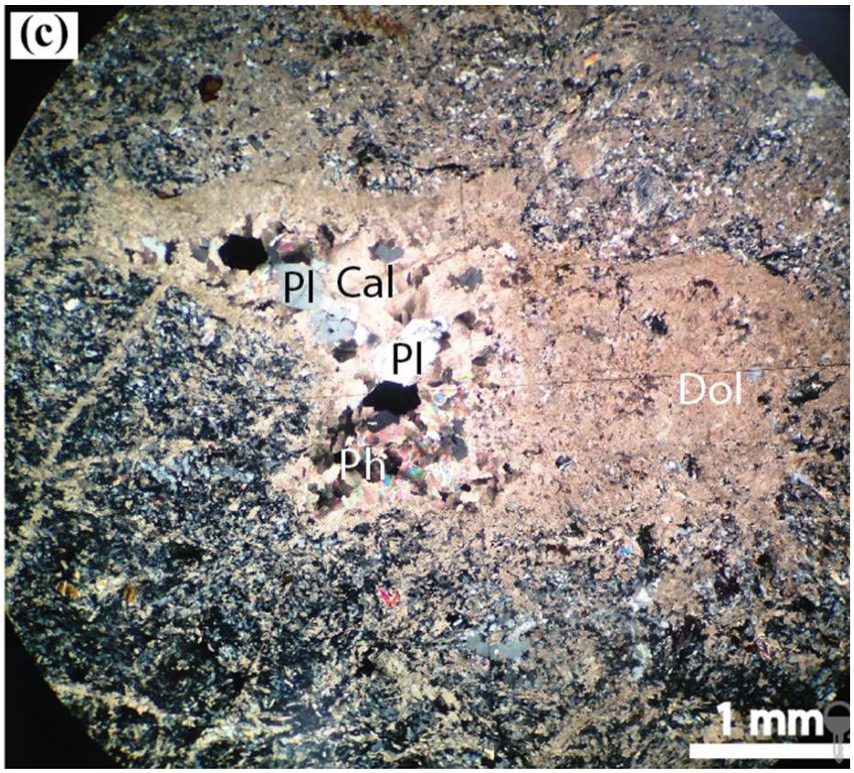

Fig.3.52 Orthogneiss (MG1228-1) surrounding eclogite bodies. Dolomite-rich micro veins intensely developed in the rock. Unknown probably magmatic mineral fully replaced by quartz, plagioclase, calcite and dolomite preserved in the orthogneiss.

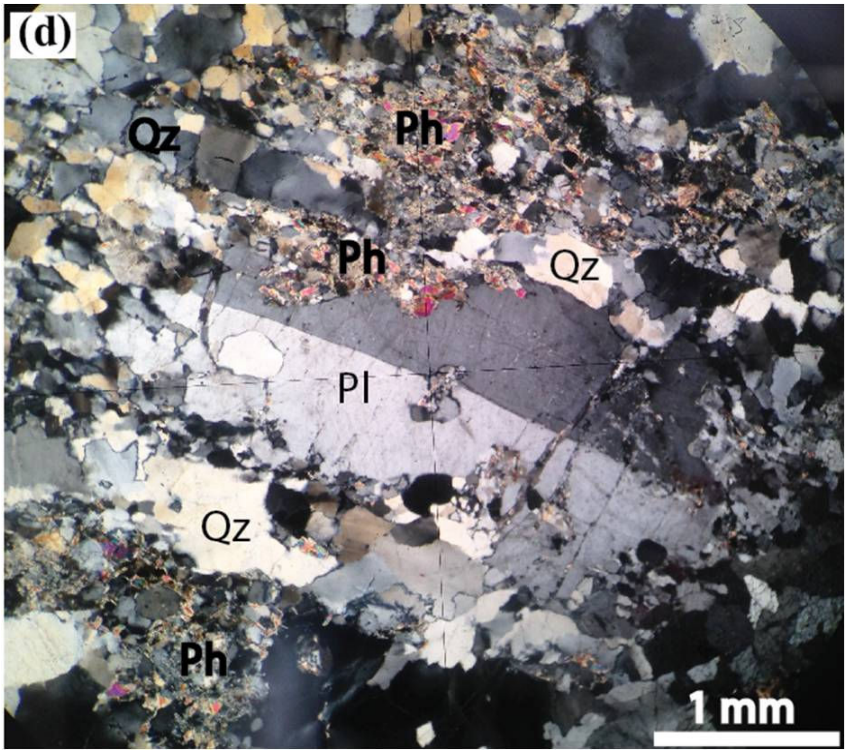

Fig.3.53 Orthogneiss (MG1229) surrounding eclogite bodies. Orthogneiss (MG1229) close to the outcrop of sample MG1228-1. Magmatic plagioclase preserved and they were partially replaced by quartz and phengite.

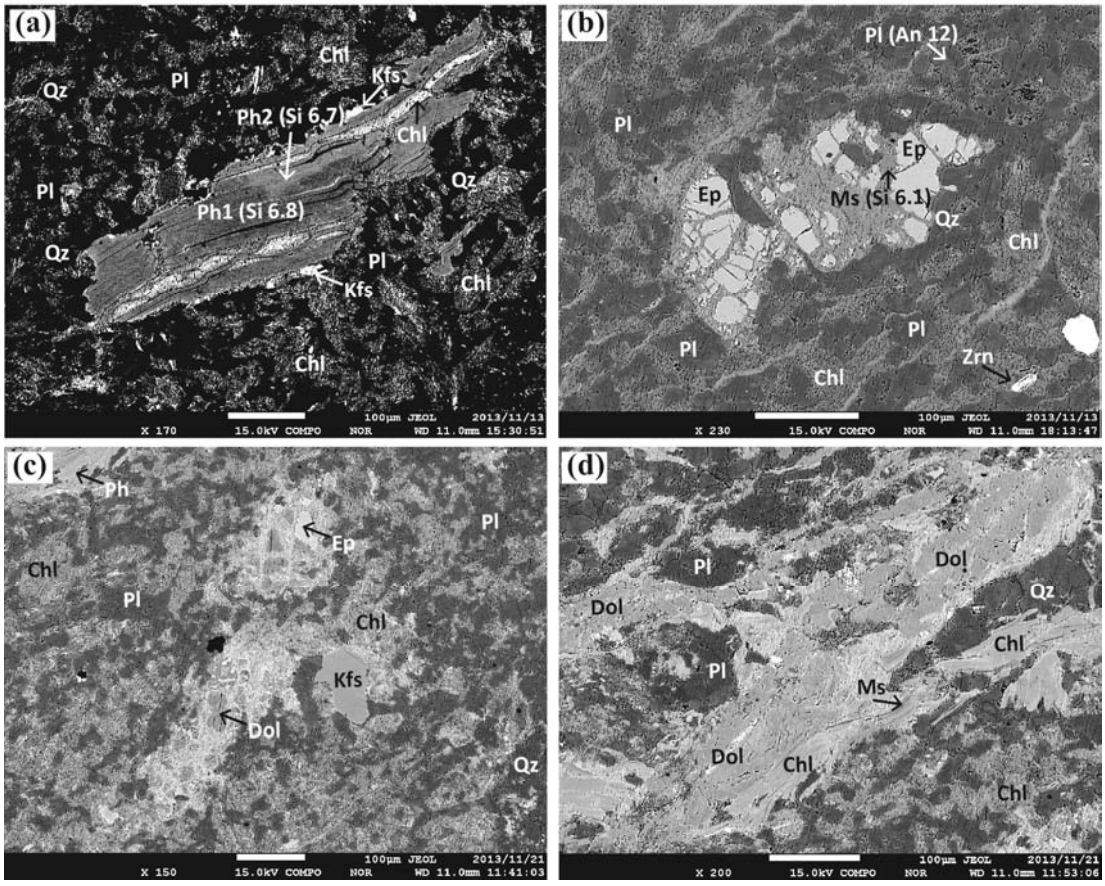

Fig.3.54 Back-scattered electron images of orthogneiss surrounding eclogite bodies (sample MG1228-1). (a) Phengite intercalated with chlorite within dolomitized quartz and plagioclase assemblage. (b) Epidote partially replaced by chlorite and muscovite within quartz and plagioclase dolomitized assemblage. (c) Discrete grains of K-feldspar, epidote, phengite and dolomite surrounded by quartz plagioclase dolomitized assemblage. (d) Dolomite-rich micro-vein mainly consisting dolomite minor chlorite and muscovite.

Phengite in the sample MG1229 occur as subhedral crystal up to 0.2 mm across. Resorbtion texture also preserved in the phengite grains that phengite with high Si content (6.59-6.84) (Ph1) overgrown by phengite with low Si content (6.39-6.42) (Ph2) (Fig. 3.55a).

In the sample MG1228-1, discrete grains of K-feldspar occur as subhedral up to 0.5 mm across (Fig. 3.54c). Epidote grains occur as subhedral up to 0.3 mm across (Fig. 3.54b). Micro-fracture developed in epidote grains, and it is filled by chlorite, dolomite, rarely muscovite (Si=6.12 pfu) and quartz (Fig. 3.54b). Dolomites which are fine grained occur as discrete grains in the matrix and filling dolomite-rich micro-

veins. Dolomite-rich vein mainly consist of dolomite with minor chlorite and quartz (Fig. 3.54d).

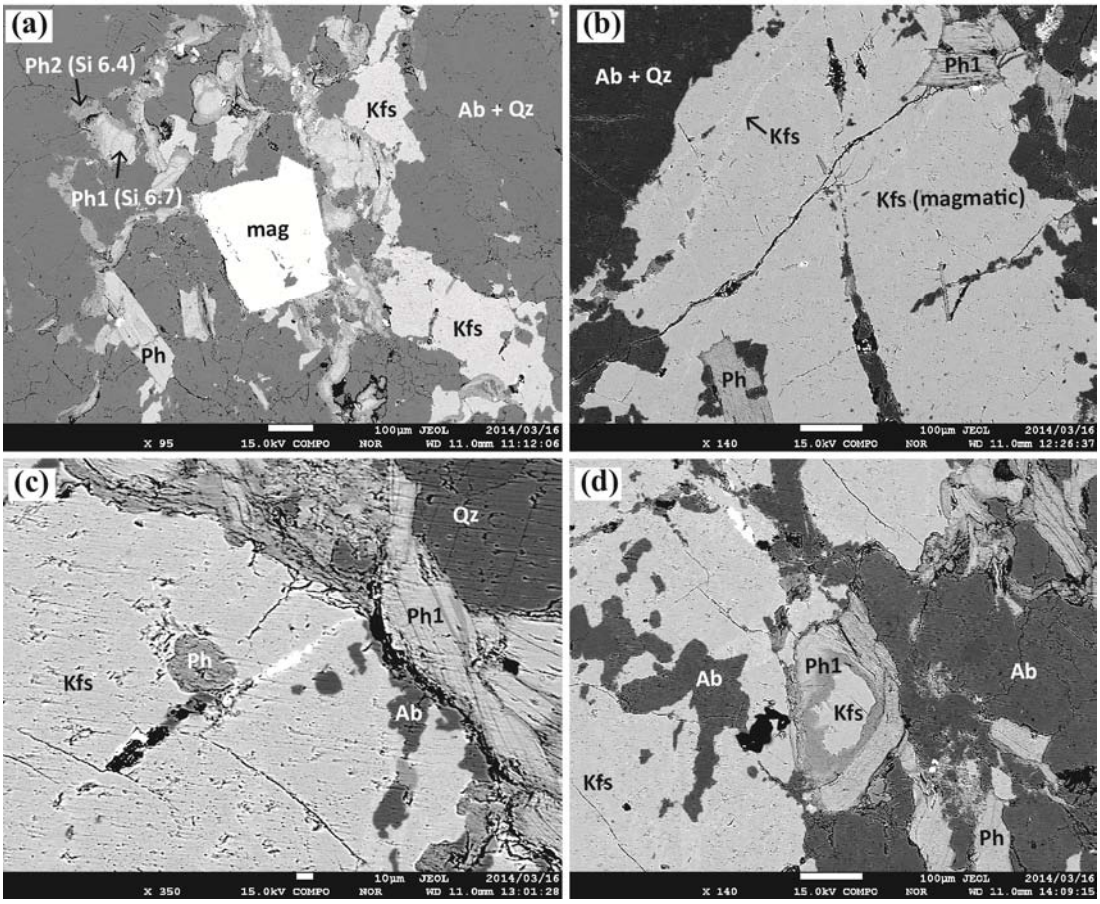

Fig.3.55 Back-scattered electron images of orthogneiss surrounding eclogite bodies (sample MG1229). (a) Phengite, magnetite, K-feldspar surrounded by albite and quartz assemblage. (b), (c) and (d) Magmatic K-feldspar partially replaced by phengite, albite and secondary K-feldspar.

3.7 Khantaishir ophiolites

Khantaishir ophiolites in the Chandman district is consist mainly of epidotized tuffs, agglomerate crystallic tuffs, greenschists, metabasalts and minor metadiorite, metadolerite, locally with serpentinite boudins. All these rocks are strongly chloritized and epidotized.

Metatuffs consist mainly of chlorite, epidote, albite and minor titanite and carbonates. Schistosity defined by chlorites, epidotes, albites and quartz (Fig. 3.56). Chlorites are anhedral, and they are up to 0.3 mm long. Epidotes are anhedral to subhedral up to 0.2 mm across. Albite are anhedral up to 0.2 mm long. Quartz are anhedral up to 0.1 mm across. Titanites are anhedral up to 0.1 mm across.

Metabasalts are massive, fine-to medium-grained and they consist of chlorite, plagioclase, epidote, and minor quartz, titanite, magnetite and carbonates. Preferred orientation defined by chlorite, epidote, albite and quartz (Fig. 3.57). Chlorite filling micro-fractures developed in the metabasalt. Epidote are anhedral to subhedral up to 0.2 mm across. It has zoning with core [$X_{Ps}(Fe^{3+}=(Al+Fe^{3+})$]=0.22-0.25 and rim ($X_{Ps}$=0.32-0.35). Chlorites are anhedral, and they are up to 0.1 mm long. Hematites are anhedral to subhedral, and up to 0.05 mm across.

Metadiorites are coarse-grained, composed of porphyrblastic amphibole (actinolite and Mg-hornblende) albite, epidote and minor quartz, chlorite, titanite and hematite (Fig. 3.58). Porphyroblastic amphibole (up to 4 mm long) has zoning with Act core (Si=7.52 pfu and Al_2O_3=2.78 wt%), Mg-hornblende mantle (Si=6.98-7.45 pfu and Al_2O_3=2.77-5.82 wt%) and actinolite rim (Si=7.79-7.86 pfu and Al_2O_3=0.85-1.12 wt%). It has a pleochroic with x'=pale yellow green and z'=pale green core x'=pale brown z'=brown mantle and x'=pale green z'=green rim. Amphiboles

surrounded by epidote, chlorite and albite. Epidotes crystallized as fine grained, fully replaced large prismatic crystal with chlorites. Prismatic euhedral chlorite (X_{Mg}=0.53) rarely identified and it surrounded by fine grained anhedral chlorites (X_{Mg}=0.60-0.65). Albite and quartz are recrystallized up to 0.5 mm across.

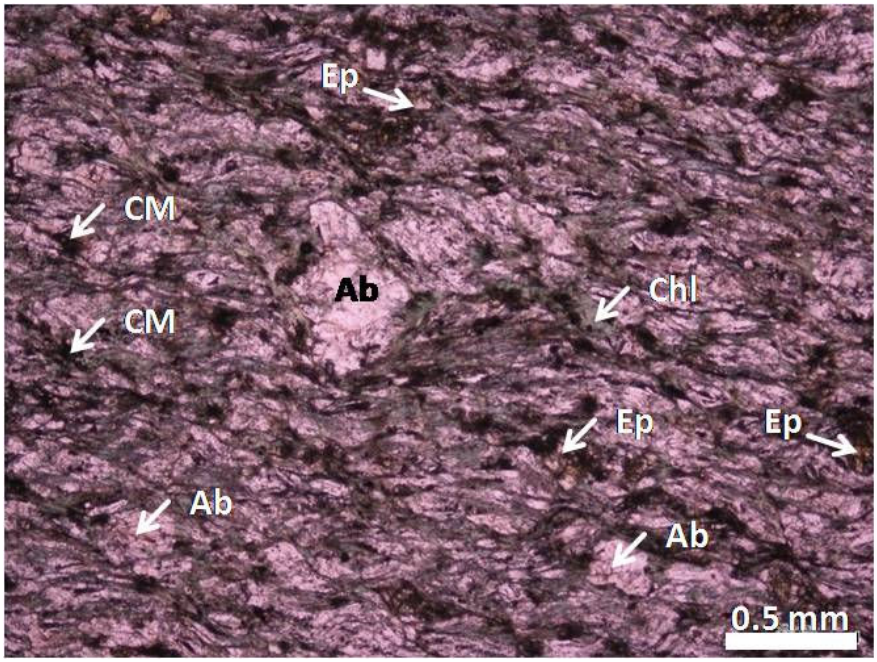

Fig.3.56 Metatuff (MG1234) of Khantaishir Formation. Metatuff consist mainly of chlorite (Chl), albite (Ab), epidote (Ep) and carbonaceous matter (CM).

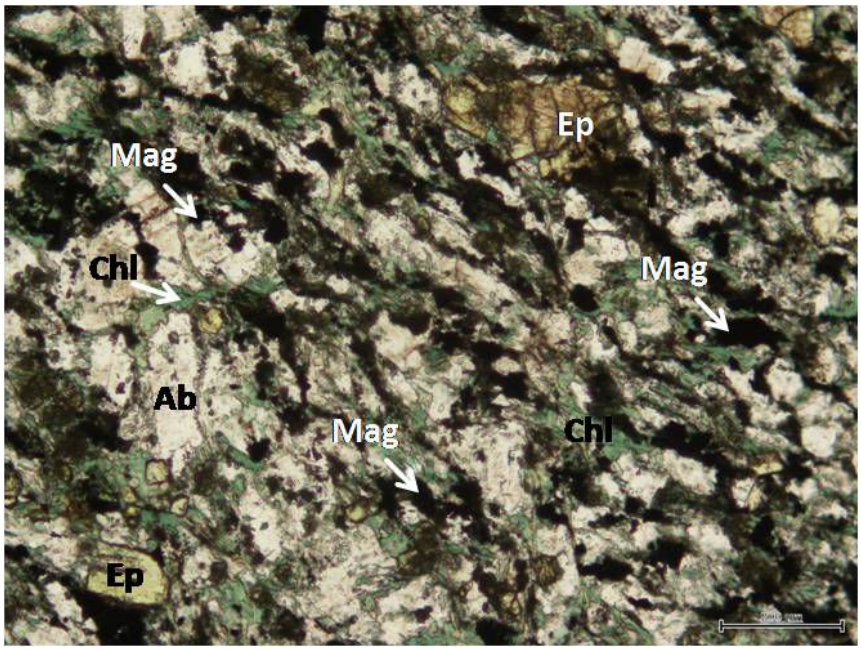

Fig.3.57 Metabasalt (MG1237) of Khantaishir Formation. Metabasalt consist mainly of chlorite (Chl), albite (Ab), epidote (Ep) and magnetite (Mag).

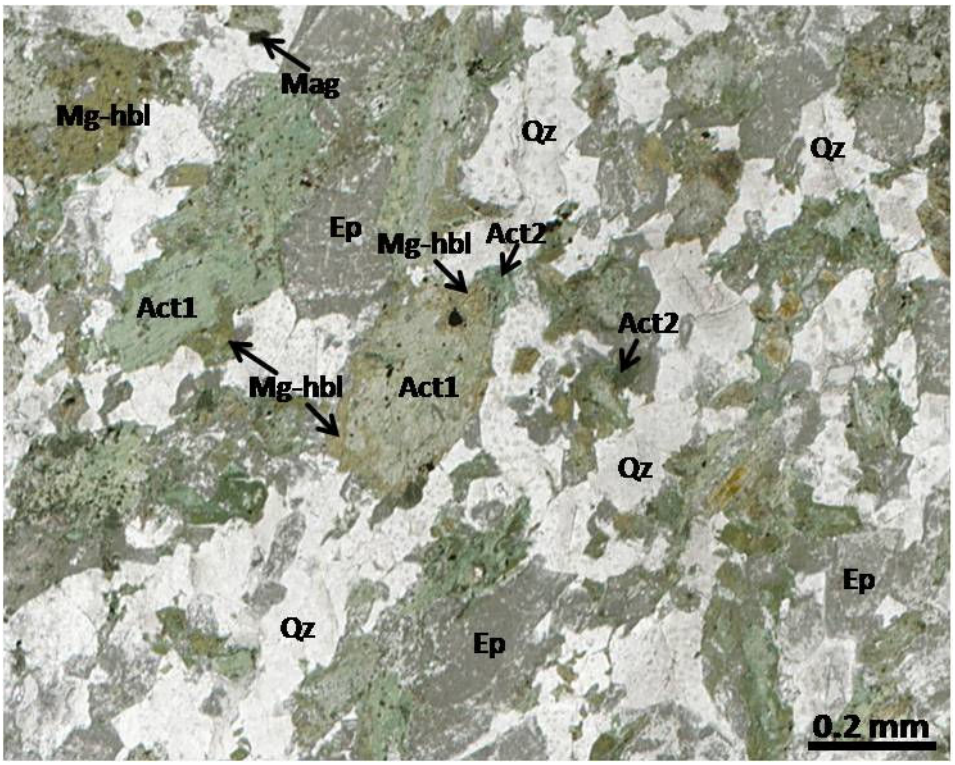

Fig.3.58 Metadiorite (MG1240) of Khantaishir Formation. Metadiorite consist mainly of zoned amphibole (Act1→Mg-Hbl→Act2), albite (Ab), epidote (Ep), quartz and magnetite (Mag).

CHAPTER 4 MINERAL CHEMISTRY

4.1 Analytical procedures

Chemical compositions of minerals were measured using electron probe microanalysers (JEOL JXA-8800M and JXA-8530F) at the Department of Geoscience, Shimane University. The analytical conditions used for all minerals were a 15 kV accelerating voltage, 20 nA beam current and 3-5 μm in diameter. Corrections were carried out using the procedures of Bence and Albee (1968). Ferric iron contents in garnet and clinopyroxene were estimated on the basis of charge balance [Fe^{3+} = 8 - 2Si - 2Ti - Al (for garnet)]; [Fe^{3+} = 4 - 2Si - 2Ti – Al + Na (for clinopyroxene)]. Jadeite, aegirine and augite contents (mol.%) in clinopyroxene were estimated as Jd=AlVI*100, Aeg=Na - Jd or Aeg = Fe^{3+}, if (Na-Jd) ≥ Fe^{3+}, and Aug = 100 - (Jd + Aeg), respectively. Ferric iron contents in amphibole were estimated as total cations 13 = Si + Al + Ti + Cr + Mg + Fe + Mn [(for O=23; 13eCNK method of Schumacher, in Leak et al. (1997)].

The mineral abbreviations used in the text, tables and figures follow Whitney and Evans (2010).

4.2 Garnets

Garnets in the eclogites-1 are pyralspite type with Alm_{45-63} Grs_{24-34} Prp_{5-20} Sps_{2-14} in the core, Alm_{54-61} Grs_{25-34} Prp_{6-21} Sps_{1-2} in the rim, and Alm_{45-61} Grs_{24-26} Prp_{15-32} $Sps_{<1}$ in the outermost rim. Garnets have prograde zoning, spessartine (X_{Sps}) decreasing from core (0.03-0.08) to rim (0.01-0.05) whereas the pyrope component (X_{Prp}) increases from core (0.05-0.06) to rim (0.05-0.15). Grossular (X_{Grs}) is relatively homogeneous in the core (0.25-0.29), slightly increasing to the rim (0.27-

0.31), but when X_{Prp} is increasing to the rim X_{Grs} decrease (0.30-0.23). Almandine (X_{Alm}) is relatively homogeneous (0.57-0.63); slightly decrease to the rim (Fig.4.2).

Garnets in amphibolized eclogites-1 are Alm_{53-62} Grs_{22-31} Prp_{14-18} $Sps_{<2}$ for aggregates of relic eclogitic garnet (Grt1), Alm_{59-66} Grs_{14-16} Prp_{16-25} Sps_{1-2} for secondary garnets (Grt2) which are replacing Grt1 and intercalating with tschermakitic amphiboles (Amp2), Alm_{65-68} Grs_{15-19} Prp_{12-15} Sps_{3-5} for fracture filling garnet (Grt3) after the Grt2 and Alm_{48-54} Grs_{31-38} Prp_{4-5} Sps_{9-11} for thin films of Mn-rich garnet (Grt4) replacing Grt1 and Grt2. All modes of occurrences of garnets (Grt1, Grt2, Grt3 and Grt4) are relatively homogeneous in compositions (Fig. 4.1).

Grt1 of amphibolized eclogites-1 are comparable in compositions with mantle and rim of garnets in the eclogites-1, whereas the Grt2 of amphibolized eclogites-1 distingtly lower in Grs and slightly higher in Prp contents than mantle and rim of garnets in the eclogites-1 (Fig. 4.1).

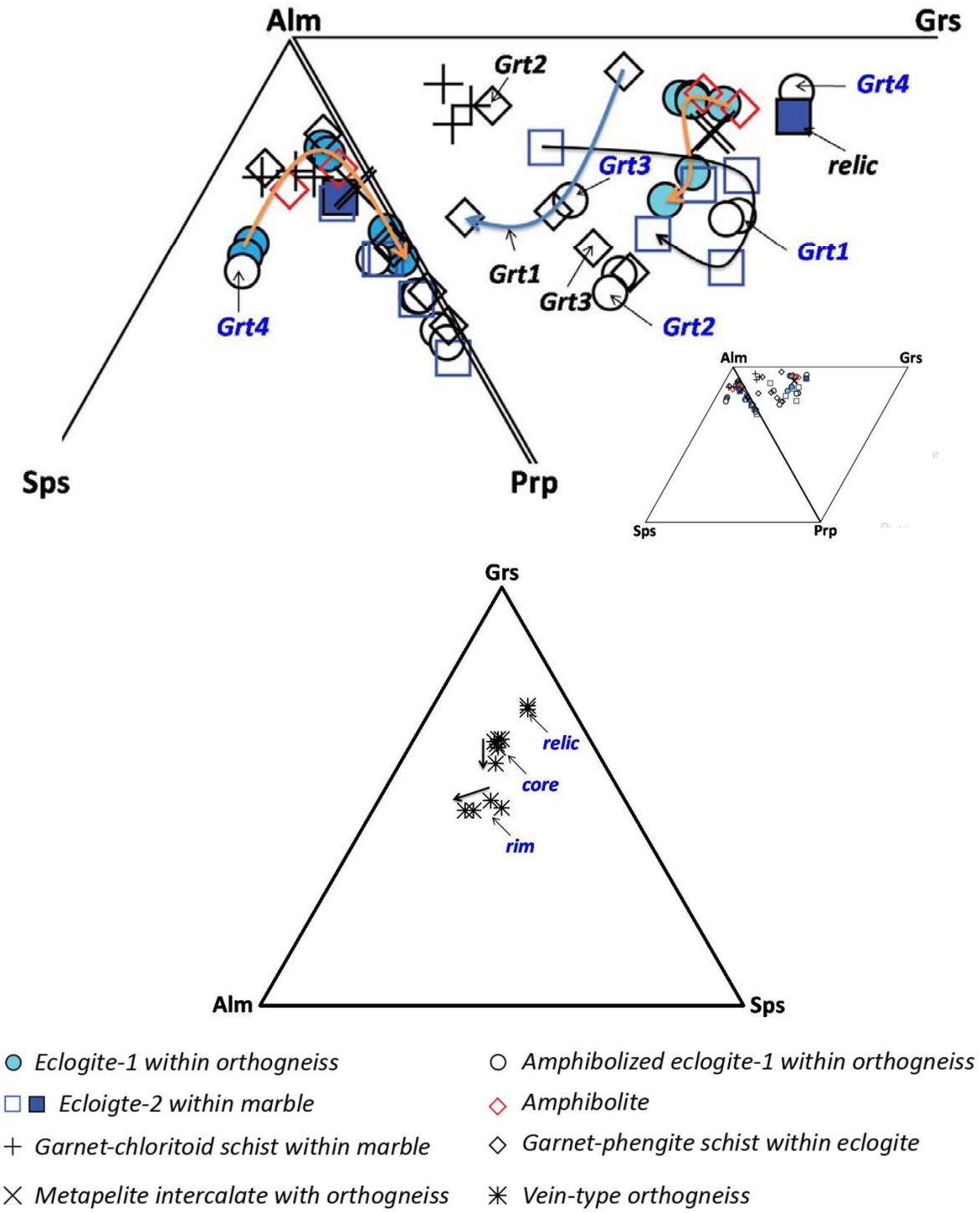

Fig.4.1 Sps-Alm-Prp-Grs diagram for eclogites and associated metamorphic rocks and Alm-Grs-Sps diagram for vein-type orthogneiss showin chemical composition garnets. Orange and sorrel colored arrows indicate zoning from core to rim for eclogite and garnet-phengite schist.

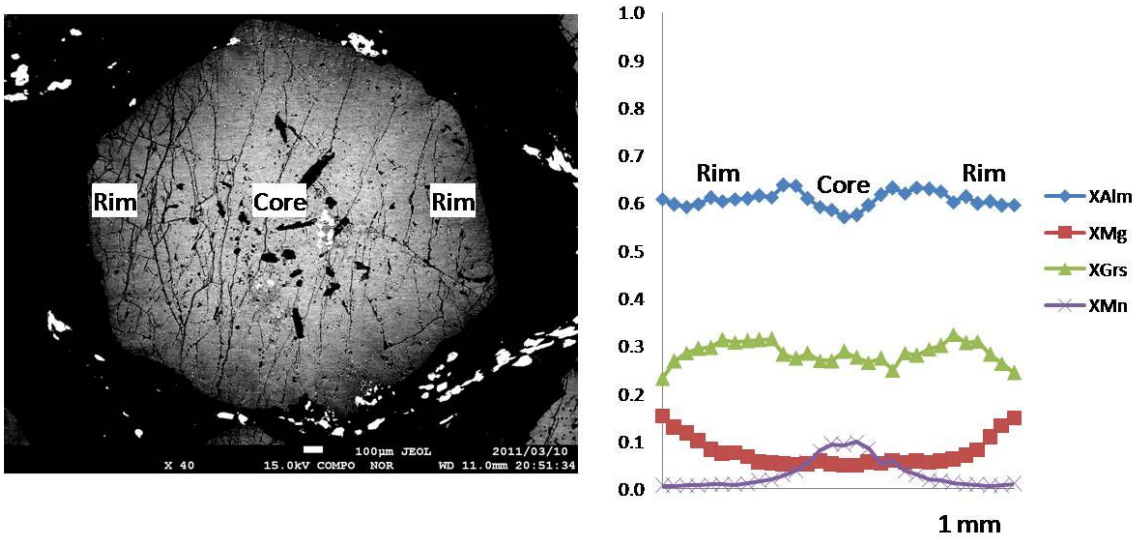

Fig.4.2 Chemical zoning pattern (rim-core-rim) of garnet crystals from the eclogite-1.

Garnet grains in the eclogites-2 divided as core (Alm_{64-74}, Grs_{8-24}, $Prp_{10-16,}$ Sps_{2-3}), mantle (Alm_{51-59}, Grs_{24-39}, $Prp_{8-17,}$ Sps_{1-3}), rim (Alm_{50-57}, Grs_{22-26}, $Prp_{18-23,}$ Sps_{1}) and outer-rim (Alm_{60-64}, Grs_{20-22}, $Prp_{12-19,}$ Sps_{1-2}). Relic garnets in the core are Alm_{49-57}, Grs_{32-42}, $Prp_{7-8,}$ Sps_{2-3} (Fig.4.3). Garnets have prograde zoning, X_{Alm} decrease from core (0.64-0.74) to mantle (0.51-0.59), then homogenized in the mantle; and then slightly decrease from mantle to rim (0.50-0.57) and then increase from rim to outermost rim (0.60-0.64). X_{Prp} relatively homogeneous in core (0.10-0.16) and mantle (0.08-0.17) and sharply increase from mantle to rim (0.18-0.23) and slightly decrease from rim to outermost rim (0.18-0.18). X_{Grs} increase dramatically from core (0.08-0.20) to mantle (0.24-0.39) and slightly decrease from mantle to rim (0.22-0.26) and outermost rim (0.20-0.22). X_{Sps} is relatively homogeneous; slightly decrease from core to the rim slightly increase to outermost rim (Fig.4.3).

Garnet compositions of eclogites-1 have lower X_{Prp}, higher X_{Grs} and X_{Sps} than garnets in the eclogites-2 (Figs.4.1).

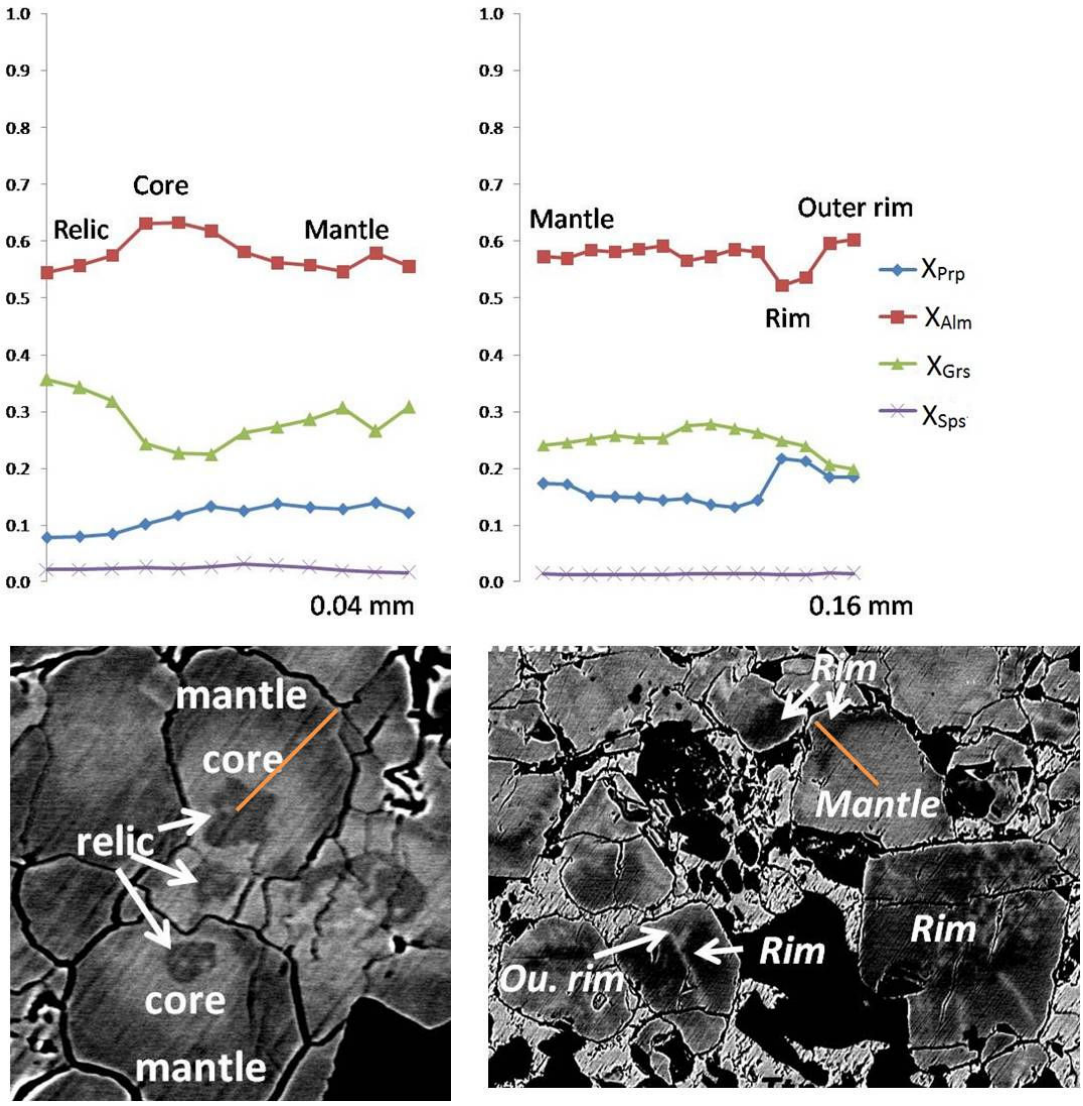

Fig.4.3 Chemical zoning pattern (relic-core-mantle and mantle-rim-outer rim) of garnet crystals from the eclogite-2

Garnets in the amphibolites have relatively homogeneous composition of $Alm_{57-62}Grs_{29-36}Pyr_{5-6}Sps_{2-5}$. X_{Sps} decreases with increasing X_{Prp} from core to rim. X_{Grs} slightly increases with homogeneous X_{Alm} from core to rim in the garnet. Those compositions of the garnet represent higher almandine and spessartine, lower grossular components than the garnets of the eclogite (Figs 4.1 and 4.4).

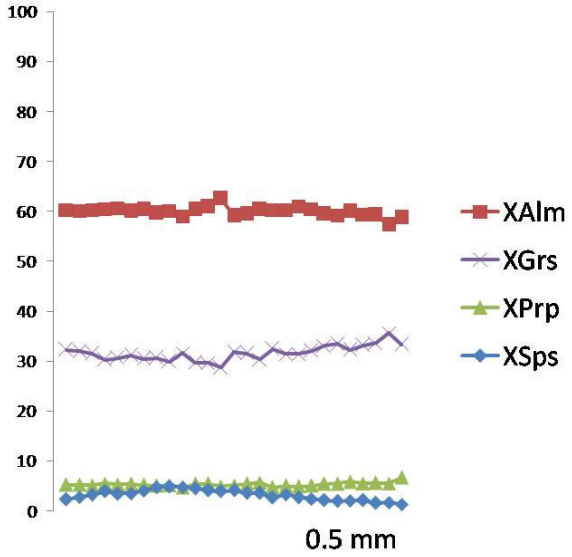

Fig.4.4 Chemical zoning pattern (rim-rim) of garnet crystals from the amphibolites.

Garnets in the garnet-phengite schists intercalating with eclogites bodies display a compositional zoning and divided as Grt1, Grt2 and Grt3. Grt1 has a zoning with core and mantle and both core and mantle of Grt1 partially replaced by relatively Fe-rich Grt2. Then both Grt1 and Grt2 partially replaced by overgrown Grt3. Composition of core of Grt1 is Alm_{55-68} Grs_{8-23} Pyr_{17-24} Sps_{1-5}. The composition of Grt2 is Alm_{69-71} Grs_{11-12} Pyr_{16-19} $Sps_{<1}$. The composition of overgrown Grt3 is Alm_{59-63} Grs_{22-25} Pyr_{15-17} $Sps_{<1}$ (Figs. 4.1 and 4.5). In the Grt1, X_{Sps} decreases continuously from core (0.02-0.05) to mantle (0.01-0.02), whereas X_{Prp} and X_{Alm} increase from core (0.17-0.21 and 0.55-0.60, respectively) to mantle (0.22-0.24 and 0.64-0.68). X_{Grs} sharply decreases from core (0.0.18-0.22) to mantle (0.09-0.12).

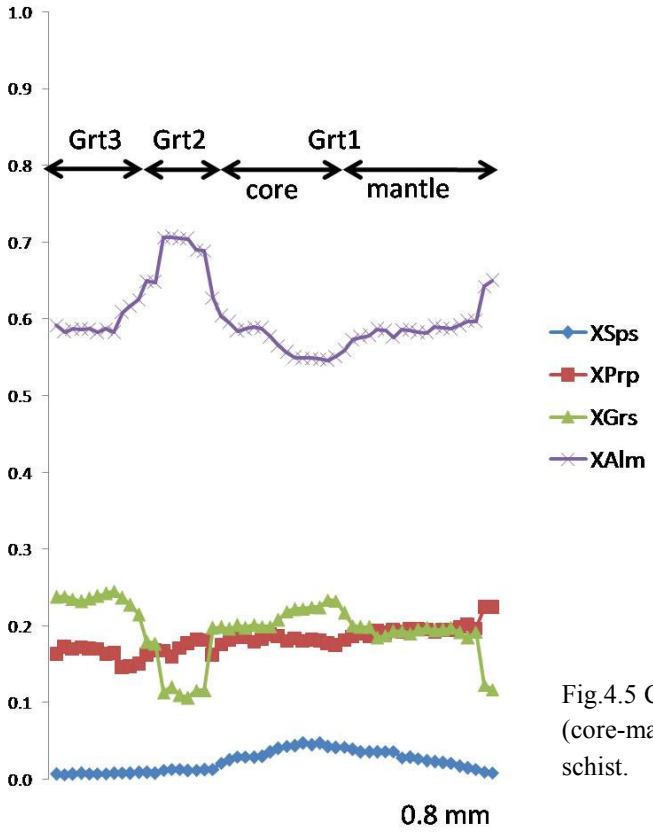

Fig.4.5 Chemical zoning pattern (Grt3-Grt2-Grt1 (core-mantle) of garnet from the garnet-phengite schist.

The composition of garnet in the garnet-chloritoid schist is $Alm_{83-86}Py_{10-11}Grs_{1-4}Sps_{1-2}$ in the rim, whereas in the core $Alm_{77-84}Py_{5-10}Grs_{4-11}Sps_{2-7}$. Garnet has a prograde zoning, X_{Sps} decreases from core to rim whereas the X_{Prp} increases from core to rim. X_{Grs} is relatively homogeneous in the core, and slightly increasing to the rim. X_{Alm} is relatively homogeneous and slightly decreases to the rim (Figs 4.1 and 4.6) (Javkhlan et al., 2013).

Garnet grains in the vein-type orthogneiss are rich in grossular (Grs=43.49-0.67.93) with significant amount of almandine (Alm=8.82-34.06) and spessartine (Sps=16.99-26.39) components. Pyrope component (Prp=0.19-0.51) is very low in the garnet (Figs 4.1 and 4.7). Garnet displays a compositional zoning, which divided as core, rim and outermost-rim. Spessartine components are increased from the core

(16.99-19.73) to the rim (18.96-20.64) then decreased to the outermost-rim (18.96-20.64).

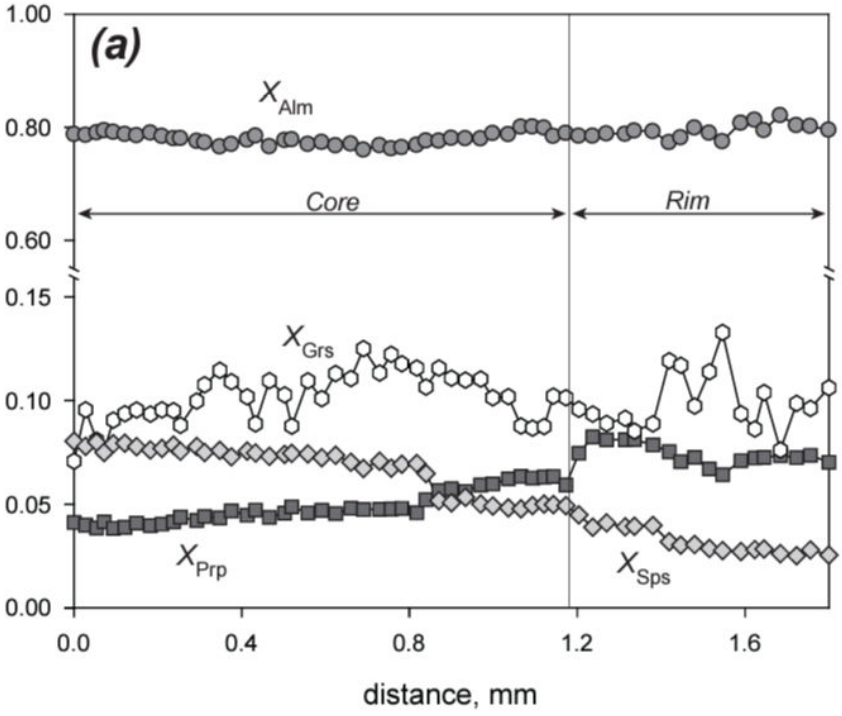

Fig.4.6 Chemical zoning pattern (core-rim) of garnet crystals from the garnet-chloritoid schists.

Almandine components are also remarkably increased from the core (17.92-19.95) to rim (26.07-27.67) and outermost-rim (32.39-34.06). Grossular components decreased from the core (56.63-60.30) to rim (43.49-45.93) and outermost-rim (45.70-46.48) (Figs.4.7). Relic garnet in the core of garnet is high in Grs (66.95-67.93), low in Alm (8.82-9.24) and similar Sps composition (19.68-20.00) with core of garnet in the vein-type orthogneiss.

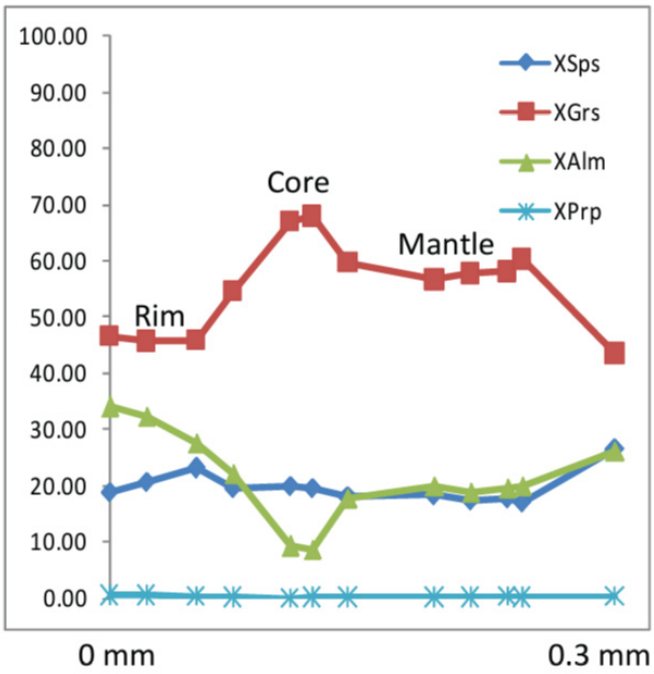

Fig.4.7 Chemical zoning pattern (rim-rim) of garnet crystals from the orthogneiss.

4.3 Clinopyroxenes

The jadeite component of clinopyroxene (Cpx1) as inclusions in the garnets is from 16% to 41% and the aegirine component is from 9 % to 23 % in the eclogites-1. Those Cpx1 are classified as omphacite and aegirine-augite (Fig.4.8). The discrete grains of clinopyroxene in the matrix (Cpx2) are classified as omphacite. Jadeite component is from 27 % to 46 % and aegirine component is from 0 % to 19 % (Fig.4.8). Cpx2 are mainly homogeneous in composition, though few Cpx2 has prograde zoned with jadeite component increase from the core (Jd_{27}) to the rim (Jd_{41}) (Fig. 3.14). Sometimes it show reverse zoning as well; jadeite component slightly decrease from core (Jd_{38-39}) to rim (Jd_{37-36}) (Fig.3.10). Symplectitic clinopyrexenes (Cpx3) with Mg-hornblende and plagioclase (An_{1-13}) are classified mainly as diopsite and rarely as aegirine-augite and omphacite composition. Jadeite component of Cpx3 is up to 25 % and aegirine component is up to 15 % (Fig.4.8).

Clinopyroxenes (Cpx1 and Cpx2) in the eclogites-2 are classified as a omphacite. Few omphacites preserved their core (X_{Jd}=0.27-0.31) whereas most of grains have compositional heterogeneity with jadeite component vary from 34 % to 48 % and aegirine component vary from 1 % to 15 % (Fig. 4.8).

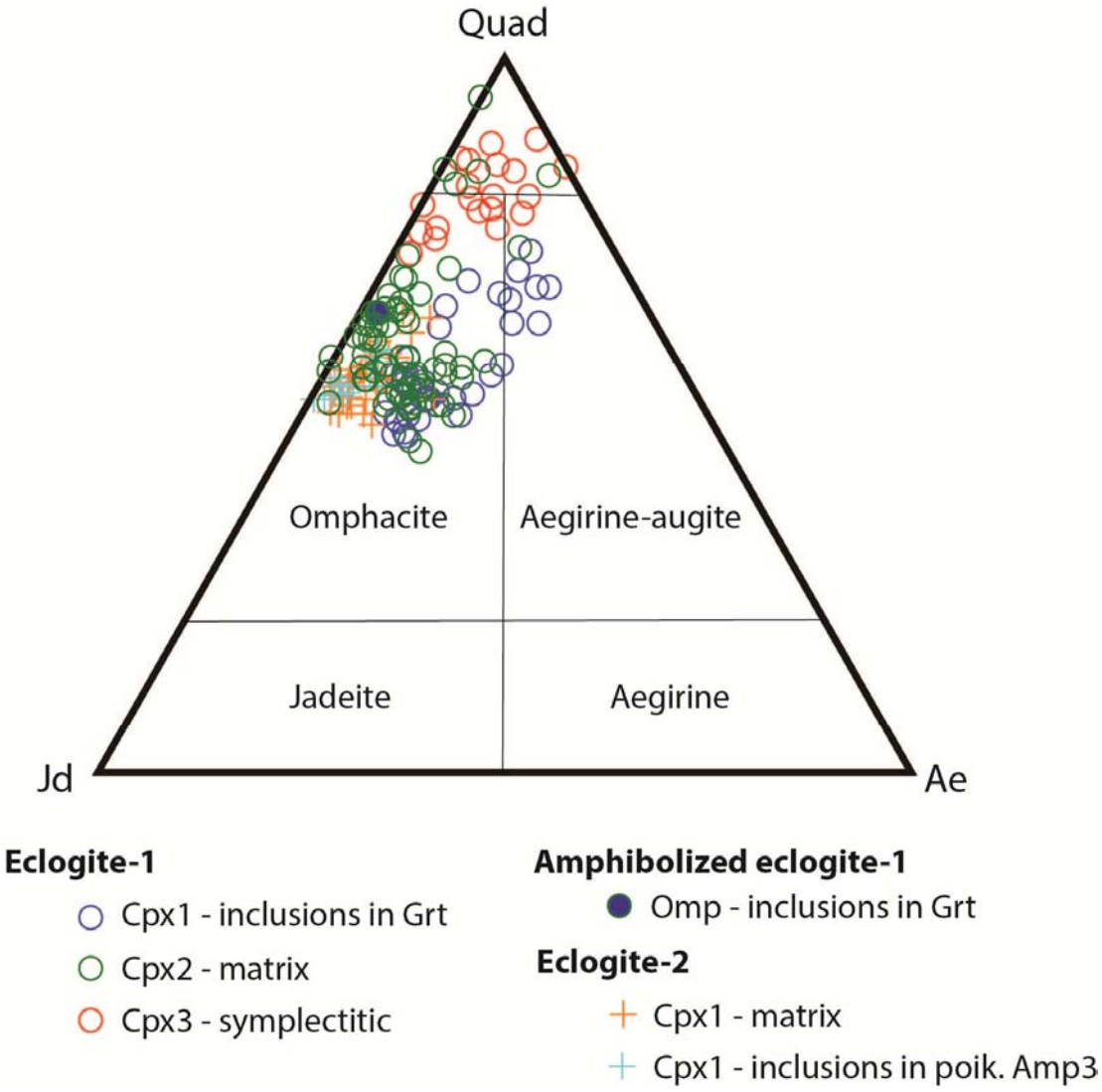

Fig.4.8 Chemical compositions of clinopyroexenes of eclogites-1, amphibolized eclogites-1 and eclogites-2.

4.4 Amphiboles

Eclogites

Amphiboles in the eclogites-1 are classified into calcic, sodic calcic, sodic groups. Amphiboles (Amp1) included in the garnets are composed mainly of sodic-calcic (taramite, Mg-taramite, Fe-barroisite, barroisite) and calcic amphiboles (pargasite, Fe-pargasite, tschermakite, Fe-tschermakite, actinolite, Fe-actinolite, Mg/Fe-hornblende and edenite; Fig.4.9). Amp1 show relatively lower Si content (5.74-7.00 pfu) and higher Na_B (0.33-1.10 pfu) than Amp4 and lower Si content and lower Na_B content than Amp2 except for some inclusions of barroisite in the garnet rim are higher Na_B (1.04-1.10 pfu) content than other compositons of inclusions (Fig.4.9). Also Amp1 show high-TiO2 content (TiO2 is up to 1.56%). Amphiboles (Amp2) coexisting omphacite (Cpx2) have a prograde and retrograde zoning (Fig.4.9), glaucophane core (Si=7.52-7.72 pfu, Na_B=1.51-1.70) with barroisite mantle (Si=6.94-7.48 pfu, Na_B=0.78-1.41 pfu) and Mg-hornblende rim (Si=6.68-6.88 pfu, Na_B=0.35-0.49 pfu) with actinolite outermost rim (Si=7.56-7.69 pfu, Na_B=0.25-0.29 pfu. Symplectitic Amp3 after omphacite are mainly with Mg-hornblende (Si=6.90-7.32 pfu, Na_B=0.05-0.39 pfu), rarely actinolite composition (Si=7.65 pfu, Na_B=0.16 pfu) (Fig.4.9). Amp4 in the matrix has a prograde and retrograde zoning, from actinolite, winchite core (Si=7.53-7.68 pfu, Na_B=0.25-0.69 pfu) to barroisite mantle (Si=6.93-7.51 pfu, Na_B=0.51-0.73 pfu) with Mg/Fe-hornblende rim (Si=7.03-7.16 pfu, Na_B=0.15-0.45 pfu). Amphiboles sorrounding garnets have (Amp5) mainly pargasite (Si=5.94-6.24 pfu, Na_B=0.15-0.36), locally Mg-hornblende compositions (Si=6.52-6.78 pfu, Na_B=0.31-0.38 pfu; Fig.4.4). Amphiboles of veins in eclogites (Amp6) show a prograde zoning, Mg-hornblende core (Si=6.56-7.55 pfu, Na_B=0.17-0.33) and pargasite rim (Si=5.72-6.35 pfu, Na_B=0.18-0.23 pfu; Fig.4.4).

Amphiboles in the amphibolized eclogites-1 are classified into sodic-calcic, calcic groups.

Relic amphibole (Amp1) has a chemical zoning with actinolite core (Si=7.62-7.78 pfu, Na_B=0.45-0.46 pfu) and barroisite rim (Si=7.04-7.39 pfu, Na_B=0.50-0.59 pfu) (Fig. 3.22), calcic amphibole (Amp2) replacing Amp1 has a zoning with Mg-hornblende core (Si=6.57-7.38 pfu, Na_B=0.29-0.45 pfu) and tschermakite, Fe-tschermakite, Fe-pargasite rim (Si=6.36-6.45, Na_B=0.37-0.44). Si contents of thin actinolite micro-vein (Amp3) vary from 7.87 pfu to 7.99 pfu and Na_B contents vary from 0.02-0.03 pfu.

Amphiboles in the eclogites-2 are classified into calcic, sodic calcic groups. Amphiboles (Amp1) coexisting omphacite (Cpx2) and garnet have a prograde zoned with actinolite (Si=7.73-7.85 pfu, NaB=0.03-0.05 pfu) core, barroisite (Si=6.32-7.17 pfu, NaB=0.50-0.74 pfu) mantle and rims with tschermakite, Mg-taramite and pargasite (Si=6.23-6.40 pfu, Na_B=0.44-0.50) in compositions (Fig.4.9). Symplectitic Amp2 after omphacite (Fig.4.9) are mainly with actinolite, Mg-hornblende (Si=7.25-7.61 pfu, Na_B=0.20-0.21 pfu), rarely pargasitic composition (Si=6.21-6.26 pfu, Na_B=0.22-0.25 pfu). Poikiloblastic Amp3 in the matrix are barroisite in composition and they have a prograde zoning with Si contents decreasing from to the rim (Si=6.69-7.01 pfu, Na_B=0.61-0.70 pfu). Amphiboles filling grain boundaries of omphacite and garnet grains (Amp4) actinolite (Si=7.66-7.92 pfu, NaB=0.02-0.05) in composition (Fig.4.9).

Amphibolite

Amphiboles occur as inclusions in the rim of the garnets (Amp1) and as discrete grains in the matrix (Amp2). Amp1 mainly has composition of Fe-pargasite, Fe-tschermakte (Si=6.15-6.47 pfu, Na_B=0.21-0.29 pfu), rarely Mg-hornblende (Si=6.64-

6.86 pfu, Na_B=0.07-0.39 pfu). Amp2 has a zoning with Mg-hornblende or actinolite core (Si=6.52-7.59 pfu, Na_B=0.17-0.49 pfu) with pargasite, Fe-pargasite or tschermakite, Fe-tschermakite rim ((Si=6.16-6.62 pfu, Na_B=0.21-0.40 pfu). This zoning texture is as same zoning as Amp6 of amphibole-rich veins in the eclogites (Fig.4.9).

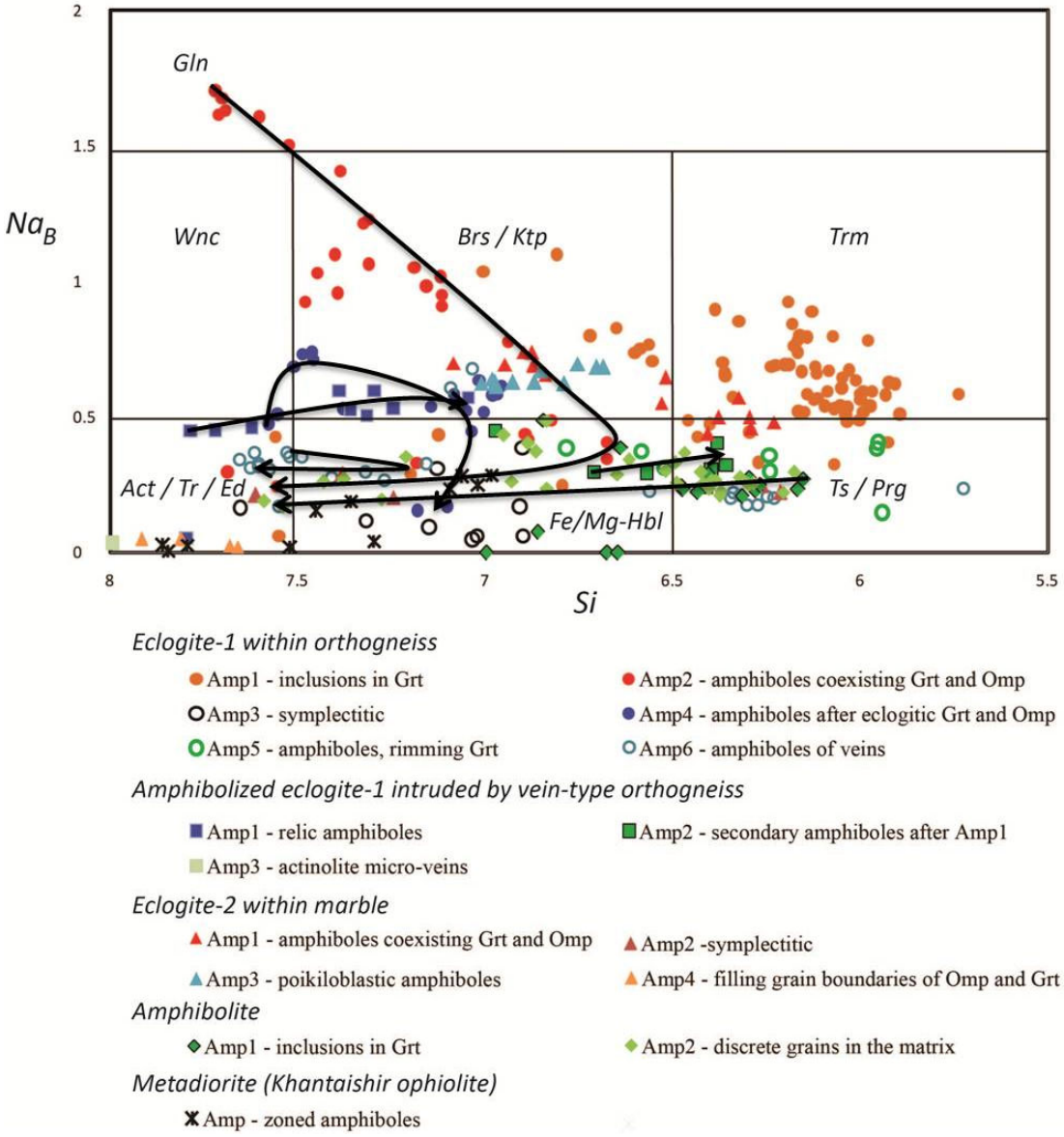

Fig.4.9 Chemical composition of amphiboles from eclogite-1, amphibolized eclogites-1, eclogite2, amphibolites and metadiorite. Arrows indicate compositional change from cores to rims in amphibole crystals.

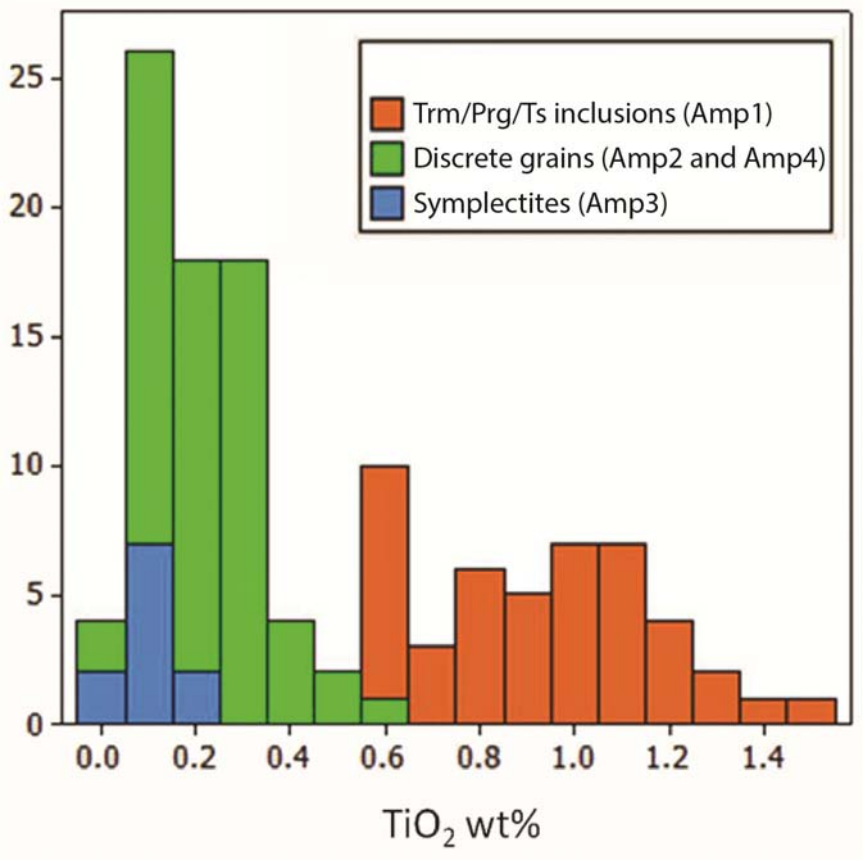

Fig.4.10 TiO_2 content in the amphiboles from the eclogites-1

4.5 White micas

Phengite as inclusion in garnet (Phn1) has Si content of 6.69-6.74 pfu. Discrete grains (Phn2) have a Si content of 6.75-7.12 pfu in the eclogites-1 (Fig. 4.11).

In the garnet-phengite schists intercalating with eclogites bodies, Si contents of phengites (Ph1) in the main schistosity vary from 6.9 to 7.2 pfu, whereas Si contents of the randomly oriented grains of phengite (Ph2) vary from 6.5 to 6.4; distinctly lower Si content than Ph1 (Fig. 4.11).

White micas occurring as inclusions in the porphyroblastic garnet in the garnet-chloritoid schists are from muscovite to phengite in compositions [Si = 6.06-6.63 pfu, X_{Na} (Na/Na+K) = 0.04-0.12] and paragonite (Javkhlan et al., 2013). Si

content of the phengite inclusions gradually increases from core to rim of the garnets. Phengites in the matrix is chemically zoned, from Si-rich core (Si = 6.34-6.64 pfu) to Si-poor rim (Si = 6.05-6.32 pfu). The phengites has higher X_{Na} (0.09-0.25) than those found as inclusions in garnet (X_{Na} = 0.04-0.12) (Fig. 4.11). Paragonite inclusions in the cores of the garnet have Si = 5.93-6.03 pfu and X_{Na} = 0.88-0.91, and those included within chloritoid have Si = 5.80-5.86 pfu and X_{Na} = 0.91-0.94. Paragonite in the matrix has similar Si (5.84-6.09 pfu) and X_{Na} (0.84-0.94) to those found as inclusions in the garnet cores. Si-poor phengitic muscovite filling fractures in the porphyroblastic garnets have compositions of Si = 6.15-6.23 pfu and X_{Na} = 0.20-0.23 (Javkhlan et al., 2013).

In the vein-type orthogneiss, Si contents of relic Ph1 vary from 6.56 pfu to 6.89 pfu (X_{Na}=0.01-0.02). Ph2 overgrowing relics of Ph1 has zoning with Si contents vary from 6.31 to 6.71 (X_{Na}=0.01-0.04) from the core to the rim.

4.6 Epidotes

Pistacite [$X_{ps}=Fe^{3+}/(Al+Fe^{3+})$] content of epidotes as inclusions of the garnets in the eclogites (Xps=0.17-0.29) are higher than discrete grain epidotes in the matrix (X_{ps}=0.04-0.16) of eclogite. X_{Ps} content of epidotes in the eclogites-2 are varied from 0.10 to 0.13 of eclogite. In the amphibolite X_{ps} in the inclusions in a garnet are higher (X_{ps}=0.16-0.24) than inclusions in a matrix amphibole (X_{ps}=0.15-0.16). X_{ps} in porphyroblastic epidotes in the metapelites are from 0.02 to 0.03 pfu. In the vein-type orthogneisses X_{Ps} of epidote is ranged from 0.14 to 0.16 whereas X_{Ps} of zoisite distinctly lower, up to 0.01.

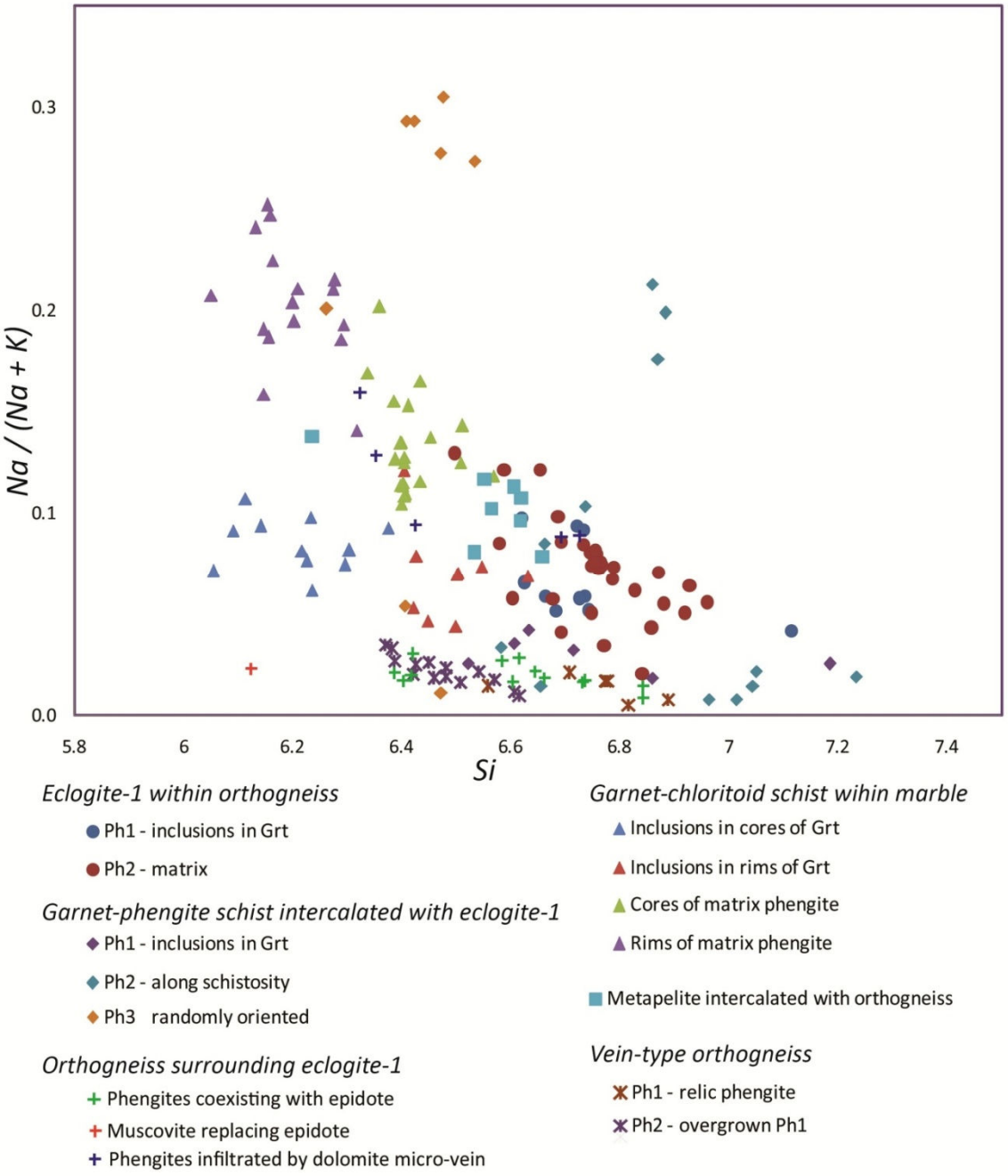

Fig.4.11 Chemical compositions of white micas of eclogites and associated metamorphic rocks in the Chandman district

4.7 Other minerals

Anorthite component of plagioclases in the garnets as inclusions varies from 2 to 17 (albite and oligoclase), and in the symplectitic plagioclases after omphacite are from 1 to 13 (albite and oligoclase) whereas the after phengite are from 2 to 18 (albite and oligoclase) in the eclogites-1. Anorthite component of albites, coexisting with Amp4 are from 2 to 7. X_{Mg}=Mg/(Fe+Mg) of chlorite in the eclogites-1 varies from 0.54-0.62.

In the amphibolite anorthite component of inclusions of plagioclase (An_{9-12}; albite, oligoclase) in the garnet rim with Amp1 (Fe-pargasite, Fe-tschermakite and Fe-edenite) are higher than plagioclase (An_{5-8}) occuring with amphibole surrounding garnet. Chloritoid is preserved high content of Fe/(Fe+Mg), varied from 0.8 to 0.9 in the garnet-chloritoid schist (Javkhlan et al., 2013). X_{Mg} [Mg/(Mg+Fe] content in chlorites as inclusion in garnets of eclogites-1 is varies from 0.62-0.64 whereas chlorite in fracture zone of garnet has X_{Mg} varying from 0.52-0.54. X_{Mg} ratio of biotite inclusions in the garnet of eclogites-1 vary from 0.52 to 0.58. X_{Mg} of symplectitic biotites with plagioclase vary from 0.41 to 0.62 in the eclogites-1. X_{Mg} of biotites filling grain boundaries of Cpx2 and garnet vary from 0.63-0.70.

CHAPTER 5 MINERAL PARAGENESIS AND PRESSURE-TEMPERATURE PATH OF METAMORPHIC ROCKS

5.1 Eclogites

5.1.1 Eclogite-1 within orthogneisses

Based on the texture and mineral chemistry, metamorphism of the eclogite-1 is divided into three different metamorphic events (Fig.5.1), i.e. low pressure (LP) and high temperature (HT) precursor metamorphic event (M1), high-pressure (HP) eclogitic metamorphic event of (M2), medium-pressure metamorphic event of the epidote amphibolite facies (M3) metamorphism. Farthermore, additional low-pressure and high-temperature metamorphic event of the amphibolites facies (M4) has been distinguished in the amphibolized eclogites-1 intruded by vein-type orthogneiss.

LP-HT precursor metamorphic event (M1)

The LP-HT precursor metamorphic event is characterized by the polyphase and discrete grain inclusions of Na-Ca (taramite, Mg-taramite; Amp1) and Ca amphiboles (Fe-pargasite, tschermakite, Fe-tschermakite; Amp1), biotite, plagioclase (An_{2-17}), epidote, rutile and quartz in the garnet core (Fig. 5.1).

The polyphase inclusions of biotite + oligoclase ($An_{<17}$) + epidote and high TiO_2-bearing taramite, Fe-pargasite, tschermakite, Fe-tschermakite (TiO_2 < 1.56 wt% of) are included in the cores of the garnet (Fig. 3.4 and 3.8). The high-TiO2 amphiboles are interpreted as relatively HT metamorphic condition (Ernst and Liu, 1998). Wakabayashi (1990) reported the discovery of pargasitic amphiboles in amphibolites from the Franciscan complex, California; these pargasitic amphiboles

crystallized during the early HT metamorphic event before the HP Franciscan metamorphism. He suggested that such HT metamorphism took place when metamorphic soles beneath ophiolites at the inception of subduction zone. The occurrence of pargasitic amphiboles from the metamorphic soles beneath ophiolites suggests that crystallization of pargasitic amphiobles requires relatively HT metamorphic conditions, such as amphibolite and/or granulite facies and is incompatible with HP-LT metamorphism in the subduction zone. Also biotite-oligoclase assemblages are common in HT conditions. Hence above the polyphase and single grain inclusions in the cores of the garnet are formed during a relatively LP-HT metamorphic event of amphibolite facies a condition (M1) before the blueschist facies conditions of eclogitic metamorphic event (M2) was attained.

The approximate pressure-temperature (P-T) condition for the first precursor metamorphic event (M1) suggested the amphibolites facies condition that the temperature conditions of 400-650 ºC and pressure condition of below the 8 kbar for inclusions of Ca-, Na-Ca amphiboles (taramite, pargasites, tschermakites), oligoclase and biotite. Upper limits of pressure conditions are constrained by oligoclase-in line (Maruyama et al., 1983; Fig. 5.2).

Second high-pressure metamorphic event (M2)

M2 metamorphic event with prograde and peak stages of metamorphism represents relatively high pressure and low temperature metamorphism of the blueschist to eclogite facies which is characterized by coexisting eclogitic mineral assemblage of omphacite, garnet and prograde zoned glaucophane bearing barrositic amphiboles.

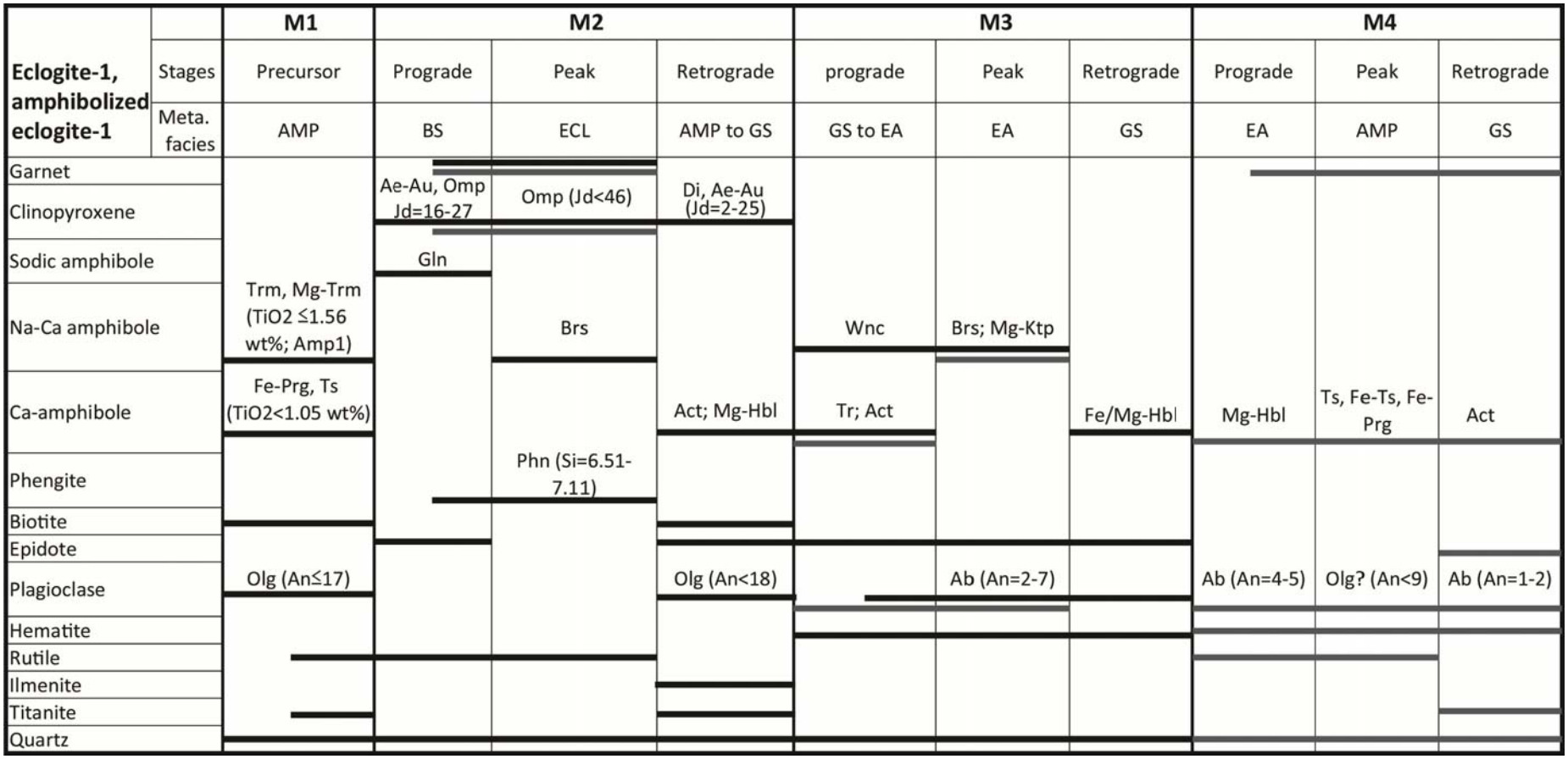

Fig.5.1 Mineral paragenesis of eclogites-1 within orthogneisses. Thick black and grey lines indicate eclogites-1 and amphibolized eclogites-1, respectively.

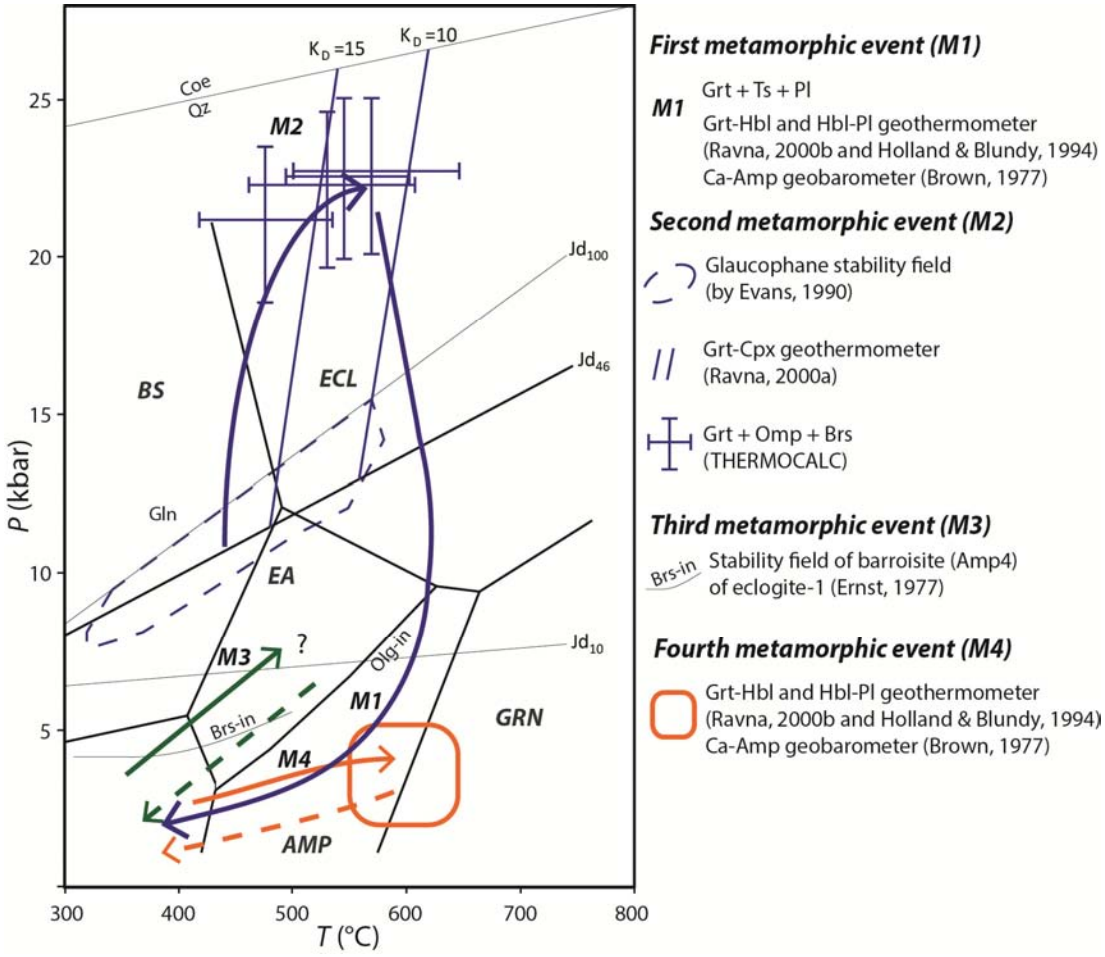

Fig.5.2 Estimated P-T conditions for eclogites of Alag Khadny metamorphic complex (P-T boundary after Takasu, 1989). ECL, eclogite facies; BS, blueschist facies; EA-AMP, epidote-amphibolite facies; AMP, amphibolite facies; GS, greenschist facies; GRAN, granulite facies. Olg-in reaction after Maruyama et al., (1983). The first metamorphic event (M1) is indicated by stability field of amphibolite facies. Purple arrow, second metamorphic event (M2); green arrow, third metamorphic event (M3); orange arrow, fourth metamorphic event (M4).

The prograde stage of second high-pressure metamorphic event (M2) is defined by glaucophane cores in the barroisitic amphibole (Fig. 3.12). The glaucophane cores are regarded as prograde stage of the HP-LT conditions as the blueschist facies before the eclogitic conditions (Fig. 5.1). Presense of inclusions of epidote occur in core and rim of garnets (Fig. 3.7 and 3.8) suggested that epidotes are stable in prograde stage of blueschist to eclogite facies conditions instead of lawsonites.

The approximate P-T condition of prograde stages is characterized by glaucophane cores and stability conditions of glaucophane suggesting 330-570 ºC and 8-16 kbar (Evans, 1990) of blueschist to eclogites facies conditions (Fig. 5.2).

Hence the glaucophane cores in the barroisites and inclusions of epidotes are suggested that after the LP-HT metamorphic event (M1), biotite + oligoclase + taramite + tschermakite/pargasite bearing amphibolites are suffered HP-LT metamorphism of blueschist facies (M2). Sometimes polyphase inclusions of taramite + omphacite (Jd40-41) + quartz and aegirine-augite (13-16) + omphacite (Jd20) + Fe-tschermakite are included in the garnet core and rim (Figs. 3.7, 3.8). These inclusions are interpreted as minerals of M1 even replaced by minerals of M2 metamorphic events.

The peak mineral assemblage of eclogite facies is defined by garnet (rim), omphacite (Cpx2; Jd<46), phengite (Si6.51-7.11), barroisite (Amp2), epidote (Ep2) quartz, and rutile (Figs. 3.9 and 5.1).

The K_D value of garnet-clinopyroxene pairs vary from 10 to 15. The temperature range was estimated by inclusions of omphacite in the garnet rim and rim-rim composition of garnet and omphacite in the matrix. K_D and maximum Jd content in omphacite (up to 46%) without coesite yield the P-T conditions of 480-620ºC and >11-26 kbar by the garnet-clinopyroxene thermometer and barometer of jadeite component (Ravna, 2000; Holland, 1983, respectively) (Fig. 5.2). Consisting estimation obtained by THERMOCALC (v.3.33) (Powell and Holland, 1994) calculations for the peak stage (garnet rim + omphacite + barroisite of Amp2) of eclogites-1 (MG802) yielded P-T conditions of 565 ± 69ºC and 22.5 ± 2.6 kbar (sigfit=1.54) (Fig. 5.2).

The retrograde stage of the M2 is characterized by symplectite of plagioclase (An1-13) + Mg-hornblende (Amp3) + Na-poor clinopyroxene (Cpx3; diopsite, agirine-augite; Jd2-25) after omphacite (Cpx2); plagioclase (An=2-18)+biotite assemblage after phengite (Fig.3.9) and the retrograde Mg-hornblende rim of barroisite (Amp2) (Fig. 5.1).

The P-T condition of the retrograde stage are estimated by symplectite consisting of plagioclase (An=5-13) + Mg-hornblende assemblage giving 530-630°C and Jd content in symplectitic Na-poor clinopyroxene (Jd=2-25) giving 4-11 kbar using a hornblende-plagioclase geothermometer (Holland and Blundy, 1994) and geobarometer of jadeite component (Holland, 1983). Estimated temperature and pressure ranges suggesting the retrograde path has been passed stability field of amphibolites facies (Fig. 5.2).

In the amphibolized eclogite-1 intruded by vein-type orthogneiss, eclogtic Grt1 containing inclusions of omphacite is strongly replaced by several generations of garnets (Grt2, Grt3 and Grt4), and barroisitic (Amp1) and tschermakitic amphiboles (Amp2) (Figs. 3.20-3.25). Chemical compositions of Grt1 are similar with rims of porphyroblastic garnets in the eclogites-1 and evidence of omphacite inclusion suggests that amphibolized eclogites-1 are preserved M2 event of HP eclogites facies metamorphism.

Third MP-MT metamorphic event (M3)

The third MP-MT metamorphism (M3) is divided into three stages, i.e. prograde, peak, and retrograde stages (Fig. 5.1).

The prograde and peak stages (Fig. 5.1) are characterized by a zoning of secondary prograde zoned Amp4 replacing eclogitic minerals of garnet, omphacite and their symplectitic assemblage. Amp4 consist of winchite, actinolite, tremolite

core with barroisite mantle and and retrograde stage of Mg-hornblende rim (Fig. 3.15). Amp4 often occur in between grain boundaries of omphacite (Cpx2) and in the pressure shadows of garnet (Fig. 3.13). Amp4 includes relic assemblage of eclogite-facies mineral such as garnet, omphacite, and symplectite of Mg-hornblende with plagioclase (An<12) and Na-poor clinopyroxene (Jd<12; Fig. 3.13 and Fig. 3.14) suggesting the amphiboles (Amp4) were grown on the retrograde assamblages of eclogite event. The barroisite mantle of Amp4 coexist with albite (An<2-7), epidote and hematite (Fig. 3.16). Hence, the mineral assemblage of prograde zoned barroisitic amphibole together with epidote, albite and hematite suggesting the second MP-MT metamorphism (M3) after the M2 metamorphic event.

The prograde zoning of amphiboles (Amp4; actinolite or winchite core with barroisite mantle) suggests the P-T trajectory passed through the stability field of actinolite, winchite and barroisite of epidote-amphibolite facies (Ernst, 1977; Otsuki and Banno, 1990). The coexisting barroisite and albite give temperature conditions of ~400-500ºC using hornblende-plagioclase geothermometer (Holland and Blundy, 1994) (Fig. 5.2).

The retrograde stage of the M3 is characterized by the retrograde zoning of Amp4, barroisite mantle with Mg/Fe-hornblende rim, suggesting a P-T trajectory from peak epidote-amphibolite-facies to the greenschist-facies conditions.

In the amphibolized eclogites-1, relic amphiboles of prograde zoned Amp1 (actinolite core with barroisite rim) containing inclusions of eclogitic Grt1 and symplectites of amphibole and plagioclase after the omphacite (Figs. 3.23 and 3.24) suggest that Amp1 were formed after the crystallization of Grt1 and symplectite (former omphacite). Farthermore, chemical zoning of Amp1 (actinolite core with barroisite rim) in the amphibolized eclogites-1 are similar with Amp4

(actinolite/winchite core with barroisite mantle and Mg-hornblende rim) of eclogites-1.These features suggest that amphibolized eclogites-1 were suffered M3 metamorphism after the M2 metamorphic event, as the same as eclogites-1.

Fourth LP-HT metamorphic event (M4)

The fourth LP-HT metamorphic event (M4) is defined by the textural evidence of barrisitic amphibole (Amp1) formed by M3 metamorphism replaced by tschermakitic amphibole (Amp2) together with Grt2 and plagioclase (An<9) in the amphibolized eclogites-1 (Figs. 3.24). M4 is divided as prograde, peak and retrograde stage (Fig. 5.1).

The prograde stage of M4 is characterized by Mg-hornblende core of Amp2 overgrown Amp1 (actinolite core with barroisite rim), core of plagioclase (An=4-5) and epidote (X_{Ps}=0.16-0.21) in amphibolized eclogites-1. Prograde mineral assemblage suggests greenshchist or possibly low-temperature portion of amphibolites facies conditions (Fig. 5.2).

The peak stage of M4 is characterized by Grt2 replacing eclogitic Grt1, rim of Amp2 (tschermakite, Fe-tschermakite, Fe-pargasite), mantle of plagioclases (An<9) and K-feldspar in the amphibolized eclogites-1 (Fig. 5.1).

Temperature conditions of the peak stage are estimated by plagioclase (An<9) + Amp2 (tschermakite / Fe-tschermakite / Fe-pargasite) giving 550-640°C using hornblende-plagioclase geothermometer (Holland and Blundy, 1994) and garnet + Amp2 giving 570-600°C using garnet-hornblende geothermometer (Ravna, 2000b). Pressure conditions of the peak stage are estimated by Al^{IV} and Na_B content in Mg-hornblende and tschermakite giving 2-5 kbar (Fig.6.1) using a geobarometer of calcic amphibole (Brown, 1977) (Fig.5.2).

Retrograde stage of characterized by fracture filling Grt3 and thin films of Mn-rich Grt4 after the Grt2. Crystallization order of Grt3 and Grt4 shown by texture and chemical composition suggest that Grt4 are formed after the Grt3 probably by the Mn-rich fluid infiltration.

In the latter part of the metamorphic history, garnets of eclogites-1 and amphibolized eclogites-1 are partly replaced by chlorite, albite and epidote along their cracks. The replacement of garnet by chlorite, albite and epidote suggest retrograde metamorphism of the greenschist facies (Fig. 5.2).

5.1.2 Eclogite-2 within marbles

Based on the textures we distinguished two metamorphic events, i.e. HP eclogite facies metamorphism (M1) and poikiloblastic amphibibole (Amp3) metamorphism (M2) are distinguished (Fig. 5.3).

The matrix of eclogite-2 shows a pseudomorpous texture, where small grains of garnet crowd cemented by titanite forming isomorphic round shape (Fig. 3.27). Some of cores of garnet grain contain relics of garnet (X_{Grs}=0.32-0.42; X_{Prp}=0.06-0.08) indicating previous mineral were larger porphyroblastic garnet. In addition, small grains of omphacite forming rectangular prismatic nature surrounded by garnet grains (Fig. 3.27). These textures suggest that the protolith of eclogite-2 were once suffered by garnet-bearing metamorphism (precursor) with garnet crystallization before the HP eclogite facies metamorphism (M1).

HP eclogite facies metamorphism (M1) divided as pre-peak, peak and decompression stages. The pre-peak stage is characterized by garnet (core) + omphacite (core) + actinolite (core of Amp1) + Ep1 + rutile +quartz. The peak eclogite facies metamorphism characterized by assemblages of garnet (mantle and

rim) + omphacite + Amp1 (barroisitic mantle) + Ep2 + paragonite + rutile. Rims of garnet (Mg-rich) sometimes crystallized as discrete grains next to the mantle of garnet grains (Fig. 3.27). This feature suggests disequilibrium crystallization for garnet indicating when mantle of garnets crystallizing, rim of garnets crystallized at the same time. Therefore, it is difficult to decide which garnet can be equillbrium with omphacites in the eclogites-2.

Eclogite-2	M1			M2	
	ECL			EA	
	Prograde	Peak	Decompression	Peak	Retrograde
Garnet	Core	Mantle and rim (?)			
Omphacite	XJd=0.27-0.31	XJd=0.34-0.48			
Amphibole	Act	Brs	Mg-Trm, Ts, Prg	Brs (poik.)	Act
Plagioclase			An=1-17		An=1-9
Chlorite					
Epidote					
Paragonite					
Biotite					
Calcite					
Rutile					
Titanite					
Quartz					

Fig.5.3 Mineral paragenesis of eclogites-2 within marble

The decompression stage is charactierzed by Amp1 (rims of tschermakite, Mg-taramite and pargasite) + plagioclase (An1-17) + titanite + quartz. The P-T condition of decompression stage suggest 470-710°C at 5-15 kbar by geothermometer of hornblende-plagioclase (Holland and Blundy, 1994).

Poikiloblastic amphibole metamorphism (M2) is characterized by poikiloblastic barroisitic amphibole, Ep3, plagioclase (An1-2) and quarz (Fig. 5.3). The poikiloblastic barroisitic Amp2 shows decreasing Si (7.01-6.69 pfu) and increasing Na_B (0.61-0.70 pfu) from core to rim, suggesting that the Amp2 grew after

the peak eclogite facies metamorphism, and probably during second prograde metamorphic event. Approximate P-T conditions of the poikiloblastic barroisitic Amp2 are estimated as 5-7 kbar at c. 450 °C.

5.2 Garnet-chloritoid schists within marbles

Based on the textural relationships and chemical compositions of minerals, three metamorphic stages are distinguished in the garnet-chloritoid schists, i.e. (i) pre-peak stage, (ii) peak metamorphic stage, and (iii) retrograde stages (Fig. 5.4) (Javkhlan et al., 2013).

The porphyroblastic garnets exhibit typical a prograde zoning, with X_{Sps} decreasing and X_{Prp} increasing from core to rim. The X_{Mg} of chlorite, chloritoid and Si contents of phenge progressively increase with increasing X_{Prp} from garnet cores to rims.

The pre-peak stage is defined by the mineral inclusions in the cores of the garnets (X_{prp}=0.03-0.05). The assemblage is phengitic muscovite (Si=6.06-6.38 pfu), paragonite, chlorite (X_{Mg}=0.07-0.24), chloritoid (X_{Mg}=0.08-0.13) and quartz. This mineral assemblage is probably stable in greenschist to epidote-amphibolite facies conditions (Baltatzis and Wood, 1977; Miyashiro, 1994).

The peak metamorphic stage (ii) of the garnet-chloritoid schists is defined by the of inclusions in the rims of the garnets (X_{Prp}<0.13), i.e. kyanite, phengitic muscovite (Si=6.40-6.63 pfu), chloritoid (X_{Mg}=0.11-0.18), Mg-rich chlorite (X_{Mg}=0.38-0.42) rutile and quartz; and by schistosity-forming minerals, i.e. chloritoid (X_{Mg}=0.08-0.21), and phengitic muscovite (Si=6.34-6.57 pfu) and paragonite, coexisting with the rims of porphyroblastic garnet. Kyanite thus coexisted with

garnet (rim), chloritoid, phengite and Mg-rich chlorite at the peak metamorphic conditions.

Metamorphic stage	Pre-peak stage	Peak stage	Retrograde stage
Garnet	X_{Prp} 0.02-0.06 (Cores)	X_{Prp} 0.06-0.13 (Rims)	
Kyanite			
Chloritoid	X_{Mg} 0.08-0.13	X_{Mg} 0.11-0.18	
Phengitic muscovite	Si=6.06-6.38	Si=6.34-6.76	Si=6.05-6.32
Paragonite			
Chlorite	X_{Mg} 0.07-0.24	X_{Mg} 0.38-0.42	X_{Mg} 0.14-0.29
Quartz			
Rutile			
Ilmenite			
Calcite			

Fig.5.4 Mineral paragenesis of garnet-chloritoid schist within marble (after Javkhlan et al., 2013).

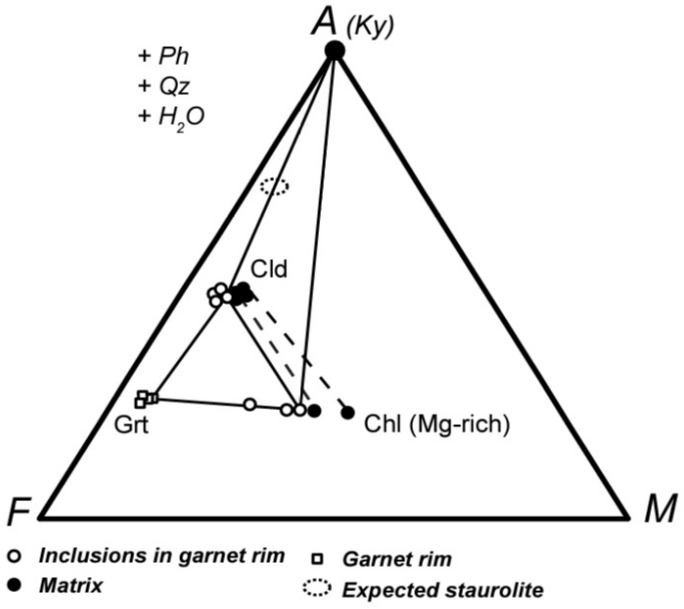

Fig.5.5 AFM diagram illustrating the compositional and mineral relationships of the peak minerals of the garnet-chloritoid schist (after Javkhlan et al., 2013).

Compositions of the peak mineral assemblage of garnet (rim), chloritoid, kyanite and chlorite are plotted in an AFM diagram (Fig. 5.5). Garnet, chlorite and chloritoid (with phengite, quartz and H_2O) occur in equilibrium as a divariant

mineral assemblage (Fig. 5.5). The garnets of the garnet-chloritoid schists also contain considerable amounts of X_{Grs} (0.09-0.12), and therefore kyanite may coexist as a divariant assemblage with ferromagnesian phases such as chloritoid and chlorite. THERMOCALC (v.3.33) (Powell and Holland, 1994) with an updated internally consistent thermodynamic data set (Holland and Powell, 1998) was used to apply an 'average PT' mode calculation for the garnet-chloritoid schists, to estimate their pre-peak and peak P-T conditions (Fig. 5.7). Quartz and H2O are present in both assemblages. THERMOCALC calculations for the pre-peak stage (garnet core + chloritoid + phengitic muscovite + chlorite) of garnet-chloritoid schists yielded P-T conditions of T=500-510 °C and P=7-8 kbar. These lie in the field of epidote-amphibolite conditions (Fig. 5.7). THERMOCALC calculations for the peak stage (garnet rim + kyanite + chloritoid + phengitic muscovite + chlorite) of garnet-chloritoid schists yielded P-T conditions of T=560-590 °C and P=10-11 kbar. These lie in the high-pressure portion of epidote-amphibolite or the low-pressure portion of eclogite facies conditions (Fig. 5.7). When decreasing the activity of water [a(H2O) = 0.9 and 0.8], the estimated temperature is generally lowered by ~10-20 °C and ~15-25 °C respectively, whereas the effect on the pressure is minimal.

The pre-peak (garnet core + chloritoid + phengitic muscovite + chlorite) and the peak mineral assemblages (garnet rim + kyanite + chloritoid + phengitic muscovite + chlorite) of the garnet-chloritoid schists are a typical high-pressure series of mineral assemblages in common metapelite (Spear and Cheney, 1989). At the estimated peak metamorphic conditions of T=560-590 ºC and P=10-11 kbar, staurolite is expected as a stable phase (Spear and Cheney, 1989). However, staurolite was not observed within the porphyroblastic garnets or in the matrix of the

garnet-chloritoid schists, suggesting that at the peak metamorphic conditions, kyanite and chloritoid were stable instead of staurolite.

The retrograde stage (iii) is defined by the minerals replacing the peak metamorphic assemblages. The porphyroblastic garnets are strongly fractured, and the fractures are filled by an assemblage of chlorite, muscovite (Si=6.15-6.23 pfu), paragonite and quartz, suggesting retrograde metamorphism during greenschist facies conditions (Fig. 5.7).

5.3 Vein-type orthogneisses

The mineral assemblage and chemical compositions of minerals particularly of garnet and phengite compositions in the vein-type orthogneiss (sample MG1220-1), two metamorphic events distinguished. First metamorphic event (M1) divided as pre-peak, peak and retrograde stages. Second metamorphic event (M2) divided as pre-peak, peak and retrograde stage (Fig. 5.6).

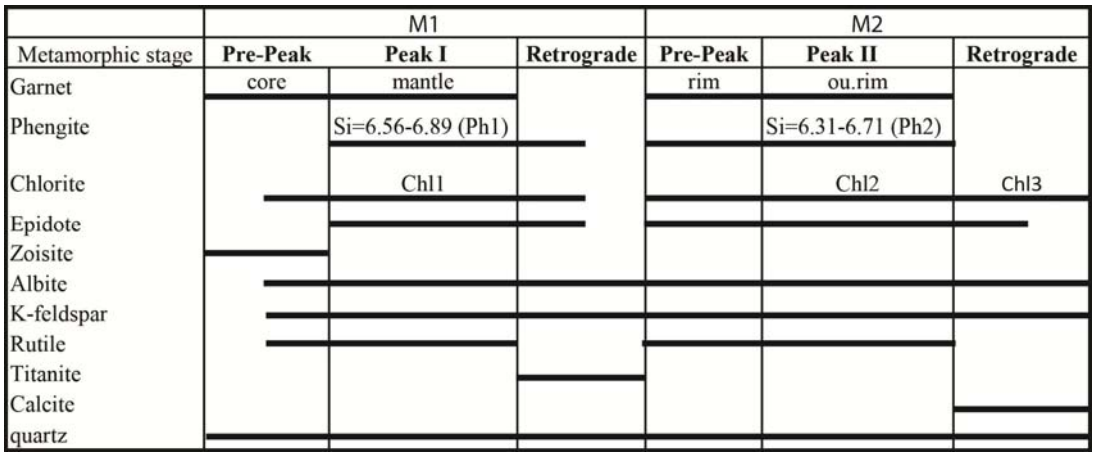

Fig.5.6 Mineral parapgenesis of vein-type orthogneiss (sample MG1220-1).

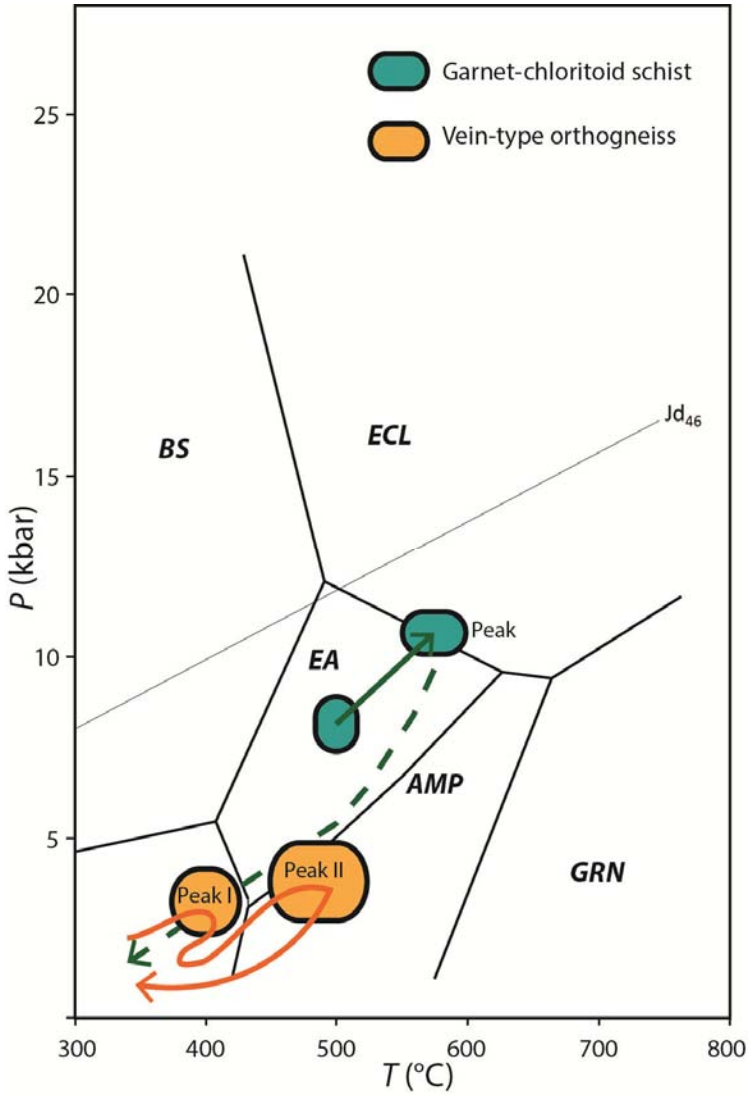

Fig.5.7 Metamorphic P-T conditions of garnet-chloritoid schist and vein-type orthogneiss from the Alag Khadny metamorphic complex, SW Mongolia. Metamorphic facies boundaries after Takasu (1989). ECL, eclogite facies; GL, glaucophane schist facies; EA, epidote-amphibolite facies; AM, amphibolites facies; GRN, granulite facies; GS, greenschist facies.

The pre-peak stage of M1 is can be defined by the core of garnet grains, inclusions of zoisite in the K-feldspar, albite and K-feldspar.

Mantles of garnet, epidote (Ep1), Ph1, chlorite intercalating epidote (Chl1), K-feldspar, albite, rutile and quartz suggest the peak metamorphic stage (peak I) minerals M1 event. THERMOCALC calculations for the peak stage (garnet mantle + Ep1 + Ph1 + Chl1 + albite + K-feldspar) of first metamorphism (M1) of the vein-type orthogneiss yielded P-T conditions of 376 ± 27 °C and 3.3 ± 1.0 kbar. These lie in the green schist facies conditions (Fig. 5.7).

Garnet (rim), Ph2 overgrowing Ph1, Ep2, Chl2, K-feldspar, albite and quartz suggest the peak metamorphic stage of M2 event minerals (peak II). Chl3 replacing garnets and calcite represent retrograde metamorphism after the peak II stage. THERMOCALC calculations for the peak stage (garnet rim + Ep2 + Ph2 + Chl2 + albite + K-feldspar) of second metamorphism (M2) of the vein-type orthogneiss yielded P-T conditions of 486 ± 33 °C and 4.3 ± 1.3 kbar (sigfit=1.85). These lie in the low-pressure portion of epidote-amphibolite and amphibolites facies conditions (Fig. 5.7).

CHAPTER 6 GEOCHRONOLOGY

6.1 K-Ar

Analytical methods

K-Ar ages of the amphiboles and phengites were determined by the Geospace Science Co., Ltd. The K content of each mineral separates were measured by flame spectrophotometry. Analytical precision was better than 2%. 25 to 30 mg samples were degassed under vacuum at aproximately 100°C for ten to twelve hours before analysis to reduce atmospheric contamination. Argon was extracted during complete sample fusion in a Mo crucible heated by a radiofrequence furnace and mixed with a known amount of ^{38}Ar spike and purified in a pyrex glass extraction line. Measurements were done in static mode with an AEI MS-10 mass-spectrometer with a permanent magnet of 4.1 kG and connected to a computer for data processing. Analytical precision on ^{40}Ar and ^{38}Ar peak heights was higher than 0.5%; and 1% on ^{36}Ar.

Eclogites

Javkhlan et al. (2014) reported K-Ar ages of amphibole-rich metamorphosed veins, i.e. amphibole (barroisite cores with Mg-hornblene/edenite rims)-sodic plagioclase (An=1-14)-phengite (Amp-NaPl-Ph) (sample MG1218) and amphibole (tremolite core with actinolite/Mg-hornblende rim)-quartz (Amp-Qz) (sample MG1222) metamorphosed veins in the eclogite bodies (eclogite-1) surrounded by orthogneisses. K-Ar ages of amphibole and phengite from the amphibole-rich metamorphosed veins were determined, and interpreted as exhumation ages of the eclogite bodies (Javkhlan et al., 2014).

Samples of both the Amp-NaPl-Ph metamorphosed vein (MG1218) and the Amp-Qz metamorphosed vein (MG1222) from the eclogites were treated for K-Ar dating. The metamorphosed veins were carefully obtained from the eclogite matrix, hand-crushed, and sieved to separate grains coarser than 0.075 mm (sieve #200). Amphiboles were separated by hand-picking, whereas phengites were concentrated using an isodynamic separator and paper shaking.

Compositions of the mineral separates were verified by EPMA analysis. The amphiboles separates from the Amp-NaPl-Ph and Amp-Qz metamorphosed veins have K2O contents ranging from 0.10 to 0.60 wt% and 0.04 to 0.17 wt%, respectively. The phengites from the Amp-NaPl-Ph vein have Si contents ranging from 6.70 to 6.92 pfu, and Na/(Na+K) of 0.07-0.10 (Fig. 6.1). The compositions of the amphibole and the phengite separates are thus concordant with the grains analyzed in thin sections, and hence are representative of the mineral populations in the metamorphosed veins.

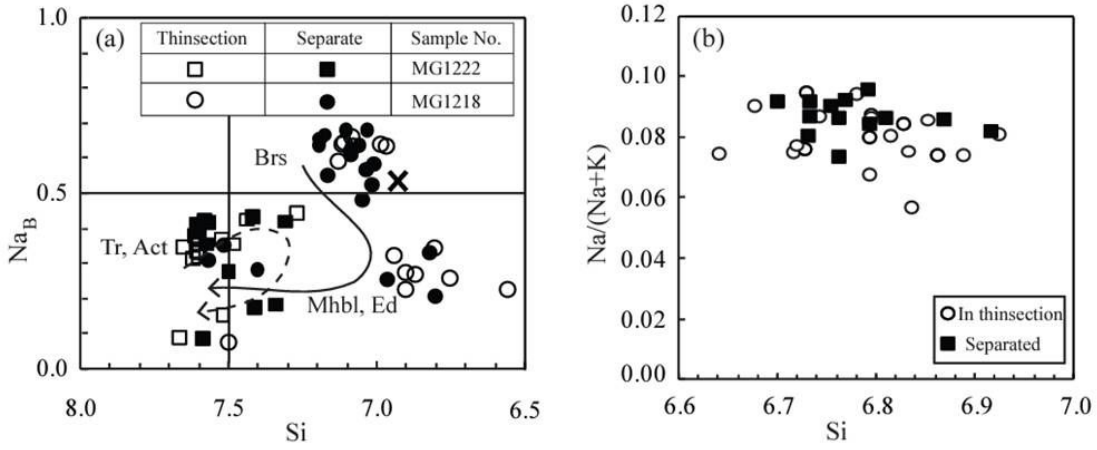

Fig. 6.1 (a) Chemical compositions of zoned amphiboles from the Amp-NaPl-Ph metamorphosed vein (sample MG1218) and Amp-Qz metamorphosed vein (sample MG1222). Dashed and solid arrows represent compositions of amphibole cores and rims. Cross indicates representative composition of barroisitic amphibole in the eclogites-1 matrix. (b) Chemical compositions of phengites in the Amp-NaPl-Ph metamorphosed vein (sample MG1218). Photos referred from Javkhlan et al. (2014).

The amphibole and the phengite concentrates separated from the Amp-NaPl-Ph metamorphosed vein in the eclogites near Mt. Ulaan Tsakhir yielded ages of 603 ± 15 Ma and 612 ± 15 Ma, respectively (sample MG1218). The amphibole concentrate from the Amp-Qz metamorphosed vein in the eclogites near Mt. Alag Khad was dated as 602 ± 15 Ma (sample MG1222) (Table 6.1).

Rock type	Sample No.	Material analyzed	Isotophic Age (Ma)	%K	Rad. ^{40}Ar (scc/gx10^{-5})	%Rad. ^{40}Ar
Eclogite-1	MG1218	Amp	603 ± 15	0.42	1.2	73.7
				0.42	1.2	70.1
		Ph	612 ± 15	7.10	19.6	97.9
				7.06	20.5	98.4
	MG1222	Amp	602 ± 15	0.16	0.5	92.2
				0.16	0.4	91.7
Vein-type orthogneiss	MG1220-1	Ph (lay.)	508 ± 13	7.92	18.1	98.1
				7.91	18.0	97.8
		Ph (with Qz + Ab)	479 ± 12	8.12	17.4	97.7
				8.10	17.2	98.6
Orthogneiss surrounding eclogite bodies	MG1228-1	Ph (mtx)	510 ± 13	7.57	17.6	98.4
				7.56	17.1	98.2
	MG1229	Ph (mtx)	459 ± 11	7.00	14.1	97.7
				6.98	14.3	97.1

Table.6.1 K-Ar analytical data for amphiboles and phengites from eclogites-1, vein-type orthogneiss intruding into eclogites-1and orthogneiss surrounding eclogites-1 of the Alag Khdany metamorphic complex (after Javkhlan et al., 2014).

The K-Ar ages of the amphibole and the phengite from the eclogites-1 cluster at about 600 Ma, and are concordant within analytical error (Table 6.1). Reported argon retention temperatures in amphibole and muscovite (phengite) are 500 ± 50 °C (Harrison, 1981; Baldwin et al. 1990) and c. 350-430 °C (Purdy and Jager 1976; McDougall and Harrison 1988; Blanckenburg et al. 1989; Kirschner et al. 1996), respectively. These temperatures are considerably lower than the peak temperatures

(T=565 ± 39°C) of the eclogites-1 (Fig. 5.2), suggesting that argon retention took place during the exhumation of the eclogites bodies.

Orthogneisses (vein-type and surrounding eclogites bodies)

Phengites segregated in the phengite-rich layer is chemically less zoned in the vein-type orthogneiss (MG1220-1). These phengite-rich layers were carefully separated from the vein-type orthogneiss sample. K-Ar age dating for both phengites from phengite-rich layers and phengites from whole domains (phengite-rich layer and quartz-albite rich domain) in the vein-type orthogneiss (MG1220-1) were performed. The samples (MG1220-1, MG1228-1 and MG1229) were hand-crushed, and sieved to separate grains coarser than 0.075 mm (sieve #200). Phengites were concentrated using paper shaking method. In addition, in the sample MG1228-1, Si contents (6.32-6.98 pfu) in phengite vary widely. And Si-poor muscovite present. Higher-Si phengites are shown higher Fe+Mg (0.75-1.16 pfu) than lower-Si phengites (0.46-0.55) in sample MG1228-1. Thus, we concentrated higher-Si phengites using an isodynamic separator after the paper shaking.

Compositions of the mineral separates were verified by EPMA analysis. Phengites in the whole domains (Ph-rich layer and Qz+Ab rich part) from sample MG1220-1 have Si contents ranging from 6.42 pfu to 6.74 pfu with X_{Na}= 0.02-0.03. Phengites from the phengite-rich layer part in the vein-type orthogneiss (sample MG1220-1) have Si contents ranging from 6.47 pfu to 6.72 pfu with X_{Na}= 0.01-0.03 (Fig. 6.2).

Phengites from sample MG1228-1 have Si contents ranging from 6.45 pfu to 6.64 pfu, and X_{Na}= 0.01-0.03. X_{Na} contents of separated phengites distinctly lower than phengites in the thinsection, indicating they were unaffected by dolomite-rich

micro-veins. Phengites from sample MG1229 have Si contents ranging from 6.35 pfu to 6.73 pfu, and X_{Na}= 0.01-0.03 (Fig. 6.2).

The compositions of the phengite separates are thus concordant with the grains analyzed in thin sections, and hence are representative of the mineral populations in the metamorphosed veins.

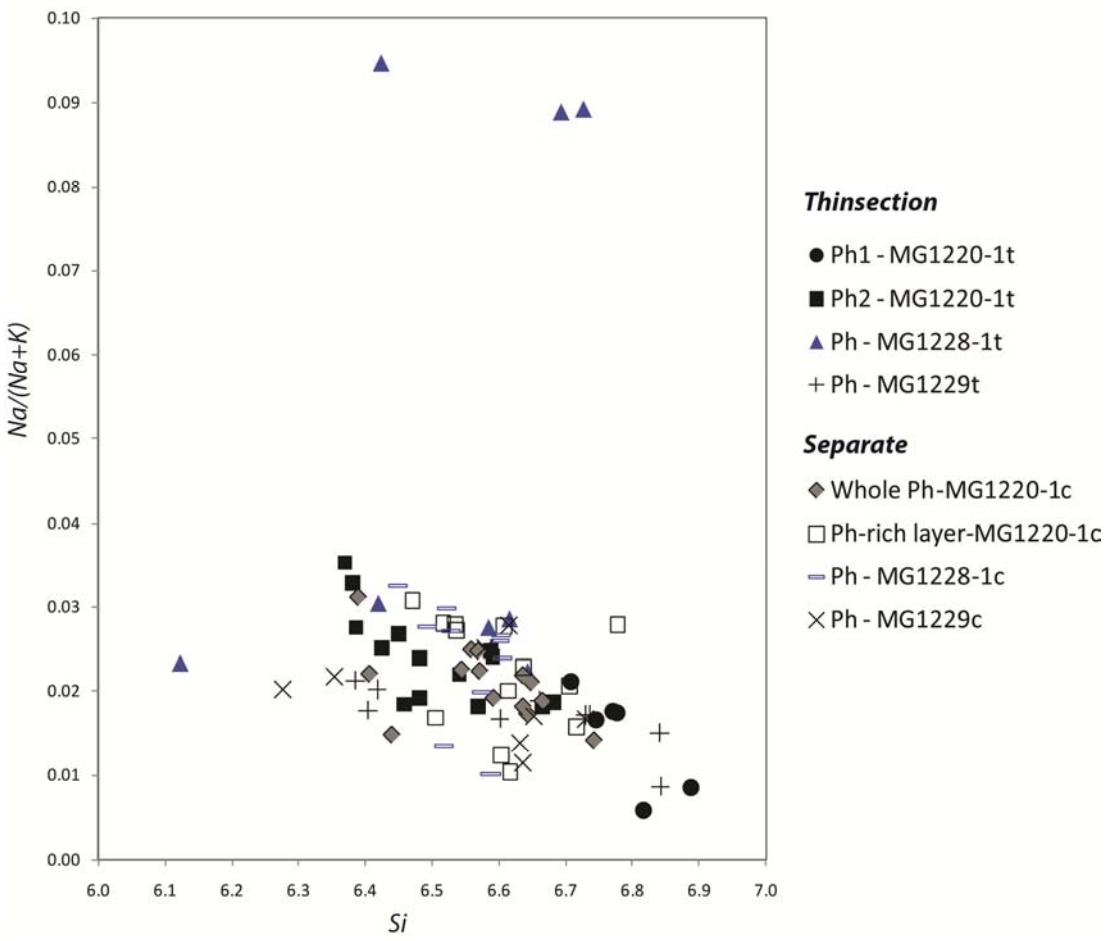

Fig. 6.2 Chemical compositions of phengites from vein-type orthogneiss (MG1220-1) and orthogneisses surrounding eclogites bodies (sample MG1228-1 and MG1229).

The phengite concentrates (whole) from the vein-type orthogneiss (sample MG1220-1) near Mt. Alag Khad yielded age of 479 ± 12 Ma whereas phengite concentrates from the phengite-rich layer yielded age of 508 ± 13 Ma (Table 7.1.1). The phengite concentrate from the orthogneisses surrounding eclogite bodies near Mt. Ulaan Tsakhir was dated as 510 ± 13 Ma for sample MG1228-1 (dolomitized

orthogneiss) and as 459 ± 11 Ma for sample MG1229 (neighboring orthogneiss) (Table 6.1).

The obtained K-Ar ages of phengites (479 ± 12 Ma) from whole phengites from both phengite-rich layer and quartz-albite rich part and phengites from phengite-rich layer (508 ± 13 Ma) in the vein-type orthogneiss (sample MG1220-1) are not concordant (Table 6.1) and older age has been obtained from phengite-rich layer. This feature suggests that the 'excess argon' probably affected for phengites in the phengite-rich layer. Phengite, epidote and garnet in the vein-type orthogneisses are preserved multiple generations of crystallization (Fig. 3.47-3.51) suggesting multiple metamorphic events took place. The obtained K-Ar age of 479 ± 12 Ma from whole phengite therefore may represent cooling age of last events of metamorphism.

Two dated orthogneiss samples which are as far as ~ 200 m each other, close to the Mt. Ulaan Tsakhir (Fig. 2) have been shown distinctly different age (459 ± 11 Ma for sample MG1229 and 510 ± 13 Ma for sample MG1228-1). By the petrographic observation, orthogneiss sample MG1229 contain large embayed phenocrystic K-feldspars which are partially replaced by metamorphic phengite, albite and secondary K-feldpar suggesting that orthogneisses was suffered by single metamorphism. In contrast, nor any magmatic phenocrysts observed in the sample MG1228-1 and some phengites shown resorbtion texture (Fig. 6a) similar as phengites in the vein-type orthogneiss (MG1220-1), may suggesting multiple events of metamorphism took place and indicates that its timing of the metamorphism probably older (510 ± 13 Ma) than neighboring orthogneiss (459 ± 11 Ma) despite the possibility of 'excess argon' affected.

459 ± 11 Ma from orthogneiss sample MG1229 and 479 ± 12 Ma for whole phengites from vein-type orthogneiss sample MG1220-1 are comparable and is interpreted as dating the last stage of the cooling age after the multiple events of metamorphism of orthogneisses.

6.2 Sm-Nd

Eclogite sample MG1223 has been chosen for Sm-Nd analyses. The eclogite consists mainly of garnet (<1.5 mm across), omphacite (Jd=31-40%) and amphibole (barroisite, Mg-hornblende, actinolite) with minor amounts of epidote, chlorite, plagioclase, quartz and accessory minerals of rutile, titanite. Garnet contains inclusions of epidote, barrosite and quartz. Fractures of garnet filled by chlorite, albite and occationally filled by epidote. Epidotes also included by omphacite.

Analytical method

Garnets and omphacites were separated using isodynamic separator and hand-picking, under a binocular microscope, then mineral separates were hand-crushed in an agate mortar. Whole rock powder is also prepared and analised together with garnets and omphacites. Surface contamination on the garnet separates was removed by washing in an ultrasonic bath in 0.5 N HCl for 20 min. in order to remove any possible REE-bearing micro-inclusions, the samples were leached in Suprapur 96% H_2SO_4 on a hot plate at 180°C for 24 h. Samples were then washed with pure DI water at least 10 times to remove any H_2SO_4 residue. The leached powders of mineral and whole rock were then spiked with a mixed ^{149}Sm-^{150}Nd tracer and dissolved in a 2:1 HF-HNO_3 acid mixture in SAvillex PFA vials on a hot plate at 180°C for several days. After complete dissolution, the samples were evaporated to dryness and then redissolved in 6 N HCl ready for cation-exchange column

extraction. Sm-Nd analysises were measured using thermal-ionisation mass spectrometry (TIMS).

Result

The results of Sm-Nd isotopic analyses on separated minerals of garnet and omphacite and whole rock from eclogites are presented in Table 6.2 and Fig. 6.2.

The $^{147}Sm/^{144}Nd$ ratio of the analysed garnets is much lower (0.0476) than omphacites (0.1719) and whole rock (0.1734) whereas similar for omphacites and whole rock. The $^{143}Nd/^{144}Nd$ ratio of the analysed garnets is also lower (0.5123) than omphacites (0.5127) and whole rock (0.5126) whereas ratio of omphacites are slightly higher than whole rock ratio (Table 6.2). Thus, in the Sm-Nd isochron diagram, a negative isochron has been shown indicated by garnet, omphacite and whole rock plots (Fig. 6.2). Whole rock data point lie outside the garnet-omphacite tie-line. This indicates that isotopic compositions of coexisting minerals were not equillibrium and that whole rock must be mass-balanced by nonanalyzed minor phases such as epidotes. The $^{147}Sm/^{144}Nd$ ratio of the analysed garnets is much lower (0.0476) than the 'normal' garnet values of 0.5 to 2.0 from various eclogitic garnets in the world.

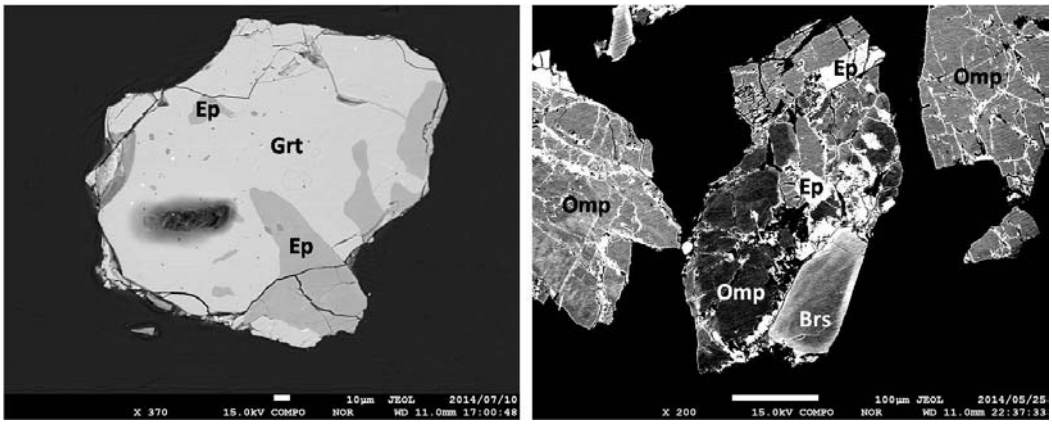

Fig. 6.1 Inclusions of epidotes in the garnet and omphacite separated grains and epidotes partially replacing garnet in the eclogite-1 (MG1223) from Alag Khadny metamorphic complex, Chandman district.

Tie-line of garnet-omphacite-whole rock gives an age of 410 ± 150 Ma (MSWD=1.3), which is appeariently negative younger age with high error comparing the previously obtained K-Ar and Ar-Ar exhumation ages (c. 600 Ma and c. 540 Ma) from the eclogites of Alag Khadny metamorphic complex (Štípská et al., 2010; Javkhlan et al., 2014) and concordant within error with K-Ar ages of orthogneisses (c. 460-500 Ma) associated with eclogites bodies.

The interpretation of failed isochron suggests that garnet and omphacite contain inclusions of epidotes and some fractures of garnet filled by later stage epidotes (Fig. 6.1). Since Sm and Nd partition coefficients for epidote group (Nd=1620; Sm=866.5) much higher than garnet (Sm=0.29; Nd=0.07) and omphacite (Sm=0.50; Nd=0.31) (Arth, 1976), most of amounts of Sm and Nd were redistributed to the epidotes during the retrograde metamorphism. Data points of whole rock and omphacite are close to each other in the Sm-Nd isochron diagram (Fig. 6.2) suggest that Sm/Nd ratios of whole rock and omphacite are essencially controlled by Sm-Nd distribution in epidotes.

	Whole rock	Omphacite	Garnet
$^{143}Nd/^{144}Nd$	0.5126	0.5127	0.5123
$^{147}Sm/^{144}Nd$	0.1734	0.1719	0.0476
Nd (ppm)	15.02	9.001	8.218
Sm (ppm)	4.306	2.559	0.647
Sm/Nd	**0.29**	**0.28**	**0.08**

Table 6.2 Whole rock, omphacite and garnet Sm-Nd data of the eclogite-1 (MG1223) from Alag Khadny metamorphic complex, Chandman district.

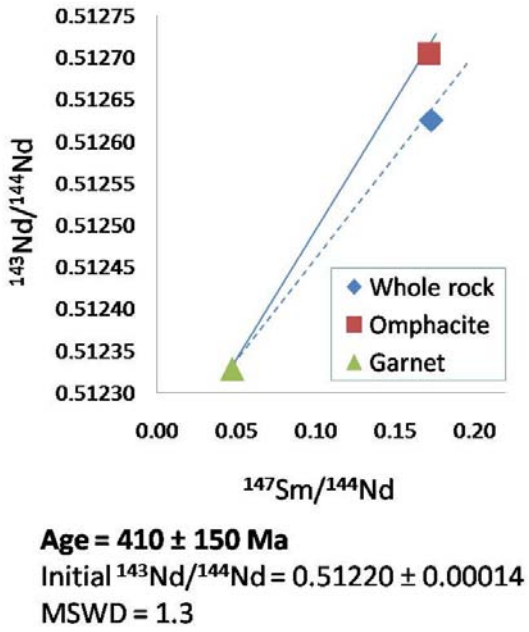

Fig. 6.2 Sm-Nd isochrons of the eclogite-1 (MG1223) at Alag Khadny metamorphic complex, Chandman district.

This interpretation also supported by some of omphacite containing epidote inclusions. The obtained Sm-Nd age (410 ± 150 Ma) somehow similar within error with K-Ar ages of orthogneisses (c. 460-500 Ma), suggesting epidote crystallization during the retrograde metamorphism probably associated with fluids related with granitic magmatism and metamorphism.

CHAPTER 7 GEOCHEMISTRY

Three samples from eclogite-1 (MG1202, MG1218, MG1223), three samples of orthogneisses (MG1220-1, MG1228-1, MG1229) and samples of ophiolitic Khantaishir Formation (metabasalts, metadiorites, porphyry dykes and metatuffs) were analyzed for determine their whole-roch chemical compositions (major and trace elements) in the Chandman district.

Analytical method

Whole-rock chemical analyses were made using a Rigaku RIX-2000 X-ray fluorescence spectrometer (XRF) at Shimane University. Loss on ignition (LOI) was calculated by weight difference after ignition at 1000 °C. Abundances of the major elements and 14 trace elements were determined from glass beads prepared with an alkali flux (80% lithium tetraborate, 20% lithium metaborate), with a sample to flux ratio of 1:2. The list of samples and major- and trace-element data are in Table 7.1.

Results of analysis

Eclogite-1 samples (MG1218, MG1202 and MG1223) from the Alag Khadny metamorphic complex have composition of tholeiitic basalts (Figs. 7.2 and 7.3). SiO_2 abundances range between 48.16% and 48.96%. The K_2O is low (0.15-0.26) with value 1.99 in sample MG1218 (Table 7.1). K_2O/Na_2O ratio is 0.18-1.74. MORB-normalized trace element patterns shown that eclogites-1 are strongly enriched in Rb and Th, slightly enriched in Nb, slightly depleted in Cr. Ba remarkably higher in eclogites sample MG1202 than other eclogites samples (Fig. 7.5).

Metabasalts (MG1235 and MG1237) of the Khantaishir Formation are calk-alkaline field of AFM diagram (Fig. 7.3). The K_2O/Na_2O ratio is 0.00-0.01. In the classification diagram metabasalts are plotted in the fields of basalt and trachybasalt (Fig. 7.2). Trace element patterns maintain consistent pattern with eclogites-1 except have a strong enrichment of Th in both samples and strong depletion of Cr in sample MG1237 (Fig. 7.5).

Porphyry dykes (MG1232 and MG1242) of the Khantaishir Formation are plotted in the field of calc-alkaline (MG1242) and boundary line of toleiitic series and calc-alkaline series (MG1232) in the AFM diagram and have a higher alkali component (Na_2O+K_2O) than eclogites-1 and metabasalts (Figs. 7.2 and 7.3). As

shown in classification diagram, they have a componsitions of trachybasalt and trachyandesite.

Orthogneisses [(MG1220-1 vein-type orthogneiss), MG1228-1 and MG1229] from the Alag Khadny metamorphic complex can be classified as granitic in composition in (Cox et al. 1979). Silica contents of orthogneisses are shown little compositional variation, range from 76.19 to 77.73 wt% (Table 7.1). However, the ratio K_2O/Na_2O (0.1-1.4) varies widely in comparison to K_2O+Na_2O (7.06-7.81 wt%) and is perhaps for some orthogneisses indicative of exchange of alkalis prior to or during metamorphism. The Rb/Sr ratios for sample MG1228-1 (3.2) and for sample MG1229 (4.5) are distinctly higher than ratio (0.2) for sample MG1220-1. The chondrite-normalized trace element patterns displays a marked depletion in Sr and Zr and slight depletion in Ba while Rb and Th show a marked enrichment for all samples MG1220-1, MG1228-1 and MG1229 (Fig. 7.6) comparing to upper and lower continental crust data (Taylor and McLennan, 1981 and Weaver and Tarney, 1984, respectively).

Metadiorite (MG1239-1, MG1239-2 and MG1240) from the Khantaishir Formation have a little compositional variations in both major and trace element Harker diagrams and they can be classified as quartzdiorite (granodiorite) in composition (Cox et al. 1979). Silica (SiO_2) contents of metadiorite shown little compositional variation, range from 63.08 to 64.17 wt% (Table 8.1). Trace element patterns display that they are distinguished as marked depletion in Ba, Ce, Nb, Rb, Sr, Y and Zr and enriched in Th comparing to upper and lower continental crusts (Fig. 7.6).

Metatuffs of the Khantaishir Formation divided as lower and upper section by their whole rock compositions. Clear negative trend with SiO_2 content and positive

trends with TiO_2, Fe_2O_3, CaO and P_2O_5 contents comparing to MgO content shown in the Harker variation diagrams (Fig. 7.1). Lower successions of metatuffs are lower in SiO_2 (53.07-57.84 wt%) and higher in MgO (3.94-6.07 wt%), TiO_2 (0.62-0.78 wt%), Fe_2O_3 (8.04-12.21 wt%), CaO (5.67-14.58 wt%) and P_2O (0.09-0.30 wt%) than upper successions of metatuffs (SiO_2=55.31-67.34 wt%; MgO=2.58-4.89 wt%; TiO_2=0.20-0.32 wt%; Fe_2O_3=7.63-14.38; CaO=0.82-7.38 wt% and P_2O=0.05-0.11 wt%) in the Khantaishir Formation. One sample from lower section are distinctly different composition higher in SiO_2 (70.15 wt%) and K_2O (2.61 wt%) and lower in Al_2O_3 (12.53 wt%), Fe_2O_3 (7.63 wt%), CaO (0.76 wt%), Na_2O (0.28 wt%) than overlying metatuffs (Fig. 8.1). By the petrographic observation, rock type regarded as deformed metasiltstone.

In variation diagrams of trace elements, lack of consistent trend shown except for positive trend with Y and Zr between lower and upper section of metatuffs (Fig. 8.4). Spider diagram for trace elements displays that trace element contents of metatuffs from both lower and upper section are generally clustered except significant variation in Rb and Sr contents. Metasiltstone from lower section is higher in Ce, Nb, Rb and Zr contents than metatuffs (Fig. 7.7).

	Eclogite-1			Orthogneisses		
	MG1218	MG1202	MG1223	MG1220-1	MG1228-1	MG1229
Major elements (wt%)						
SiO2	48.76	48.96	48.18	76.94	77.73	76.19
TiO2	1.42	1.41	1.95	0.01	0.01	0.17
AL2O3	13.80	13.36	13.33	13.85	14.07	13.99
Fe2O3	15.49	14.96	15.98	0.57	0.58	1.35
MnO	0.24	0.21	0.22	0.01	0.01	0.02
MgO	6.84	7.49	7.32	0.21	0.20	0.32
CaO	10.22	11.51	11.17	1.31	0.13	0.11
Na2O	1.14	1.85	1.45	6.52	5.36	3.28
K2O	1.99	0.15	0.26	0.55	1.89	4.53
P2O5	0.09	0.10	0.15	0.03	0.04	0.04
Trace elements (ppm)						
Ba	222.05	17.76	38.82	66.68	141.40	537.44
Ce	12.67	16.43	26.60	35.96	28.86	89.73
Cr	125.27	126.74	98.83	0.50	1.01	1.51
Ga	16.76	15.98	19.60	14.53	22.76	19.70
Nb	6.88	6.32	9.20	6.03	15.00	18.27
Ni	74.37	85.64	95.09	3.20	1.01	0.23
Pb	6.15	1.57	1.39	36.45	66.94	28.75
Rb	59.53	15.33	14.34	23.51	142.41	229.56
Sc	42.45	40.66	35.16	3.92	5.91	5.25
Sr	69.10	138.84	111.17	124.99	43.82	50.67
Th	1.78	2.50	2.94	9.31	24.73	37.73
V	425.80	399.10	430.74	1.30	1.01	13.32
Y	24.50	25.61	23.66	11.92	34.73	29.12
Zr	77.04	80.65	110.46	45.15	70.21	143.78

Table. 7.1 Whole rock compositions of eclogites-1 and orthogneisses of Alag Khadny Metamorphic complex, Chandman district.

	Lower metatuffs						Upper metatuffs						Metabasalts		Metadiorites			Porphyry dykes	
	MG1230	MG1231	MG1233	MG1234	MG1236	MG1238	MG1241	MG1243	MG1244	MG1246	MG1247	MG1248	MG1235	MG1237	MG1239-1	MG1239-2	MG1240	MG1232	MG1242
Major elements																			
SiO2	70.15	53.07	57.84	53.45	57.48	54.51	73.17	55.31	59.29	67.34	67.32	62.09	50.78	49.69	63.08	64.17	63.74	56.17	49.85
TiO2	0.84	0.62	0.70	0.78	0.70	0.70	0.18	0.32	0.30	0.20	0.20	0.26	1.39	2.18	0.22	0.22	0.24	2.03	1.79
AL2O3	12.53	15.19	15.81	15.73	15.26	13.98	12.23	17.03	17.16	14.08	14.70	13.74	14.77	17.16	11.33	11.54	11.83	14.31	17.02
Fe2O3	7.63	12.21	11.88	10.12	9.62	8.04	5.53	14.38	10.97	7.82	7.63	10.43	12.50	15.19	9.77	9.22	9.22	12.23	10.23
MnO	0.11	0.20	0.16	0.21	0.14	0.15	0.09	0.16	0.16	0.17	0.20	0.19	0.19	0.24	0.17	0.16	0.16	0.22	0.17
MgO	4.96	6.07	3.94	5.71	5.19	4.63	3.57	4.89	3.78	2.58	3.57	3.11	7.75	5.38	6.37	5.95	5.37	2.40	6.19
CaO	0.76	9.41	5.67	8.48	7.10	14.58	2.19	0.92	5.33	3.09	0.82	7.38	9.26	4.31	6.61	5.73	7.34	5.44	8.12
Na2O	0.28	2.66	3.18	5.30	4.15	3.32	2.86	6.93	2.37	4.24	5.42	2.43	3.28	5.53	2.16	2.79	1.66	3.46	3.44
K2O	2.61	0.44	0.53	0.06	0.20	0.00	0.09	0.00	0.55	0.41	0.06	0.32	0.00	0.07	0.17	0.11	0.36	2.88	2.29
P2O5	0.13	0.14	0.30	0.16	0.15	0.09	0.08	0.11	0.08	0.07	0.08	0.05	0.16	0.26	0.11	0.11	0.09	0.86	0.89
Trace elements																			
Ba	393.23	178.60	238.78	85.82	117.21	32.30	83.28	97.43	206.10	260.33	48.75	128.83	31.70	36.78	105.58	104.60	212.75	947.72	1216.89
Ce	58.93	13.06	27.02	13.37	20.09	17.82	13.87	13.42	11.15	13.29	11.26	11.12	22.29	24.61	8.46	10.47	12.96	75.65	66.52
Cr	331.64	48.59	4.99	147.04	65.31	555.35	75.92	22.67	5.73	7.64	0.63	10.60	233.52	22.33	234.66	215.89	203.47	2.01	169.10
Ga	14.73	14.17	15.76	10.72	13.72	10.93	9.91	13.38	18.81	11.86	12.24	13.44	17.34	19.39	9.75	8.88	10.03	21.82	17.92
Nb	12.29	1.67	1.27	3.75	3.17	2.98	2.97	3.87	3.26	3.77	3.86	1.50	5.18	6.16	1.86	2.44	2.18	15.48	12.20
Ni	135.48	34.08	2.94	55.92	40.32	30.76	10.40	5.40	3.95	1.96	3.75	2.98	66.17	23.19	28.66	26.75	27.57	0.50	90.07
Pb	9.53	4.80	6.97	4.87	2.26	1.92	3.99	1.51	5.68	3.88	2.89	5.78	1.97	1.85	3.02	2.92	5.55	14.62	5.43
Rb	109.70	11.14	6.76	3.74	2.66	1.49	5.01	1.81	7.44	4.56	3.29	5.15	2.14	4.13	3.78	3.93	5.85	70.10	54.74
Sc	14.50	35.62	24.09	33.30	31.43	40.46	16.25	36.50	37.49	26.71	23.04	41.68	38.89	37.29	36.89	36.24	37.46	23.33	27.94
Sr	79.06	469.40	723.56	151.21	153.39	130.66	162.52	35.98	195.74	101.24	22.40	447.09	115.32	80.73	381.19	256.99	323.83	319.92	600.62
Th	9.20	3.70	2.20	7.43	3.98	1.29	1.23	1.74	1.85	2.18	1.83	1.99	2.18	2.43	1.19	2.25	1.84	8.70	3.64
V	146.75	281.47	359.00	324.98	361.52	168.87	133.30	372.34	192.72	157.45	147.86	356.80	301.22	536.31	257.36	226.32	223.26	247.25	217.80
Y	23.48	16.71	15.27	19.19	18.78	14.79	4.35	8.30	13.78	10.23	8.79	7.94	34.86	52.81	5.96	5.52	6.70	51.06	31.79
Zr	160.10	46.98	64.92	46.39	49.94	39.71	35.63	21.89	22.55	20.36	18.70	16.20	115.10	125.21	23.65	22.64	25.09	312.75	238.39

Table. 7.2 Whole rock compositions of metatuffs, metabasalts, metadiorites and porphyry rocks of Khantaishir ophiolitic Formation, Chandman district.

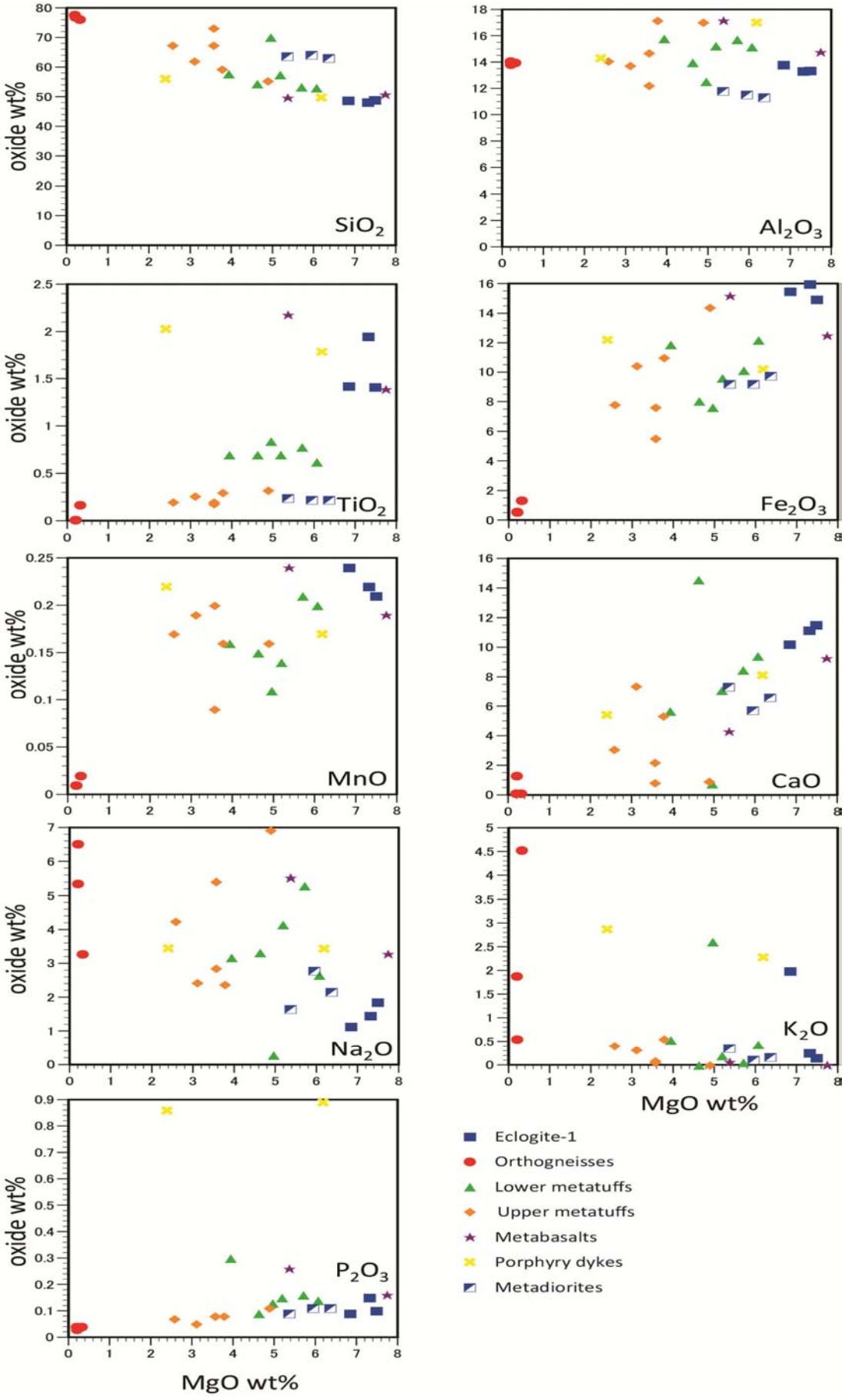

Fig. 7.1 Major elements Harker variation diagram of metamorphic rocks and ophiolitic rocks of Khantaishir Formation, Chandman district.

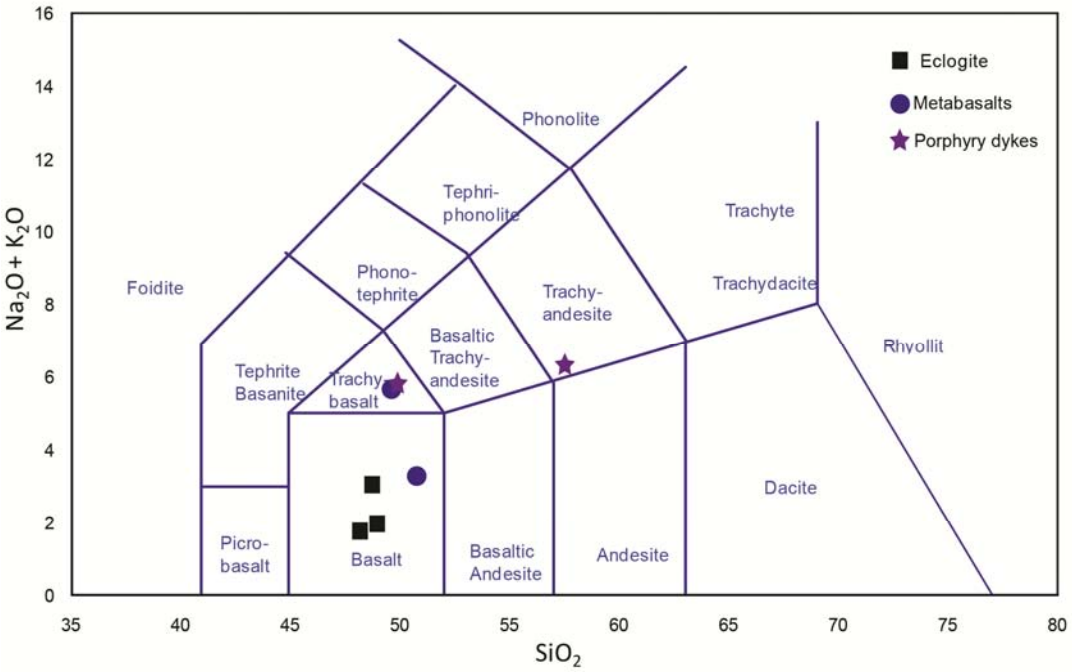

Fig. 7.2 Classification of eclogites-1 from the Alag Khadny metamorphic complex and metabasalts and porphyry dykes from the Khantaishir Formation in the TAS diagram (Le Bas, 1986).

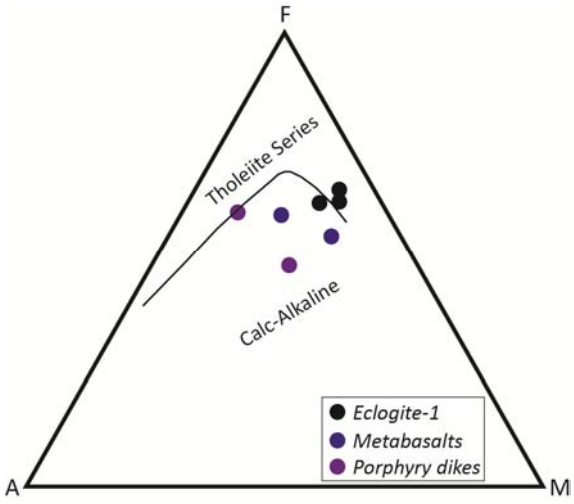

Fig. 7.3 Plots of eclogites-1, metabasalts and porphyry dykes in the AFM diagram (Irvine and Baragar, 1971). A - Alkali (Na2O+K2O), F - FeO, M - MgO.

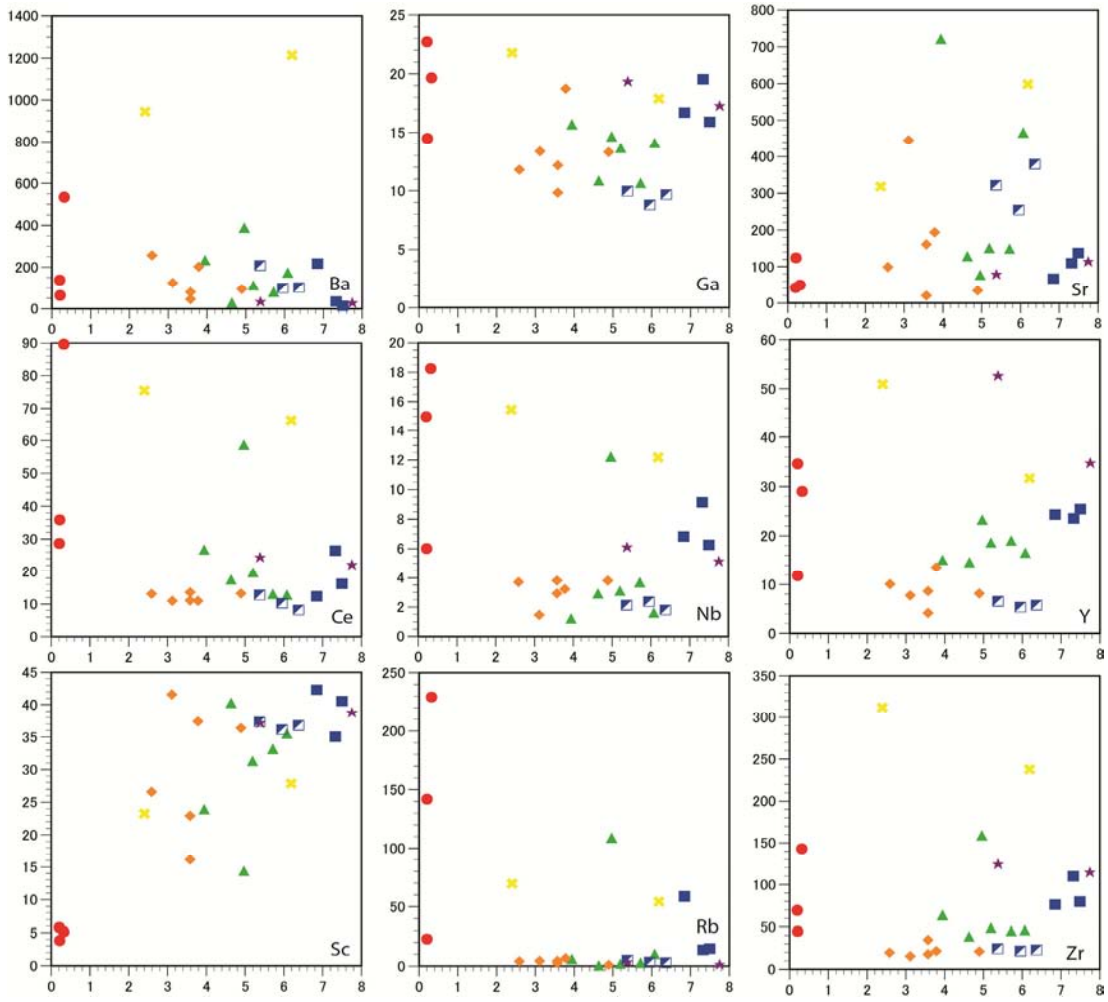

Fig. 7.4 Trace elements Harker variation diagram of metamorphic rocks and ophiolitic rocks of Khantaishir Formation, Chandman district. Symbol describtion is same as Fig. 8.1.

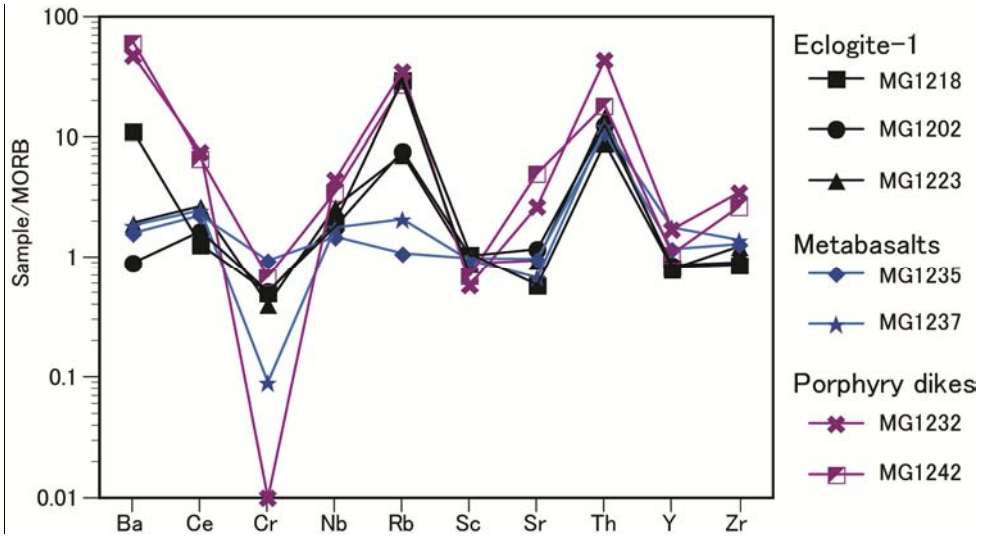

Fig. 7.5 Trace elements Spider diagram of eclogites-1 of Alag Khadny metamorphic complex and ophiolitic metabasalts and porphyry dikes of Khantaishir Formation, Chandman district. MORB values after Pearce, 1983.

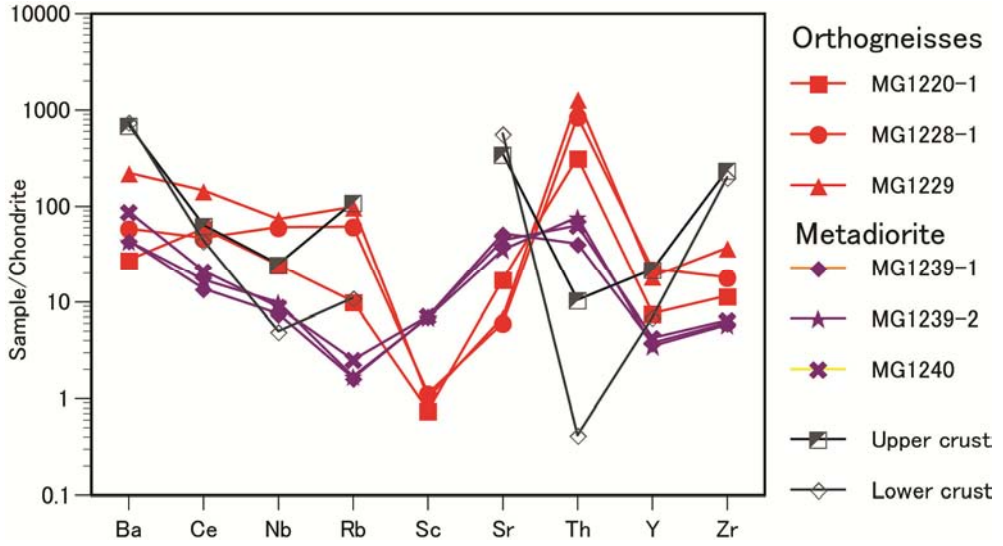

Fig. 7.6 Chondrite normalized trace elements Spider diagram of orthogneisses of Alag Khadny metamorphic complex and metadiorites of Khantaishir Formation, Chandman district; compared with Upper and Lower continental crust. Chondirte values after Sun and McDonough (1989).

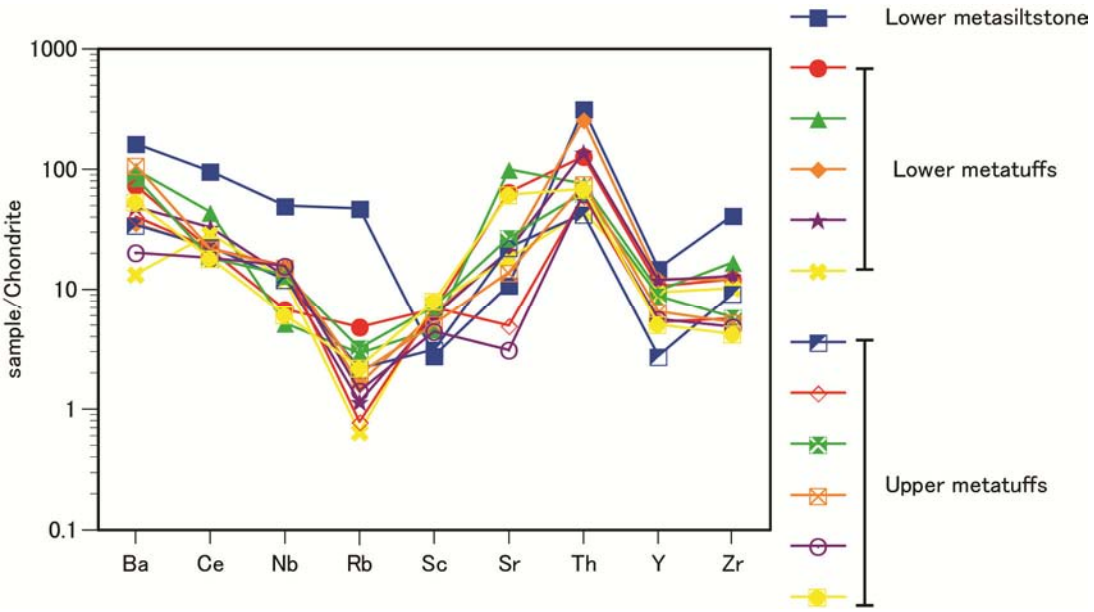

Fig. 7.7 Chondrite normalized trace elements Spider diagram of metasiltstone and metatuffs of Khantaishir Formation, Chandman district. Chondirte values after Sun and McDonough (1989).

CHAPTER 8 DISCUSSIONS

8.1 Tectonic settings of associated basement block and ophiolite units in the Chandman district

The eclogite-bearing Alag Khadny metamorphic complex is over-thrusted by the Neoproterozoic ophiolite-bearing Khantaishir Formation (Hanžl and Aichler, 2007; Lehmann et al., 2010). The Neoproterozoic-Lower Paleozoic Zamtyn Nuruu metamorphic complex is thrusted over by a part of the Alag Kadny metamorphic complex (Lehmann et al., 2010). The Zamtyn Nuruu metamorphic complex is regarded a basement block (microcontinent) which is affected by amphibolite facies metamorphism (c. 950 Ma, Kroner et al., 2010).

The ophiolites of the Khantaishir Formation represent as two types of igneous rocks, i.e tholeiite and calc-alkaline (Hanžl and Aichler, 2007). Khantaishir plagiogranite have yielded concordia intercept U-Pb zircon age of 568±4 Ma (Gibsher et al., 2001). However, Jian et al. (2014) obtained distingtly young $^{206}Pb/^{238}U$ zircon ages of c. 520 Ma from the layered gabbro and the leucogabbro of ophiolitic Khantaishir Formation close to the Chandman district (~10 km far).

The Zamtyn Nuruu basement block intruded by small bodies of diorite (542 ± 4 Ma; ICP-MS zircon; Hanžl and Aichler 2007), granitic pluton (513 ± 5 Ma and 506 ± 4 Ma; ICP-MS zircon and monazite respectively; 485 ± 3 Ma; $^{40}Ar/^{39}Ar$ muscovite age of pegmatite dike cutting the granite; Hrdličková et al., 2008) and a leucogranite dike (510 ± 6 Ma; SHRIMP zircon; Kröner et al. 2010). The obtained K-Ar ages of c. 510-460 Ma from Alag Khadny orthogneisses are comparable with ICP-MS and SHRIMP zircon ages granitic rocks and $^{40}Ar/^{39}Ar$ muscovite age of pegmatite dike,

suggesting Alag Khadny orthogneisses were probably originated from the same magmatism emplaced into the Zamtyn Nuruu basement block.

Jian et al. (2014) obtained U-Pb zircon ages of c. 523-518 Ma from gabbros from the Khantaishir ophiolite associated with the eclogites-bearing Alag Khadny metamorphic complex and they interpreted that the generation and obduction of Khantaishir ophiolites over the Zamtyn Nuruu basement block and subsequent granitic episodes (c. 513-506 Ma) in short span.

$^{40}Ar/^{39}Ar$ age of c. 573 Ma from the orthogneiss close to eclogite body (Lehmann et al., 2010) and K-Ar ages of amphibole-rich veins developed in the eclogite bodies (c. 600 Ma) (Javkhlan et al., 2014) of Alag Khadny metamorphic complex and $^{40}Ar/^{39}Ar$ ages of eclogite and garnet-chloritoid schist (c. 540 Ma) within marbles of Maykhan Tsakhir Formation (Štípská et al. 2010) have been obtained. These ages are distinctly older than obtained K-Ar ages (c. 510-460 Ma) of orthogneisses in this study. Eclogites are considered to be originated from Khantaishir ophiolites (Kröner et al., 2010; Štípská et al., 2010; Jian et al., 2014).**8.2 Protoliths of eclogites and associated metamorphic rocks**

Eclogites represent an affinity to toleiitic mid-ocean ridge basalt (T-MORB) based on major and trace element compositions (Figs 7.3 and 7.5) and rare earth element (REE) contents (Štípská et al., 2010). In the AFM diagram eclogites plotted in the field of toleiite series. One sample (MG1218) plotted in the field of calc-alkaline series; its K_2O/Na_2O ratio (1.74) is much higher than other eclogites (0.08 and 0.18) may indicate metasomatic infiltration of K^+ during post-metamorphic stage. This also supported by development of K-feldspar micro veins developed in the eclogite (MG1218). Trace elements of Ba, Ce, Nb, Sc, Sr, Y and Zr contents of eclogites are comparable with MORB compositions. Major and trace element

compositions of eclogites are comparable with ophiolitic metabasalts of Khantaishir Formation (Figs. 7.1-7.5). Khantaishir metabasalts are plotted in the field of calc-alkaline series by AFM diagram, however, toleiitic ophiolitic metabasalts from Khantiashir Formation reported as well (Hanžl and Aichler, 2007). Matsumoto and Tomurtogoo (2003) reported that the sheeted dykes of Khantaishir ophiolite are boninite-type high-Mg andesites (HMA), and they were formed in an intra-oceanic subduction zone.

The protolith of the garnet-chloritoid schists is considered to have been sedimentary rocks derived from the continental crust, based on bulk rock compositions rich in K_2O (~3 wt%) and Al_2O_3 (~20 wt%) (Štípská et al., 2010). The protolith of orthogneisses are regarded to be granitic rocks. The chondrite-normalized spider plot displays a marked depletion in Sr while Rb and Th show a marked enrichment comparing to upper and lower continental crust (data from Taylor and McLennan, 1981).

8.3 Comparison of pressure-temperature-time paths of the eclogites and associated metamorphic rocks

Based on the mineral paragenesis and pressure-temperature (P-T) evaluation, eclogite-1 within orthogneisses was suffered four distinct metamorphic events, i.e., LP-HT metamorphism (M1), HP metamorphism (M2) and MP metamorphism (M3). The peak metamorphic conditions of M2 events for eclogite-1 in the Alag Khadny metamorphic complex have been estimated as 565 ± 39 ºC and 22 ± 1.6 kbar. Estimated P-T conditions are slightly lower in temperature than previously reported peak metamorphic conditions (T=590-610 °C and P=20-22.5 kbar) by Štípská et al., 2010, and estimated P-T conditions (565 ± 39 ºC and 22 ± 1.6 kbar) correspond to

subduction type with lower geothermal gradient of 9-10 °C/km. Eclogite-1 retrogressed at conditions of 530-630°C and 4-11 kbar corresponding with previously reported decompression stage (T=600-630 ºC and P< 16 kbar; Štípská et al., 2010) after the peak metamorphism (Fig. 8.1).

Garnet-chloritoid schists in the Maykhan Tsakhir Formation are distributed close to the eclogite bodies in the Alag Khadny metamorphic complex, in the Chandman district of the Lake Zone. Textural relationship, mineral assemblage and thermobarometric estimates suggest a high-pressure intermediate type metamorphic evolution for the garnet-chloritoid schists in the Maykhan Tsakhir Formation. The metamorphic conditions of pre-peak (*T*=500-510 °C; *P*=7-8 kbar) and peak (*T*=560-590 °C; *P*=10-11 kbar) stages were determined for the garnet-chloritoid schists. The deduced *P-T* path represents the epidote-amphibolite facies, or the eclogite facies of high-pressure intermediate type metamorphism (Miyashiro, 1961). The *P-T* conditions pre-peak and peak stages correspond to geothermal gradients of 20-22 °C/km and 19-20 °C/km, respectively. These geothermal gradients consistent with 'standard' geothermal gradient with collision type (e.g. Thompson et al., 2001).

The peak metamorphic pressures for the garnet-chloritoid (~10 kbar) schist are distinctly lower than those of the peak pressure of eclogite-1 (~20 kbar), whereas the temperature conditions are similar at *T* = ~ 600 ºC (Fig. 8.1).

The third MP metamorphic event (M3) preserved in the eclogite-1 suggest that their P-T path and geothermal gradient deduced by prograde zoned Amp4 are corresponded with garnet-chloritoid schist metamorphism. These suggest eclogites were affected by the garnet-chloritoid metamorphism.

The third poikiloblastic amphibole (Amp3) metamorphism (M2) preserved in the eclogite-2 within marbles corresponding with M3 metamorphic event preserved

in the eclogite-1 within orthogneiss; and M3 metamorphism of eclogite-2 also therefore corresponding with garnet-chloritoid schist metamorphism (Fig. 8.1). These interpretation also supported by field relation between eclogite-2 and garnet-chloritoid schists which they are both occurred as lenses within marbles close to each other.

The fourth metamorphic event (M4) defined in the amphibolized eclogites-1 can be corresponding with metamorphism of the vein-type orthogneisses which suffered two metamorphic events, i.e., first (M1) greenschist facies metamorphism (~380°C and 3 kbar), second (M2) epidote amphibolite facies metamorphism (~500°C and 4 kbar) (Fig. 8.1). The P-T conditions of peak stages of M1 and M2 for vein-type orthogneiss correspond to geothermal gradients of ~35 °C/km and ~30 °C/km, respectively. The peak temperature conditions of M2 event (~ 500 °C) for the vein-type orthogneiss are lower than peak temperature of M4 metamorphic event of intruded amphibolized eclogites-1 (550-640 °C) whereas the pressure conditions of vein-type orthogneiss (4 kbar) correspond with peak pressure of M4 for amphibolized eclogites-1 (2-5 kbar) (Fig. 8.1). This feature suggests that geothermal gradient of M4 metamorphic event of amphibolized eclogites-1 same as vein-type orthogneiss.

Thus, eclogites-1 within orthogneiss were suffered by HP low geothermal gradient metamorphism (9-10 °C/km) and subsequently they were again suffered by MP relatively higher geothermal gradient metamorphism (19-20 °C/km) together with garnet-chloritoid schist and finely more higher geothermal gradient metamorphism (30-35 °C/km) together with vein-type orthogneiss (Fig. 8.1).

This kind of lithologies with differing geothermal gradient has been also reported by Štípská et al. (2013), that high-pressure eclogite lenses (~ 20 kbar) in the

orthogneiss and associated medium-pressure garnet-staurolite metapelites (~ 7 kbar) intercalated with marbles occur in Orlica-Śnieżnik dome, Bohemian Massif, are juxtaposed during upright folding which can be explained by the model of the crustal-scale folding due to horizontal shortening (Burg et al., 2004). Furthermore, two episodes of lower and higher geothermal gradient metamorphism related with subduction and subsequent collision tectonic have also been documented in the Aktyuz Formation of the Northern Tien-Shan (Orozbaev et al., 2010). The eclogites (T=550-660 ºC; P=21-23 kbar) formed in the low-geothermal gradient conditions (~10 ºC/km), and pelitic gneisses (T=635-745 ºC; P=13-15 kbar) and associated garnet amphibolites (former eclogites) (T=675-735 ºC; P=14-15 kbar) subsequently underwent higher geothermal gradient metamorphism (~17 ºC/km). Similar high-geothermal gradient metamorphism related with collision has been reported from several orogenic belts, such as in metapelites (T=700-800 ºC; P=13-16 kbar; Indares, 1995) in the Gagnon Terrane of Grenville Province, Canadian Shield, which crystallized during an early stage of a crustal shortening/thickening event after subduction of the Laurentian margin (Indares, 1995; Rivers et al., 1993), and eclogites (T=650-780 ºC; P=15-18 kbar) in Weinschenk Island (NE Greenland), which formed during crustal imbrication and subhorizontal shortening during Caledonian collision (Elvevold and Gilotti, 2000). These reported high-geothermal gradients (12-14 km^{-1}) are characteristic of collision type with 'standard' geothermal gradient (e.g. Thompson et al., 2001).

Based on the above, we suggest that a similar collisional setting with a 'standard' geothermal gradient (Thompson et al., 2001) probably responsible for M3 and M4 metamorphic events for eclogites as well as generation of orthogneisses (vein-type orthogneiss) and the Maykhan Tsakhir garnet-chloritoid schists.

Thus, eclogites-1 within orthogneiss were suffered by HP low geothermal gradient metamorphism (M2; 9-10 °C/km) after the M1 event, and subsequently they were again suffered by MP relatively higher geothermal gradient metamorphism (19-20 °C/km) together with garnet-chloritoid schist and finely more higher geothermal gradient metamorphism (30-35 °C/km) together with vein-type orthogneiss.

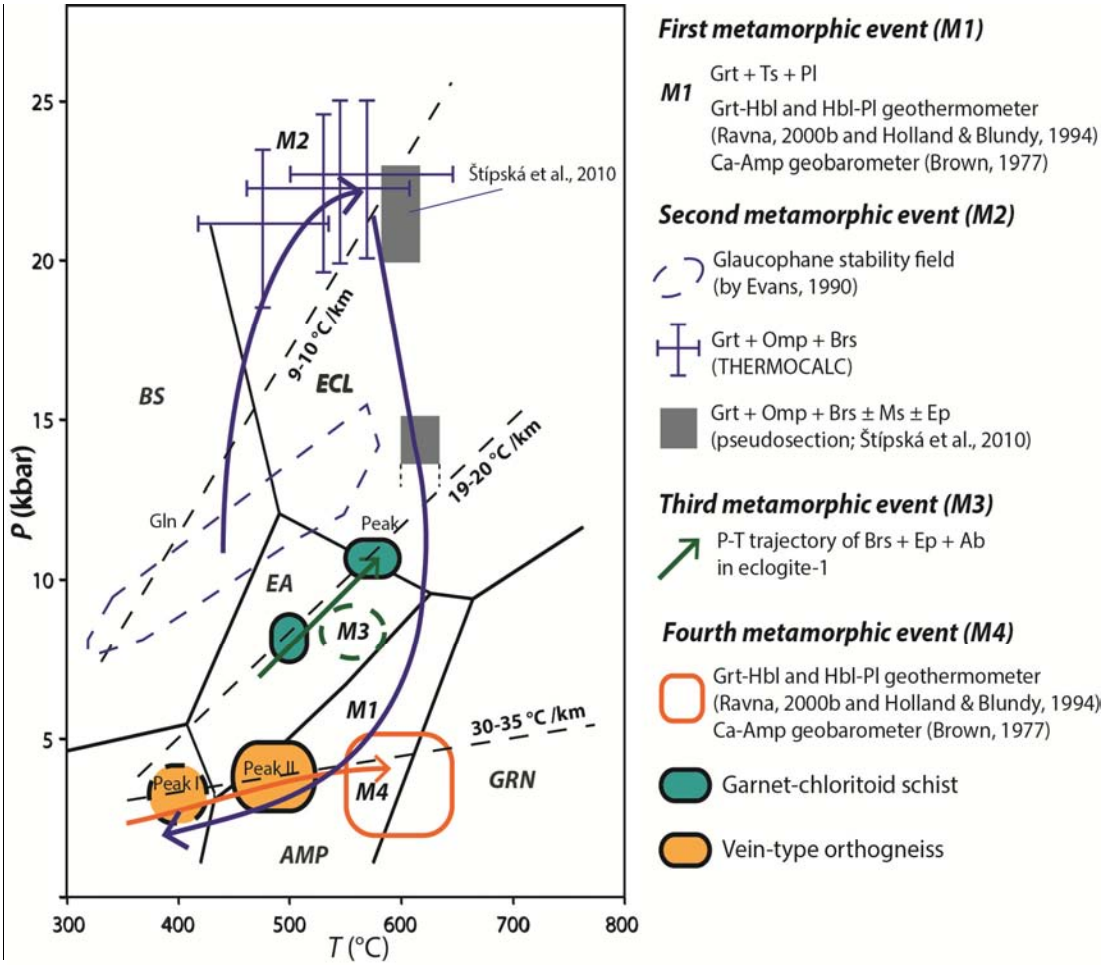

Fig. 8.1 P-T conditions of eclogites-1 and vein-type orthogneiss of Alag Khadny metamorphic complex and garnet-chloritoid schists of Maykhan Tsakhir Formation.

The obtained K-Ar ages of c. 500-480 Ma from the vein-type orthogneiss intruded into eclogite-1 as well as c. 500-460 Ma from the orthogneisses surrounding eclogite bodies. These ages indicate that an exhumation ages of eclogite-1 and vein-type orthogneisses.

8.4 Tectonic implications

Hrdličková et al. (2010) predicted possible collision of Dzabkhan-Baydrag and Zamtyn Nuruu basement blocks based on the age similarity in post-orogenic plutonic rocks of Zamtyn Nuruu (517 ± 7 Ma, 511 ± 5 Ma and 513 ± 5 Ma) (Hanžl and Aichler, 2007; Hrdličková et al., 2010) and Dzabkhan-Baydrag (519±9 Ma) (Demoux et al., 2009) basement blocks.

The U-Pb zircon age (~540-520 Ma) reported for plutonic rocks of the Zamtyn Nuruu Formation (Hanžl and Aichler, 2007) is comparable with the 519±9 Ma zircon age determined for post-accretion plutonic rocks in the Dzabkhan-Baydrag basement block (Demoux et al., 2009), suggesting collision of the Zamtyn Nuruu and the Dzabkhan-Baydrag microcontinents (Hrdličková et al., 2010).

The Alag Khadny eclogites were formed by subduction of oceanic crust beneath the Zamtyn Nuruu microcontinent (M2 metamorphism) (Fig. 8.2b), whereas the Maykhan Tsakhir garnet-chloritoid schists were metamorphosed during subsequent collision of the Dzabkhan-Baydrag and Zamtyn Nuruu microcontinents (Fig. 8.2d). During the collision the eclogites were juxtaposed and metamorphosed with the garnet-chloritoid schists (M3 metamorphism) (Fig. 8.2d), and this amalgamated sequence of metamorphic rocks was then exhumed to shallower levels at ~540 Ma (Fig. 8.2e). Furthermore, eclogites were intruded and surrounded by granitic rocks during the collision (Fig. 8.2f). Since collision related deformation and metamorphic process eclogites and intruded granitic rocks were suffered by LP-HT metamorphism (M4); and exhumed to the surface at c.460-500 Ma (Fig. 8.2j).

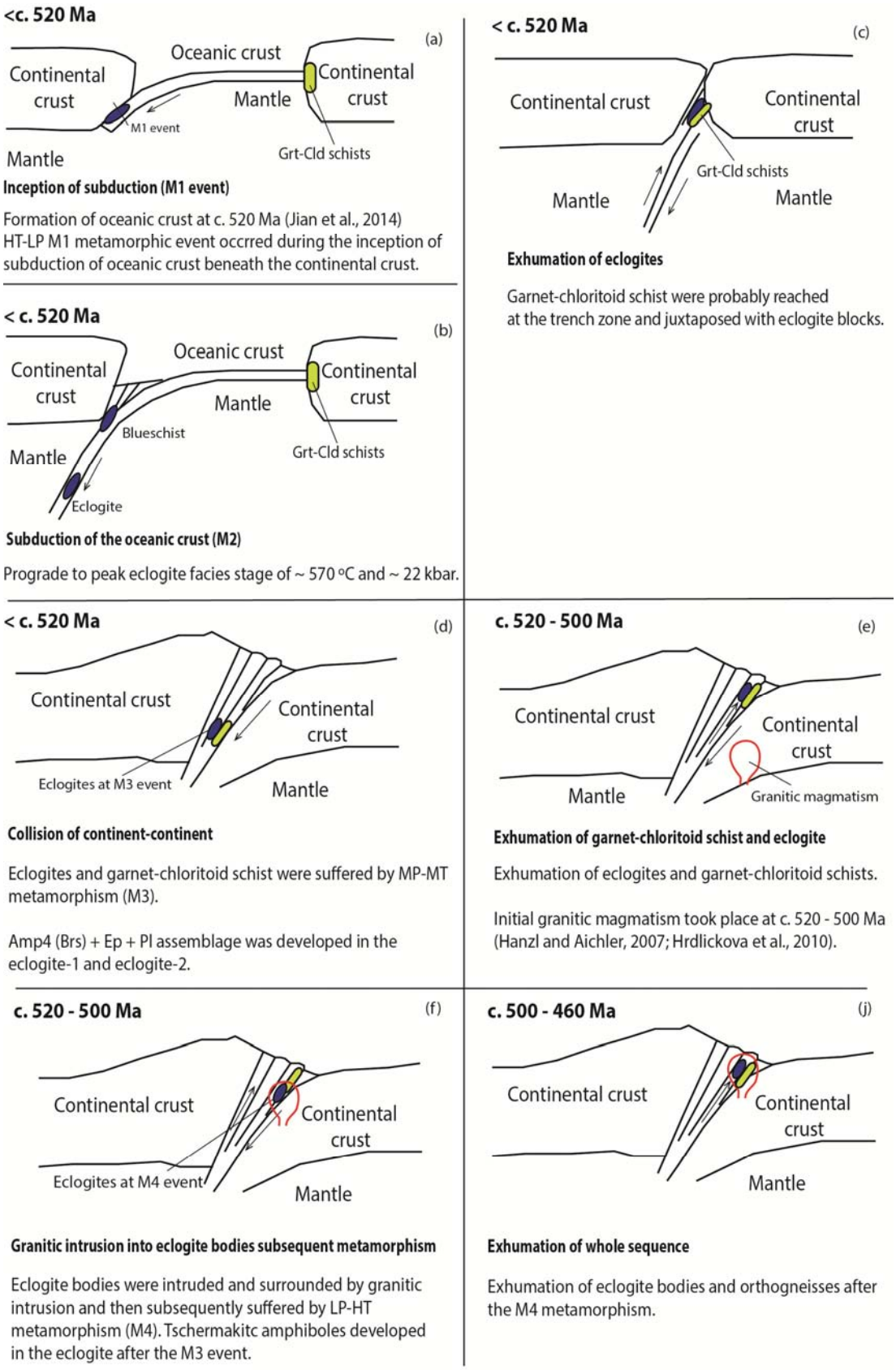

Fig. 8.2 Schematic geodynamic evolution of eclogites and associated metamorphic rocks in the Chandman district, Lake Zone, SW Mongolia.

CHAPTER 9 CONCLUSIONS

Alag Khadny eclogites consist mainly of garnet, omphacite, and sodic, sodic-calcic, and calcic amphiboles (glaucophane, taramite, barroisite, winchite, pargasite, tschermakite, Fe/Mg-hornblende, actinolite) with subordinate amounts of epidote, phengite, paragonite, plagioclase (An1-18), biotite, K-feldspar, rutile, titanite, quartz, calcite, hematite, ilmenite, and zircon.

They are experienced four metamorphic events (M1, M2, M3 and M4). The first metamorphic event (M1) is characterized by polyphase and single grain of inclusions in the garnet. The approximate pressure-temperature (P-T) conditions for the first metamorphic event (M1) suggested that the temperature conditions of 500-650 ºC and pressure condition of <4-5 kbar.

After the LP-HT metamorphic event (M1), eclogites suffered by second HP metamorphic event (M2) of the blueschist (HP-LP) to eclogite facies (HP-HT) metamorphism.

The prograde stage of pre-eclogitic metamorphism represent P-T conditions of 420-550ºC and 10-17 kbar. The peak metamorphic assemblages were stable in HP-HT eclogite facies conditions of 670-700ºC and 25-27 kbar. In retrograde stage, eclogites were passed the P-T stability conditions of 530-630°C and 4-11 kbar.

The third metamorphic event (M3) of epidote amphibolite facies MP-MT metamorphism characterized by the prograde zoning of amphiboles, suggesting the P-T trajectory passed through the stability field of actinolite, winchite and barroisite of epidote-amphibolite facies. The coexisting barroisite and albite give temperature conditions of 410-510ºC.

The associated garnet-chloritoid schists and garnet-phengite schists are experienced MP-MT metamorphism same as M3 metamorphic events of eclogites.

Garnet-chloritoid schists in the Maykhan Tsakhir Formation are distributed close to the eclogite bodies in the Alag Khadny metamorphic complex, in the Chandman district of the Lake Zone. Textural relationship, mineral assemblage and thermobarometric estimates suggest a high-pressure intermediate type metamorphic evolution for the garnet-chloritoid schists in the Maykhan Tsakhir Formation. The metamorphic conditions of pre-peak (T=500-510 °C; P=7-8 kbar) and peak (T=560-590 °C; P=10-11 kbar) stages were determined for the garnet-chloritoid schists. The deduced P-T path represents the epidote-amphibolite facies, or the eclogite facies of high-pressure intermediate type metamorphism. The P-T conditions pre-peak and peak stages correspond to geothermal gradients of 20-22 °C/km and 19-20 °C/km, respectively.

The peak metamorphic pressures for the garnet-chloritoid (~10 kbar) schist are distinctly lower than those of the peak pressure of eclogite-1 (~20 kbar), whereas the temperature conditions are similar at T = ~ 600 ºC.

The third MP metamorphic event (M3) preserved in the eclogite-1 suggest that their P-T path and geothermal gradient deduced by prograde zoned Amp4 are corresponded with garnet-chloritoid schist metamorphism. These suggest eclogites were affected by the garnet-chloritoid metamorphism.

The fourth metamorphic event (M4) defined in the amphibolized eclogites-1 can be corresponding with metamorphism of the vein-type orthogneisses which suffered two metamorphic events, i.e., first (M1) greenschist facies metamorphism (~380°C and 3 kbar), second (M2) epidote amphibolite facies metamorphism

(~500°C and 4 kbar). The P-T conditions of peak stages of M1 and M2 for vein-type orthogneiss correspond to geothermal gradients of ~35 °C/km and ~30 °C/km, respectively. The peak temperature conditions of M2 event (~ 500 °C) for the vein-type orthogneiss are lower than peak temperature of M4 metamorphic event of intruded amphibolized eclogites-1 (550-640 °C) whereas the pressure conditions of vein-type orthogneiss (4 kbar) correspond with peak pressure of M4 for amphibolized eclogites-1 (2-5 kbar). This feature suggests that geothermal gradient of M4 metamorphic event of amphibolized eclogites-1 same as vein-type orthogneiss.

The obtained K-Ar ages of c. 508-479 Ma from the vein-type orthogneiss intruded into eclogite-1 as well as c. 510-459 Ma from the orthogneisses surrounding eclogite bodies. These ages indicate that an exhumation ages of eclogite-1 and vein-type orthogneisses.

Tectonic implications of eclogites and associated metamorphic rocks suggest that M1 event of LP-HT metamorphism occurred during the inception of subduction of Khantaishir oceanic crust beneath the Zamtyn Nuruu continental crust. Then causing the continuous subduction, eclogites were subsequently dragged to deeper parts of subduction zone and suffered M2 events of HP-LT blueschist to eclogite facies metamorphism. After the exhumation of eclogite blocks which were decoupled from subducted oceanic slab, eclogites were suffered by the medium-pressure prograde collisional metamorphism (M3) together with garnet-chloritoid schists. Metamorphosed orthogneisses intruding into and surrounding eclogite-1 suggest the M4 event of low-pressure metamorphism took place during the collision, and subsequent exhumation of together with orthogneisses at c. 500-460 Ma.

The P-T-t evolution of the Chandman metamorphic rocks thus reconstructs the entire tectonic sequence from initiation of subduction (M1 and M2) to collision events (M3 and M4).

Acknowledgement

I thank my supervisors prof. Drs A. Takasu, D. Bat-Ulzii and O. Gerel. I am also grateful to Drs. B.P. Roser, M.F. Kabir and to members of the Metamorphic Geology and Geoscience seminars of Shimane University for discussion and helpful suggestions. I also thank prof. Drs. Y. Sampei and A. Kamei for helping with the Raman spectroscopy and Thermal-ionisation mass spectrometry analysises. I thank my mother Y. Majigsuren for her help during field survey. This study fully supported by Special Course Program of Shimane University and Japanese Government Scholarship Program.

References

Ao, S.J. Xiao, W.J. Han, C.M. Mao, Q.G. and Zhang, J.E. (2010) Geochronology and geochemistry of Early Permian mafic-ultramafic complexes in the Beishan area, Xinjinag, NW China: implications for late Paleozoic tectonic evolution of the southern Altaids. Gondwana Research, 18, 466–478.

Arth, J.G. (1976) Behaviour of trace elements during magmatic process - a summary of theoretical models and their applicantion. Journal of Research of the U.S Geological Survey, 4, 41-47.

Badarch, G., Cunningham, C.W. and Windley, B.F. (2002) A new terrane subdivision for Mongolia: implications for the Phanerozoic crustal growth of Central Asia. Journal of Asian Earth Sciences, 21, 87–110.

Baltatzis, E. and Wood. B.J. (1977) The occurrence of paragonite in chloritoid schists from Stonehaven, Scotland. Mineralogical magazine, 41, 211–216.

Bence, A.E. and Albee, A.L., 1968. Empirical correction factors for the electron microanalysis of silicates and oxides. *Journal of Geology,* 76, 382-403

Blanckenburg FV, Villa IM, Baur H, Morteani G and Steiger RH (1989) Time calibration of a PT-path from the Western Tauern Window, Eastern Alps: the problem of closure temperatures. Contributions to Mineralogy and Petrology, 101: 1–11.

Brown, E.H, 1976 The crosstie content of Ca-amphibole as a guide to pressure of metamorphism. *Journal of Petrology,* 18, 53–72.

Brown, E.H., Wilson, D.L., Armstrong, R.L. and Harakal, J.E., 1982. Petrologic, structural, and age relations of serpentinite, amphibolite, and blueschist in the Shuksa Suite of the iron Mountain-Gee Point area, North Cascades, Washington. *Geological Society of America Bulletin,* 93, 1087-1098.

Buslov, M.M., Saphonova, I.Y., Watanabe, T., Obut, O.T., Fujiwara, Y., Iwata, K., Semakov, N.N., Sugai, Y., Smirnova, L.V. and Kazansky, A.Y. (2001) Evolution of the Palaeo-Asian ocean (Altai Sayan region, Central Asia) and collision of possible Gondwana-derived terranes with the southern marginal part of the Siberian continent. Geoscience Journal, 5, 203–224

Coleman, R.G. (1989) Continental growth of northwest China. Tectonics, 8, 621–635.

Connolly JAD, Multivariable phase diagrams: and algorithm based on generalized thermodynamics. American Journal of Science 290, 666-718

Cox KG, Bell JD, Pankhurst RJ (1979) The interpretation of igneous rocks, George Allen & Unwin, London, pp 1-450

Dale, J. and Holland, T.J.B. (2003) Geothermobarometry, *P-T* paths and metamorphic field gradients of high-pressure rocks from the Adula Nappe, Central Alps. Journal of Metamorphic Geology, 21, 813–829.

Demoux, A., Kröner, A., Badarch, G., Jian, P., Tomurhuu, D. and Wingate, M.T.D. (2009) Zircon ages from the Baydrag Block and the Bayankhongor Ophiolite Zone: time constraints on late Neoproterozoic to Cambrian subduction and accretion-related magmatism in Central Mongolia. Journal of Geology, 117, 377–397.

Dergunov, 2001 Tectonics, magmatism, and Metallogenny of Mongolia. *Routledge, London*

Dilek, Y. and Whitney, D.L., 1997. Counterclockwise P-T-t trajectory from the metamorphic sole of a Neo-Tethyan ophiolites (Turkey). *Tectonophysics,* 280, 295-310.

Doin, M.-P. and Henry, P., 2001. Subduction initiation and continental crust recycling: the roles of rheology and eclogitization. *Tectonophysics,* 342, 163-191.

Elvevold, S. and Gilotti, J.A. (2000) Pressure-temperature evolution of retrogressed kyanite eclogites, Weinschenk Island, North-East Greenland Caledonides. Lithos, 53, 127–147.

Ernst, W.G. and Liu, J., 1998. Experimental phase-equilibrium study of Al- and Ti-contents of calcic amphibole in MORB-A semiquantitative thermobarometer. *American Mineralogist*, 83, 952-969.

Evans, B.W. (1990) Phase relations of epidote-blueschists. Lithos, 25, 3–23.

Gerdes A, Buriankova K (2007) Radiometric dating. In: Hanžl P, Aichler J (eds) Geological survey of the Mongolian Altay on the scale of 1:50,000 (Zamtyn Nuruu-50), Geological Information Centre, MRPAM, Ulaanbaatar, pp 205-217

Gibsher, A.S., Khain, E.V., Kotov, A.B., Sal'nikova, E.V., Kozakov, I.K., Kovach, V.P., Yakovleva, S.Z. and Fedoseenko, A.M. (2001) Late Vendian age of the Han-Taishiri ophiolite complex in western Mongolia: Russian Geology and Geophysics, 42, 1110–1117.

Glorie, S., De Grave, J., Buslov, M.M., Zhimulev, F.I., Izmer, A., Vandoorne, W., Ryabinin, A., Van den Haute, P., Vanhaecke, F. and Elburg, M.A. (2011) Formation and Paleozoic evolution of the Gorby-Altai – Altai-Mongolia suture zone (South Siberia): zircon U/Pb constraints on the igneous record. Gondwana Research, 20, 465–484.

Hanžl, P. and Aichler, J. (2007) Geological Survey of the Mongolian Altay at a scale 1:50,000 (Zamtyn nuruu-50). Final Report, Geological Information Centre, MRPAM, Ulaanbaatar, 389 p.

Henry, D. J., Guidotti, C.V., Thomson, J.A., 2005. The Ti-saturation surface for low-to-medium pressure metapelitic biotite: implications for geothermome-try and Ti-substitution Mechanisms. *American Mineralogist,* 90, 316-328.

Holland, T.J.B. & Blundy, J.D., 1994. Non-ideal interactions in calcic amphiboles and their bearing on amphibole-plagioclase thermometry. *Contributions to Mineralogy and Petrology,* 116, 433-447.

Holland, T.J.B. (1983) Experimental determination of the activities in disordered and short-range ordered jadeitic pyroxenes. Contributions to Mineralogy and Petrology, 82, 214–220.

Holland, T.J.B. and Powell, R. (1998) An internally consistent thermodynamic data set for phases of petrological interest. Journal of Metamorphic Geology, 16, 309–343.

Holland, T.J.B., 1983. Experimental determination of the activities in disordered and short-range ordered jadeitic pyroxenes. *Contributions to Mineralogy and Petrology,* 82, 214–220.

Hrdličková, K., Gerdes, A., Gilíková, H., Bat-Ulzii, D. and Hanžl, P. (2010) Burd Gol Granite Massif as a product of the Late Cambrian post-orogenic magmatism in the SE part of the Lake Zone, Gobi Altay, SW Mongolia, 55, 369–386.

Indares, A. (1995) Metamorphic interpretation of high-pressure-temperature metapelites with preserved growth zoning in garnet, eastern Grenville Province, Canadian Shield. Journal of Metamorphic Geology, 13, 475–486.

Jahn, B.-m., Windley, B., Natal'in, B. and Dobretsov, N. (2004) Phanerozoic crustal growth in central Asia. Journal of Asian Earth Sciences, 23, 599–603.

Jahn, B.-m., Wu, F-y.and Chen, B. (2000) Granitoids of the Central Asian Orogenic Belt and continental growth in the Phanerozoic. Transactions of the Royal Society of Edinburgh: Earth Sciences, 91, 181–193.

Katayama, I., Maruyama, S., Parkinson, C.D., Terada, K. and Sano, Y. (2001) Ion micro-probe U-Pb zircon geochronology of peak and retrograde stage of ultrahigh-pressure metamorphic rocks from the Kokchetav massif, northern Kazakhstan. Earth and Planetary Science Letters, 188, 185–198.

Khain, E.V., Bibikova, E.V., Sal'nikova, E.E., Kröner, A., Gibsher, A.S., Didenko, A.N., Degtyarev, K.E. and Fedotova, A.A. (2003) The Palaeo-Asian Ocean in the Neoproterozoic and early Palaeozoic: new geochronologic data and palaeotectonic reconstructions. Precambrian Research, 122, 329–358.

Kirschner DL, Cosca MA, Masson H and Hunziker JC (1996) Staircase Ar/Ar spectra of fine grained white mica: timing and duration deformation and empirical constraints on argon diffusion. Geology, 24: 152–168.

Kovalenko, V.I., Yarmolyuk, V.V. and Bogatikov, O.A. (1995) Magmatism, Geodyanimics and Metallogeny of Central Asia: Moscow, MIKO, Commercial Herald Publishers, 272 p.

Kröner, A., Lehmann, J., Schulmann, K., Demoux, A., Lexa, O., Tomurhuu, D., Štípská, P., Liu, D. and Wingate, M.T.D. (2010) Lithostratigraphic and geochronological constraints on the evolution of the Central Asian Orogenic Belt in SW Mongolia: early Paleozoic rifting followed by late Paleozoic accretion. American Journal of Science, 310, 523–574.

Lehmann J, Schulmann K, Lexa O, Corsini M, Kröner A, Štípská P, Tomurhuu D and Otgonbaatar D (2010) Structural constraints on the evolution of the Central Asian Orogenic Belt in Southern Mongolia. American Journal of Science, 310: 575–628.

Maruyama, S., Suzuki, K. & Liou, J.G., 1983. Greenschist amphibolite equilibria at low pressures. *Journal of Petrology,* 24, 583–604.

Massonne, H.-J. and Schreyer, W., 1987. Phengite geobarometry based on the limiting assemblage with K-feldspar, phlogopite and quartz. *Contributions to Mineralogy and Petrology,* 96, 212-224.

Matsumoto, I. and Tomurtogoo, O. (2003) Petrological characteristics of the Hantaishir Ophiolite Complex, Altai Region, Mongolia: Coexistence of podiform chromitite and boninite. Gondwana Research, 6, 161–169.

McDougall I and Harrison TM (1988) Geochronology and Thermochronology by the Ar/Ar Method. 212, Oxford University Press, New York.

Miyagi, Y. & Takasu, A., 2005. Prograde eclogite from the Tonaru epidote amphibolite mass in the Sambagawa metamorphic Belt, central Shikoku, southwest Japan. *The Island Arc*, 14, 215–235.

Miyashiro, A. (1961) Evolution of metamorphic belts. Journal of Petrology, 2, 277–311.

Miyashiro, A. (1994) Metamorphic Petrology. London, 404 p. UCL London.

Mossakovsky, A.A., Rzhentsev, S.V., Samygin, S.G. and Kheraskova, T.N. (1994) Central Asian fold belt: geodynamic evolution and formation history. Geotectonics, 24, 445–474.

Orozbaev, R.T., Takasu, A., Bakirov, A.B., Tagiri, M. and Sakiev, S. (2010) Metamorphic history of eclogites and country rock gneisses in the Aktyuz area, Northern Tien-Shan, Kyrgyzstan: a record from initiation of subduction

through to oceanic closure by continent-continent collision. Journal of Metamorphic Geology, 28, 317–339.

Otsuki, M. & Banno, S., 1990. Prograde and retrograde metamorphism of hematite-bearing basic schists in the Sanbagawa belt in central Shikoku. *Journal of Metamorphic Geology,* 8, 425–439.

Peacock, S.M., 1996. Thermal and petrologic structure of subduction zones. In: Subduction: Top to Bottom (ed. Bebout, G.E.), *Geophysical Monograph, Series* 96, pp. 119-133. AGU, Washington DC.

Powell, R. and Holland, T.J.B. (1994) Optimal geothermometry and geobarometry. American Mineralogist, 79, 120–133.

Purdy JW and Jager E (1976) K-Ar ages on rock forming minerals from the Central Alps. Memorie degli Istituti di Geologia e Mineralgia dell'Universita di Padova, 30: 1–31.

Rauzer, A.A., Zhanchiv, D.I., Golyakov, V.I. et al., 1987. Report on Results of Geological Survey at a Scale of 1:200,000, Performed in Southeast part of the Mongolian Altay, Mongolian national Republic in 1983-1986. *Tecknoexport, Moscow*, 769 pp. (in Russian).

Ravna, E.J.K. & Terry, M.P., 2004. Geothermobarometry of UHP and HP eclogites and schists-an evaluation of equilibria among garnet – clinopyroxene – kyanite – phengite – coesite/quartz. *Journal of Metamorphic Geology*, 22, 579–592.

Ravna, E.J.K., 2000. The garnet-clinopyroxene Fe2+-Mg geothermometer: an updated calibration. *Journal of Metamorphic Geology*, 18, 211–219.

Rivers, T., van Gool, J. and Connelly, J. (1993) Contrasting styles of crustal shortening in the northern Grenville orogen. Geology, 21, 1127–1130.

Rojas-Agramonte, Y., Kröner, A., Demoux, A., Xia, X., Wang, W., Donskaya, T., Liu, D. and Sun. M. (2011) Detrital and xenocrystic zircon ages from Neoproterozoic to Paleozoic arc terranes of Mongolia: significance for the origin of crustal fragments in the Central Asian Orogenic Belt. Gondwana Research, 19, 751–763.

Şengör AMC and Natal'in BA, (1996) Paleotectonics of Asia: fragments of a synthesis. In Yin, A. and Harrison, T.M. (eds) The tectonic evolution of Asia, Cambridge University Press, 486–640.

Şengör AMC, Natal'in BA and Burtman VS (1993) Evolution of the Altaid tectonic collage and Paleozoic crustal growth in Eurasia. Nature, 364: 299–307.

Smye, A.J., Greenwood, L.V. and Holland, T.J.B. (2010) Garnet-chloritoid-kyanite assemblages: eclogite facies indicators of subduction constraints in orogenic belts. Journal of Metamorphic Geology, 28, 753–768.

Spear, F.S. and Cheney, J.T. (1989) A petrogenetic grid for pelitic schists in the system SiO2 - Al2O3 - FeO - MgO - K2O - H2O. *Contributions to Mineralogy and Petrology*, 101, 149-164.

Stipska, P., Schulmann, K., Lehmann, J., Corsini, J., Lexa, O., and Tomurhuu, D. 2010, Early Cambrian eclogites in SW Mongolia: evidence that the Palaeo-Asian Ocean suture extends further east than expected. *Journal of Metamorphic Geology,* 1-19.

Takasu A (1989) *P-T* histories of peridotite and amphibolite tectonic blocks in the Sambagawa metamorphic belt, Japan. In: Evolution of Metamorphic Belts (Daly, J.S., Cliff, R.A. and Yardley, B.W.D. ed.), Geological Society of London, Special Publication, 43, 533–538.

Takasu, A., Javkhlan, O., and Batulzii, D., 2008, Eclogites from the Chandman district in the Lake zone, Western Mongolia: The first occurrence of eclogites in Mongolia. *Abstract of the 115th Annual Meeting of the Geological Society of Japan.* 246p. (in Japanese)

Taylor SR and McLennan SM (1981) The composition and evolution of the continental crust: rare earth element evidence from sedimentary rocks. Philosophical Transactions of the Royal Society, A301, 381-399.

Thompson RN (1982) British Tertiary volcanic province. Scotland Journal of Geology, 18, 49-107.

Thompson, A.B., Schulmann, K., Jezek, J. and Tolar, V. (2001) Thermally softened continental extensional zones (arcs and rifts) as precursors to thickened orogenic belts. Tectonophysics, 332, 115–141.

Volkova, N.I.l, Stupakov, S.I., Tret'yakov, G.A., Simonov, V.A., Travin, A.V. and Yuding, D.S., 2005. Blueschists from the Uimon Zone as evidence for Ordovician accretionary-collisional events in Gorny Altai. *Geologiya I Geofizika (Russian Geology and Geophysics)*, 46, 367-382. (361-378).

Wakabayashi, J., 1990. Counterclockwise P-T-t path from amphibolites, Franciscan complex, California: relics from the early stages of subduction zone metamorphism. *Journal of Geology*, 98, 657-680.

Whitney DL and Evans BW (2010) Abbreviations for names of rock-forming minerals. American Mineralogist, 95: 185–187.

Windley, B.F., Alexeiev, D., Xiao, W., Kröner, A. and Badarch, G. (2007) Tectonic models for accretion of the Central Asian Orogenic Belt. Journal of the Geological Society, London, 164, 31–47.

Wu,C. and Zhao,G., 2006. Recalibration of the Garnet–Muscovite (GM) Geothermometer and the Garnet–Muscovite–Plagioclase–Quartz (GMPQ) Geobarometer for Metapelitic Assemblages. *Journal of Petrology*, V.47, 12, 2357-2368.

Xiao, W., Huang, B., Han, C., Sun, S. and Li, J. (2010) A review of the western part of the Altaids: a key to understanding the architecture of accretionary orogen. Gondwana Research, 18, 253–273.

Xiao, X.C., Tang, Y.Q., Zhao, M. and Wang, J. (1994) Tectonic evolution of the Northern Xinjiang, NW China: an introduction to the tectonics of the southern part of the Paleo-Asian Ocean. In: Coleman, R.G. (Ed.), Reconstruction of the Paleo-Asian Ocean. Proceeding of the 29th International Geological Congress, Part B. VSP, Utrecht, The Netherlands, pp. 25–37.

Yakubchuk, A. (2004) Architecture and mineral deposit settings of the Altaid orogenic collage: a revised model. Journal of Asian Earth Sciences, 23, pp. 761–779.

Zonenshain, L.P. and Kuzmin, M.I. (1978) The Khan-Taischir ophiolitic complex of Western Mongolia, its petrology, origin and comparison with other ophiolitic complexes. Contributions to Mineralogy and Petrology 67, 95–109.